1-1-1994

Regio- and stereo-specific propylene-carbon monoxide alternating copolymers :: synthesis, characterization, and application/

Frank Yi Xu
University of Massachusetts Amherst

REGIO- AND STEREO-SPECIFIC PROPYLENE-CARBON MONOXIDE ALTERNATING COPOLYMERS: SYNTHESIS, CHARACTERIZATION, AND APPLICATION

A Dissertation Presented

by

FRANK YI XU

Submitted to the Graduate School of the University of Massachusetts Amherst in partial fulfillment of the requirement for the degree of

DOCTOR OF PHILOSOPHY

September 1994

Polymer Science & Engineering

REGIO- AND STEREO-SPECIFIC PROPYLENE-CARBON MONOXIDE ALTERNATING COPOLYMERS: SYNTHESIS, CHARACTERIZATION, AND APPLICATION

A Dissertation Presented

by

FRANK YI XU

Approved as to style and content by:

James C.W. Chien, Chair

Scott W. Barton, Member

H. Henning Winter, Member

William J. MacKnight, Department Head

Polymer Science & Engineering

TO MY GRANDPARENTS

AND PARENTS

ACKNOWLEDGEMENTS

I would like to thank my advisor, Professor James C. W. Chien, for the support, advice, and encouragement that enabled me to complete this dissertation. His enthusiasm for science and his superior ability to create good ideas had great influences on my scientific thinking. I would also like to thank Professor Scott W. Barton and Professor H. Henning Winter for serving on my thesis committee and for providing me with valuable suggestion.

Many of the faculty and students of the Department of Polymer Science & Engineering contributed intellectually to this dissertation. I would particularly like to thank Dr. L. Charles Dickinson and Dr. Jiefeng Shi for their help on both liquid and solid state NMR experiments, Dr. Allen X. Zhao for his advice on polymer synthesis, and Professor Edward Atkins for his suggestion on unit cell assignment. Special thanks are due H. J. Tao, Mario Perez, Sizhong Dong, Zhengtian Yu, and Hsin-Lung Chen for providing invaluable assistance toward the FTIR, X-ray, and computer simulation studies.

I am grateful for the friendship and help I received from my research group, roommates, and fellow students. The individuals who deserve thanks and mention are numerous. I

must thank all of my friends and loved ones who have supported me.

My deepest love and appreciation for my parents and grandparents cannot be adequately expressed by mere words. Without their love and encouragement I could never have come this far.

Finally, I would like to thank the *Center for University of Massachusetts-Industry Research on Polymers* for the financial support throughout my dissertation work.

ABSTRACT

REGIO- AND STEREO-SPECIFIC PROPYLENE-CARBON MONOXIDE ALTERNATING COPOLYMERS: SYNTHESIS, CHARACTERIZATION, AND APPLICATION

SEPTEMBER 1994

FRANK YI XU, B.S., SPRING HILL COLLEGE
M.S., UNIVERSITY OF MASSACHUSETTS AMHERST
Ph.D., UNIVERSITY OF MASSACHUSETTS AMHERST

Directed by: Professor James C. W. Chien

Compounds of palladium with many different chelated bisphosphine ligands were investigated for their catalysis of alternating copolymerization of propylene (P) with carbon monoxide (CO). The bisphosphine structure and chelate ring size influence strongly the activity, regio- and stereo-selectivity of the catalysts. Molecular mechanics calculations on π-olefin complex showed that the non-bonded interaction between propylene and the ligands on Pd is both regio- and stereo-selective. Electronic factor and presence of chiral center were crucial for the regio- and stereo-regularity control of the

catalyst, respectively. Primary insertion is more probable than secondary insertion, and the enantioselective catalysts favor the *meso* enchainment of propylene. The crystalline copolymer has the hexagonal unit cell structure with a = b = 15.5 Å, and c = 8.97 Å. The single crystalline copolymer chain is a 3_1 fold helix. GC-MS of oligomers showed that most chains are initiated by Pd-H species; and β-hydrogen elimination is the dominant chain termination process.

The anaerobic photodegradation behaviors of bulk alternating copolymers of P-CO and E-CO have been studied by irradiation with 2537 Å light. Photolysis of the former resulted in weight loss, molecular weight depression, cross-linking, and the formation of hydroxyl and terminal vinyl groups. The room temperature quantum yields of chain scission and Norrish type II reactions were found to be 0.015 ± 0.002 and 0.011 ± 0.002.

P-CO alternating copolymer was blended with poly(methyl methacrylate) (PMMA) by solution precipitation. Various aspects of blends behavior were studied by DSC, DMTA, DETA, FTIR, and CP-MAS solid state NMR. The blends exhibited single T_g's at all compositions, which is an indication of the miscible blends. β-relaxation of P-CO copolymer was detected by DETA at -65 °C for the first time. The measurement of rotating frame NMR relaxation time, $T_{1\rho}{}^H$, showed that the average distance between P-CO and PMMA is less than 30 Å.

TABLE OF CONTENTS

LIST OF TABLES

LIST OF FIGURES

CHAPTER 1

INTRODUCTION

1.1 Polymerization with Coordination Catalysts

In the early 1950s, Karl Ziegler in Germany discovered that certain combinations of transition metal compounds and organometallic compounds polymerize ethylene at low temperatures and pressures to give polyethylene that has an essentially linear structure.[1] Following Ziegler's discovery was the recognition by Natta in Italy that catalysts of the type described by Ziegler were capable of polymerizing 1-alkenes (or α-olefin) to yield stereoregular polymers.[2] Ziegler's discovery, together with the ensuing work by Natta and his coworkers, has given rise to the development of new classes both of catalysts and polymers. Due to their commercial and scientific importance Ziegler-Natta and related catalysts have been extensively reviewed in the scientific literature.[3-9]

Most Ziegler-Natta catalysts contain Group IV transition metals from periodic table. The catalytic systems are very sensitive to the H_2O, and they usually can not polymerize any polar monomer. Another class of the catalysts containing

Group VIII transition metals behaves markedly different. Pd cation complexes with bisphosphine ligand can catalyze the alternating copolymerization of α-olefin with carbon monoxide. The presence of polar monomer, carbon monoxide, and CH_3OH (as coinitiator) don't have any negative effect on the catalytic activity. In this copolymerization, α-olefin and carbon monoxide alternately insert into propagating metal-polymer bonds. The resulted copolymers have the general structures of polyketones.

1.2 Copolymers of α-Olefin with Carbon Monoxide

Copolymers of ethylene with carbon monoxide can be prepared through either a free radical or transition metal catalyzed copolymerization. The free radical initiators copolymerized ethylene (E) and carbon monoxide (CO) into random copolymers with usually low carbon monoxide content.[10]

In 1967, Gaugh patented a method of producing copolymer of ethylene and carbon monoxide in the presence of $[(Bu_3P)_2PdCl_2]$.[11] Since this discovery, several Group VIII transition metal complexes have been used as catalysts for this copolymerization.[12-22] The most distinguish character of the copolymer prepared by using a transition metal catalyst is its

linear alternating structure as shown in Figure 1.1. The resulting α-olefin-CO copolymers have a strictly alternating structure under various copolymerization conditions.

1.3 Structure of Propylene-CO Copolymer

In the copolymerization process of ethylene and carbon monoxide, neither regiochemistry nor stereochemistry is of concern. When this catalysis is extended to propylene (P) - carbon monoxide copolymerization, the issue of regiochemical mode of insertion, primary (1,2) versus secondary (2,1), stereochemical mode of enchainment, *meso* versus *racemic*, arise for the microstructure of the product.[23-29] Because propylene is an asymmetric molecule, the sequence structure of the copolymer is expected to be complicated. Regio-chemically propylene can insert in both 1,2 mode and 2,1 mode (Figure 1.2). Straight 1,2 insertion will give regioregular copolymer; the 2,1 misinsertion will lower the regioregularity. Stereochemically, *meso* enchainment competes against *racemic* enchainment of the prochiral propylene monomer to form different stereo-sequence.

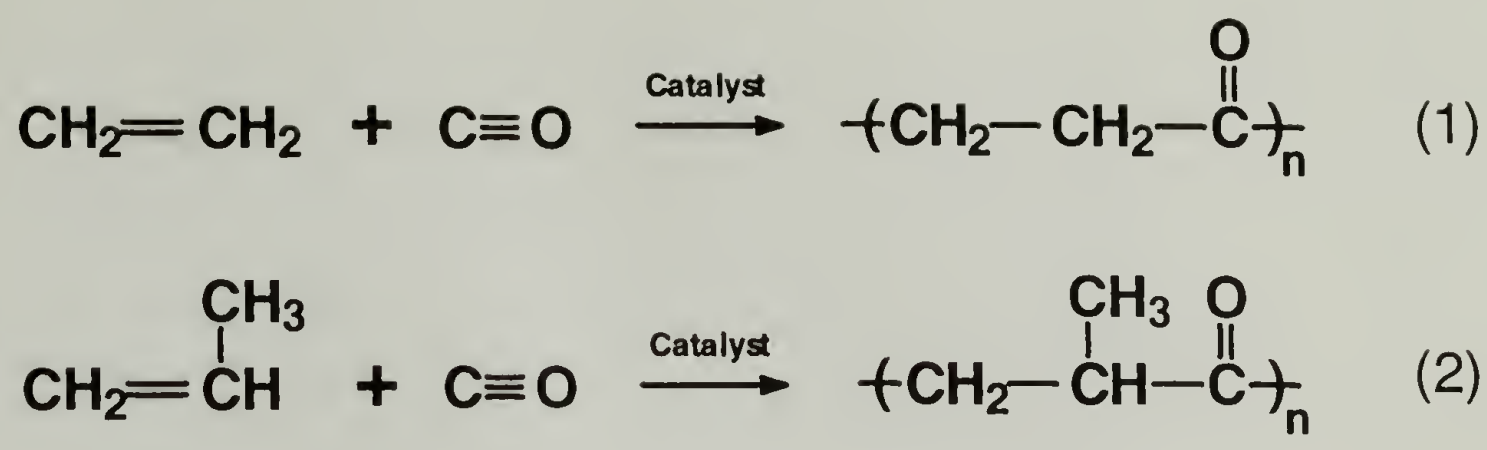

Figure 1.1 Strictly alternating structures of ethylene-CO and propylene-CO copolymers produced by transition metal catalysts.

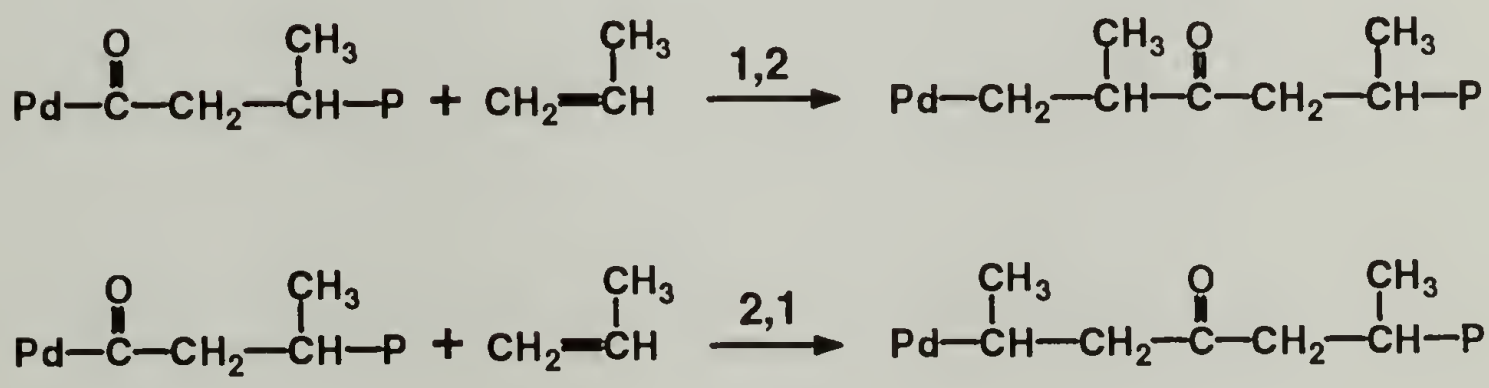

Figure 1.2 1,2 and 2,1 mode of propylene insertion.

1.4 Photo-degradation of α-Olefin-CO Copolymers

The ketone group C=O in the copolymers is one of the most important chromophores from a photochemical point of view.[30] The real progress of photochemistry of carbonyl-containing polymers followed the classic studies of Bamford and Norrish.[31-33] A particular advantage of the ketone carbonyls is that although they are photochemically labile, they are thermally stable. Furthermore, they absorb in the near ultraviolet and hence can be excited selectively in the presence of large numbers of other chemical groups.

In most simple ketones the highest energy occupied molecular orbital (MO) is non-bonding (n) and the lowest unoccupied MO is a π^* orbital. The weak absorption usually observed between 280 and 350 nm in ketones corresponds to the n-π^* transition. Since the n and π^* orbitals are orthogonal, the n-π^* transition violates both symmetry and orbital selection rules. This explains the low intensity of these absorptions, usually ε_{max}, from 10 to 100, in contrast to completely allowed transition which have ε_{max} of the order of 10^5.

The random copolymers of ethylene and carbon monoxide with low content of the latter component have been shown as photo-degradable materials. These polymers degrade by the so called Norrish type I and II processes, and they are marketed

as Ecolyte plastics.[34] The efficiency of type I and type II reactions per photon absorbed has been revealed to depend on the both chemical and physical natures of the materials. The strictly alternating propylene-CO copolymers are expected to exhibit different photochemistry in the areas of degradation mechanism and quantum yields of the degradation process.

1.5 Overview of Dissertation

This thesis work includes six subjects: synthesis and determination of sequence structures of alternating copolymers, mechanism of the polymerization, molecular mechanics calculation of the regio- and stereo-control energy, unit cell structure of the crystalline copolymer, photo- and thermo-degradation of the copolymer, and miscibility and dynamics of the polymer blends contained P-CO copolymer.

One of goals of this work is to synthesize the P-CO alternating copolymers with various morphologies and properties by the control of regio- and stereo-sequences which can be achieved by using different catalysts of bisphosphine/ palladium complexes. To search the right catalysts, we have used two approaches which are altering the ring size of the chelated ring structured catalyst and changing substituent

groups on phosphorus atoms. The details are reported in Chapter 2.

Chapter 3 discusses the two possible polymerization mechanisms expected. First is the conventional mechanism with monomer forming complex with catalyst, then the migration taking place. The second one involves dynamic ring opening. Oligomers and model compounds were analyzed by both GC-MS and NMR methods on the purpose of revealing the nature of the polymerization mechanism.

Molecular mechanics calculation has been proved to be powerful in predicting catalyst regio- and stereo-selectivities.[35] Chapter 4 describes such calculation for the two palladium/ bisphosphine catalytic systems.

The P-CO copolymer is a relatively new polymer. There is no literature report on its crystal structure yet. E-CO copolymer was reported to have the zig-zag structure.[36] With the presence of additional methyl group in P-CO copolymer, a helical structure is expected. The disclosure process of unit cell structure is described in Chapter 5.

The ketone group C=O contained in the α-olefin-CO alternating copolymer is a photoactive chromophores as described previously. Packaging materials fabricated from a bio- or photo-degradable polymer[37] is deemed more friendly to the environment. The alternating P-CO copolymer has the

potential to be served as photo-degradable material. The photolysis mechanisms of olefin-CO alternating copolymer have been examined, and the results are shown in Chapter 6.

Another possible application of the P-CO alternating copolymer is in the field of polymer blends. Poly(methyl methacrylate) is known as a brittle material. The amorphous P-CO copolymer has been selected to blend with PMMA in the hope of increasing the impact strength of the PMMA. The glass transition temperatures of the selected P-CO copolymer and PMMA are around 20 and 110 °C. Since two T_gs are well separated, the glass transition temperatures of the blends can be used as an indicator for the miscibility. Chapter 7 summarizes the various aspects of the blends by the methods of solid state NMR, FTIR, DSC, DMTA, and DETA.

References

(1) Ziegler, K. *Belg. Pat.* 53362, **1953**.

(2) Natta, G.; Pino, P.; Danusso, F.; Mantica, E.; Mazzanti, G.; Moragio, G. *J. Am. Chem. Soc.* **1955**, *77*, 1708.

(3) Bovey, F. A.; Tiers, G. V. D. *J. Polym. Sci.* **1960**, *44*, 173.

(4) Doi, Y.; Asakuru, T. *Makromol. Chem.* **1975**, *176*, 507.

(5) Pino, P.; Muelhaupt, R. *Angew. Chem., Int. Ed. Engl.* **1980**, *19*, 857.

(6) Natta, G.; Corradini, P.; Bassi, I. W.; Porri, L. *Atti. Accad. N. az. Lincei, Cl. Sci. Fis., Mat. Nat., Rend.* **1958**, *24*, 121.

(7) Longi, P.; Giannini, U.; Cassata, A. (issued to Montedison) *Belg. Pat.* 774,600, **1971**.

(8) Busico, V.; Corradini, P.; De Martino, L.; Proto, A.; Savino, V.; Albizzati, E. *Makromol. Chem.* **1985**, *186*, 1279.

(9) Langer, A. W.; Burkhardt, T. J.; Steger, J. J. *Proceedings of the MMI International Symposium on 'Transition Metal Catalyzed Polymerization: Unsolved Problems'*, Midland, MI, **1981**.

(10) Brubaker, M. M.; Coffman, D. D.; Hoehn, H. H. *J. Am. Chem. Soc.* **1952**, *74*, 1509.

(11) Gaugh, A. *Great Britain Pat.* 1,081,304, **1967**.

(12) Fenton, D. M. *U.S. Pat.* 3,530,109, **1970**.

(13) Nozaki, K. *U.S. Pat.* 3,689,460, **1972**.

(14) Nozaki, K. *U.S. Pat.* 3,835,123, **1974**.

(15) Lai, T. W.; Sen, A. *Organometallics* **1984**, *3*, 866.

(16) Shryne, T. M.; *U.S. Pat.* 3,948,388, **1976**.

(17) van Broekhoven, J. *Eur. Pat. Appl.* A1, 0,213,671, **1986**.

(18) Drent, E. *Eur. Pat. Appl.* A1, 0,264,159, **1987**.

(19) Drent, E. *Eur. Pat. Appl.* A2, 0,272,728, **1987**.

(20) Sen, A.; Lai, T. W. *J. Am. Chem. Soc.* **1980**, *104*, 3520.

(21) Sen, A. *Chemtech.* **1986**, 48.

(22) Sen, A. *Adv. Polym. Sci.* **1987**, *73/74*, 125.

(23) Jiang, Z.; Dahlen, G. M.; Houseknecht, K.; Sen, A. *Macromolecules* **1992**, *25*, 2999.

(24) Batistini, A.; Consiglio, G.; Suter, U. W. *Angew. Chem. Int. Ed. Engl.* **1992**, *31*, *No. 3*, 303.

(25) Chien, J. C. W.; Zhao, A. X.; Xu, F. *Polym. Bull.* **1992**, *28*, 315.

(26) Batistini, A.; Consiglio, G. *Organometallics* **1992**, *11*, 1766.

(27) Batistini, A.; Consiglio, G.; Suter, U. W. *PMSE Preprint*, **1992**, *67*, 104.

(28) Xu, F. Y.; Zhao, A. X.; Chien, J. C. W. *Markomol. Chem.* **1993**, *194*, 2579.

(29) Wong, P. K.; van Doorn, J. A.; Drent, E.; Sudmeijer, O.; Stil, H. A. *Ind. Eng. Chem. Res.* **1993**, *32(5)*, 986.

(30) Guillet, J. *Polymer Physics and Photochemistry* New York: Cambridge University Press, **1985**.

(31) Bamford, C. H.; Norrish, R. G. W. *J. Chem. Soc.* **1935**, 1504.

(32) Bamford, C. H.; Norrish, R. G. W. *J. Chem. Soc.* **1938**, 1521.

(33) Bamford, C. H.; Norrish, R. G. W. *J. Chem. Soc.* **1938**, 1544.

(34) Allen, N. S.; Edge, M. *Fundamentals of Polymer Degradation and Stabilisation* New York: Elsevier Applied Science, **1992**.

(35) Yu, Z.; Chien, J. C. W. *J. Am. Chem. Soc.* submitted.

(36) Chatani, Y.; Takizawa, T. *J. Polym. Sci.* **1961**, 55, 811.

(37) Bremer, Y. P. *Polym. Plast. Technol. Eng.* **1982**, *18*, 137.

CHAPTER 2

SYNTHESIS OF REGIO- AND STEREO-SPECIFIC ALTERNATING COPOLYMERS OF PROPYLENE WITH CARBON MONOXIDE

2.1 Introduction

The alternating copolymerization of carbon (CO) and ethylene (E) was discovered in 1951.[1] The mechanism had been investigated by Sen et al.[2] and Drent et al.[3] The catalyst system patented by Shell Chemical Co.[3,4] was formed by the combination of palladium acetate with a bisphosphine ligand, a Bronsted acid, and an oxidizing agent. We have found[5] that very high activity catalyst could be obtained with palladium tetrafluoroborate, bisphosphine ligand, and methanol which serves as the cocatalyst. The alternating E-CO copolymer is a high-melting (melting temperature T_m = 257 °C) material which is difficult to process and not amenable to characterize.

Recently, propylene (P) and CO have been polymerized into semicrystalline alternating P-CO copolymers,[6,7] as well as into amorphous copolymers.[6,8] Alternating copolymerization of 1-butene with CO and 1-hexene with CO have also been

achieved.[6] The semicrystalline P-CO copolymers have T_m much lower than that of E-CO alternating copolymer and are soluble in common organic solvent, thus offering ease of both processing and characterization.

Regiochemically the insertion of P can occur either by the 1,2 (primary) or the 2,1 (secondary) mode. Furthermore, the prochiral propylene can be enchained in *meso* or *racemic* configuration. NMR methods have been devised to determine the degree of regio- and stereo-regularity. The structure of the bisphosphine ligand was varied to study the effect of its chelation on the regio- and stereo-chemical control in the P-CO copolymerization. These results are reported in this chapter.

2.2 Experimental

2.2.1 Materials

Propylene (CP grade, 99% minimum), carbon monoxide (CP grade, 99.0% minimum) and argon (prepurified, 99.998%) were supplied by Linde Gas Co., U. S. A. Most chemicals were purchased from Aldrich Chemical Co., U. S. A. Some bisphosphines were the gifts of Texas Eastman Chemical Co., U. S. A.

Acetonitrile was distilled after being dried with anhydrous $MgSO_4$. Methanol was distilled from magnesium powder and small amount of iodine.[9] 1,2 dichloroethane was distilled from P_2O_5 then refluxed over CaH_2.

2.2.2 Synthesis of Catalysts

$[Pd(CH_3CN)_4](BF_4)_2$ (**1**)[2b]: In an air bag covered under argon, Pd sponge (1.064 g, 0.01 mol) and $NOBF_4$ (2.336 g, 0.02 mol) and 50 mL of CH_3CN were transferred to a 150 mL flask along with a stir bar. This reaction mixture was stirred under a slow flow of argon at room temperature for 24 hours. The reaction solution was filtrated through a cannulate tipped with filtrating paper and precipitated into anhydrous ether. The pale yellow precipitant was washed with anhydrous ether three times and dried under vacuum. A yield of 80-90 % was obtained. Anal. (Calcd for $PdC_8H_{12}N_4B_2F_8$): C, 21.7 (21.7); H, 2.8 (2.7); N, 12.3 (12.6).

$[(Ph_2P(CH_2)_2PPh_2)Pd(CH_3CN)_2](BF_4)_2$ (catalyst **2**, dppe ligand): The reaction of $(Ph_2P(CH_2)_2PPh_2)PdCl_2$ (5.76 g, 10 mmol) with $AgBF_4$ (3.89 g, 20 mmol) in 150 mL of acetonitrile was carried out at room temperature for 6 h. The white solid product was filtered and excess acetonitrile removed with

evacuation. The yellow colored **2** was obtained in ca. 95 % yield.

$[(Ph_2P(CH_2)_nPPh_2)Pd(CH_3CN)_2](BF_4)_2$ (n = 3-6), catalyst number/ligand, **3**/dppp, **4**/dppb, **5**/dpppe, **6**/dpph: These catalysts were synthesized by reacting **1** (0.444 g, 1 mmol) with $Ph_2P(CH_2)_nPPh_2$ (1 mmol) in 150 mL acetonitrile. The product was worked up as for **2**. Anal. (Calcd for catalyst **4** $PdC_{32}H_{34}P_2N_2B_2F_8$): C, 48.7 (47.8); H, 4.3 (4.2); N, 3.6 (3.9).

$[2PPh_3 \bullet Pd(CH_3CN)_2](BF_4)_2$ (**7**): The catalyst was synthesized by mixing **1** (0.444 g, 1 mmol) with PPh_3 (2 mmol) in 150 mL acetonitrile. The product was worked up as for **2**.

Other catalysts: The same procedure for preparation of the complex **3** to **6** was employed to synthesize the catalyst **8-19** using the appropriate bisphosphine ligands shown in Table 2.1. The synthesis procedures for catalyst **15** and **18** were reported by Batistini et al.[7]

2.2.3 Copolymerization

The standard copolymerization conditions are: catalyst (0.02 mmol), methanol (1 mL), 1,2-dichloroethane as solvent (150 mL), 60 psig propylene, 720 psig CO, at 50 °C for 4 h. A 300 mL Paar reactor was dried, purged with argon, the catalyst, methanol and solvent was cannulated into it, then

Table 2.1 Structures of bisphosphine ligands.

Cat. No.

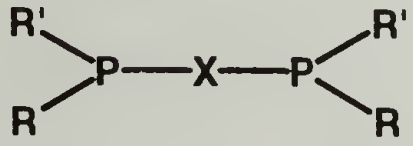

8	X = $-(CH_2)_3-$	R = $-C_6H_5$ R' = $-o\text{-}CH_3C_6H_5$
9	X = $-(CH_2)_3-$	R and R' = $-o\text{-}CH_3C_6H_5$
10	X = $-(CH_2)_4-$	R = $-C_6H_5$ R' = $-o\text{-}CH_3C_6H_5$
11	X = $-(CH_2)_4-$	R and R' = $-o\text{-}CH_3C_6H_5$
12	X = $-(CH_2)_4-$	R and R' = $-m\text{-}CH_2C_6H_4F$
13	X = $-(CH_2)_4-$	R and R' = $-p\text{-}CH_2C_6H_4Cl$
14	X = 	R and R' = $-C_6H_5$
15	X = $-(CH_2)_3-$	R and R' = 
16	X = $-(CH_2)_4-$	R and R' = 
17	X = $-(CH_2)_3-$	R and R' = 
18	X = 	R and R' = 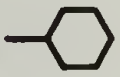
19	X = 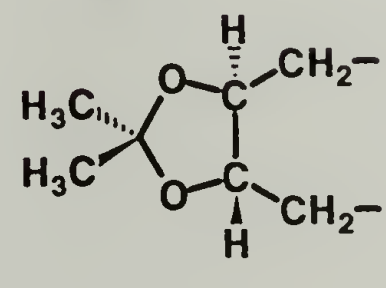	R and R' = $-C_6H_5$

propylene was introduced first through a high-pressure hose followed by carbon monoxide. The mixture was heated to the polymerization temperature. At the end of a copolymerization the unreacted monomers were vented, and the copolymer was purified by precipitation with methanol and dried in vacuo at ambient temperature for 24 h. Other copolymerization conditions were used as stated. The overall procedures of both catalyst and polymer synthesis are depicted in Figure 2.1 by using *n*+3-membered ring catalyst as an example.

2.2.4 Epimerization

Copolymer was heated to 70 °C under nitrogen for 5 days in *o*-chlorophenol in the presence of sodium *o*-chlorophenolate (0.0022 mol/L).[10] The product was precipitated with methanol and worked up as above.

2.2.5 Measurement

^{13}C Nuclear magnetic resonance (^{13}C-NMR) spectra were recorded on a Varian XL-200 spectrometer using $CDCl_3$ as solvent. Differeential scanning calorimetry (DSC) was performed on a Du Pont 2000 thermoanalysis system with 20 °C/min heating rate . X-ray diffraction pattern of palletized

(1) Catalyst Synthesis

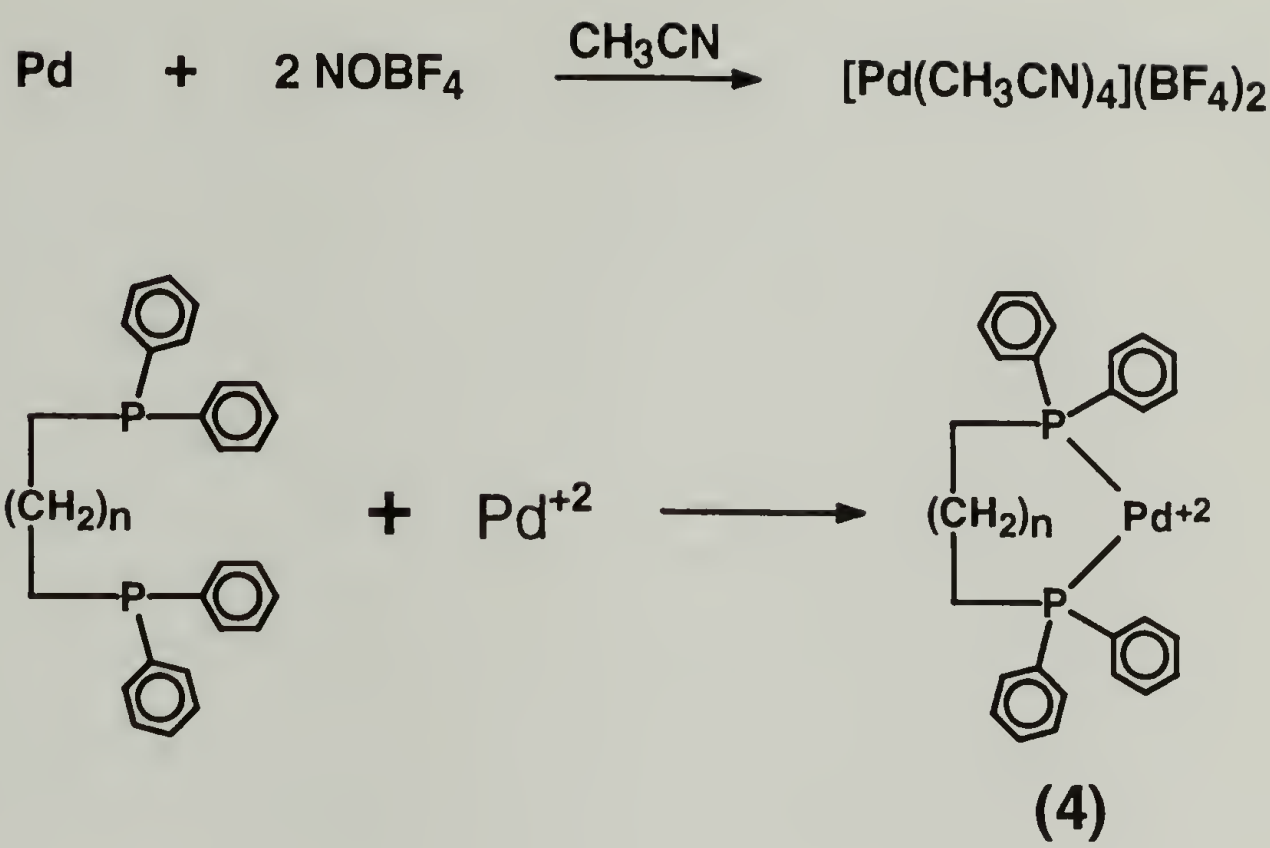

(4)

(2) Polymerization

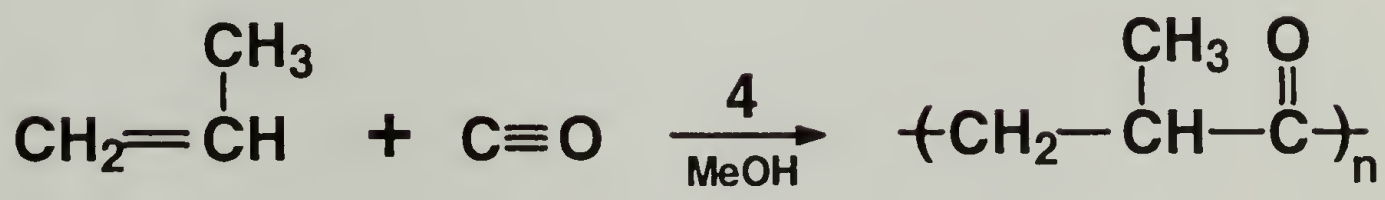

Figure 2.1 The overall procedures of both catalyst and polymer synthesis with *n*+3-membered ring catalyst.

copolymer was recorded on a Siemens D-500 diffractometer using a Ni-filtered Cu-K_α radiation excited at 40 kV. The crystallinity was calculated by Ruland's method.[11]

2.3 Results and Discussion

2.3.1 ^{13}C-NMR Characterization

Unlike the alternating copolymers of carbon monoxide with ethylene, which are very high melting and insoluble, the P-CO copolymer is either semicrystalline having lower T_m depending on its micro-structure and molecular weight[6,7] or amorphous.[6,8] The copolymers are quite soluble in common polar organic solvents such as chloroform, acetonitrile. The high molecular weight P-CO copolymer can be precipitated by cold methanol; the low molecular weight copolymer can be recovered by evaporation of methanol and solvent.

^{13}C-NMR spectroscopy is probably the best technique to determine the regiochemical arrangement and stereochemical configuration of the P-CO copolymer. Figure 2.2 shows a typical ^{13}C-NMR spectrum of the alternating copolymer made by means of catalyst **4**. The broad bands above 200 ppm have been assigned to the carbonyl group.[2e,5] The resonance at 16 ppm is readily attributed to the side chain methyl groups. We

Figure 2.2 ^{13}C-NMR spectrum of the alternating P-CO copolymer made by catalyst **4** at 0 °C. $CDCl_3$ was used as solvent.

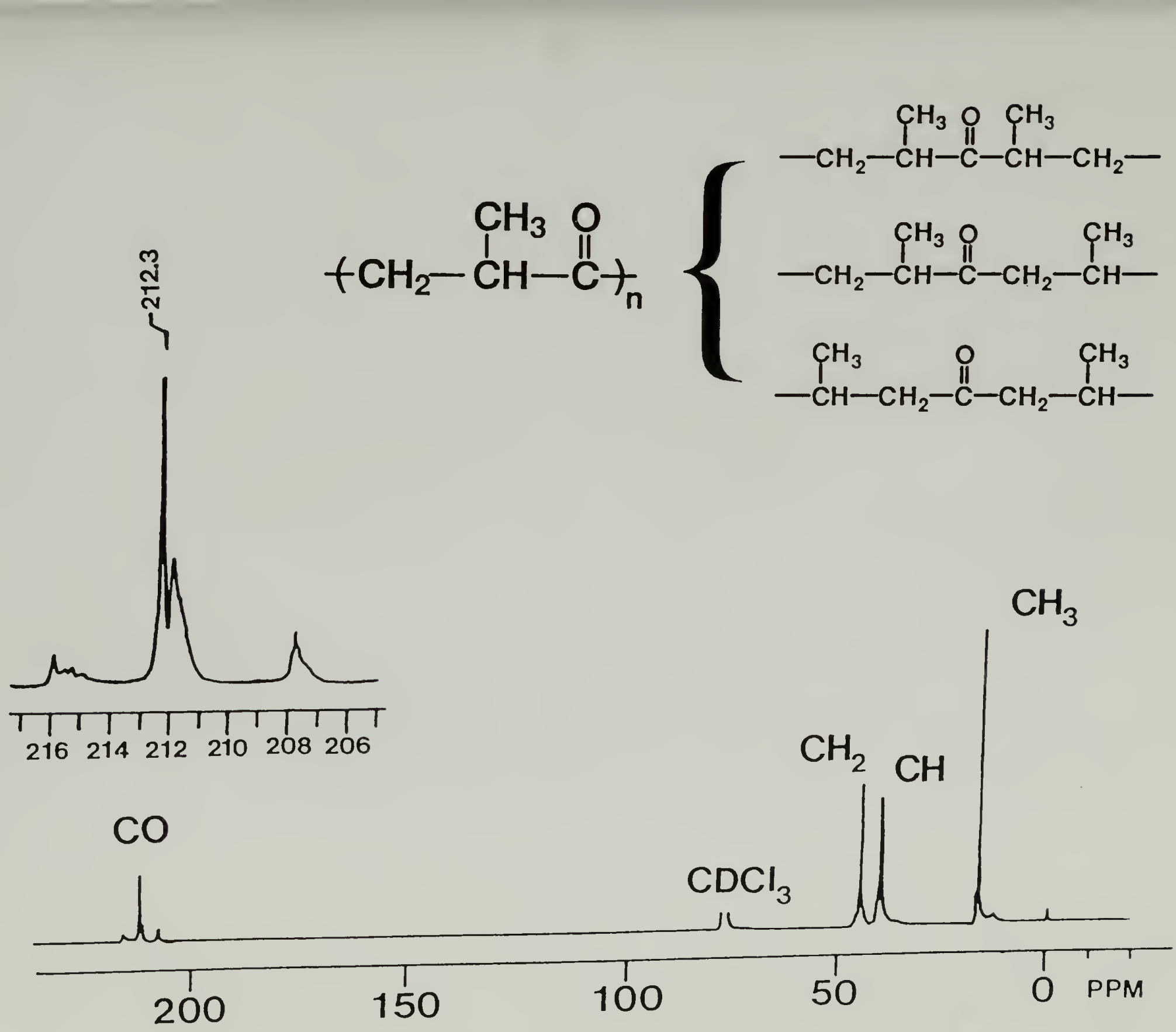
212.3
216 214 212 210 208 206
CO
CDCl3
CH2
CH
CH3
200 150 100 50 0 PPM

applied the Distortionless Enhancement by Polarization Transfer (DEPT) technique to show that the signal at 44-45 ppm is due to the methylene carbons. The integrated areas of carbonyl, main chain CH and CH_2 and side chain CH_3 ^{13}C peaks maintain a ratio of 1:1:1:1. Therefore, these high molecular weight P-CO copolymers have the alternating structure.

Propylene and CO were copolymerized with catalyst **3** at 70 °C to produce very low molecular weight products for end-group analysis by means of ^{13}C-NMR. Figure 2.3 illustrates a ^{13}C-NMR spectrum of such a copolymer.

Three kinds of end groups were detected. Peaks a, b, c (at 198.3, 142, and 131.5 ppm) are assigned to the carbonyl carbon, β- and α-carbon nuclei of an α,β-unsaturated keto end group, respectively. Peak d at 51.5 ppm is the methyl chemical shift of methoxycarbonyl end group, peak e at 13.5 ppm is attributed to the γ-carbon of a linear propylketo end group. The intensities of these resonances decrease with the increase of molecular weight of the specimen consistent with their end-group assignments.

Regioregularity in copolymers arises from different modes on propylene insertion. The first mode is 1,2 insertion (primary insertion) that gives a primary alkyl group attached to the palladium. Second mode is 2,1 insertion (secondary

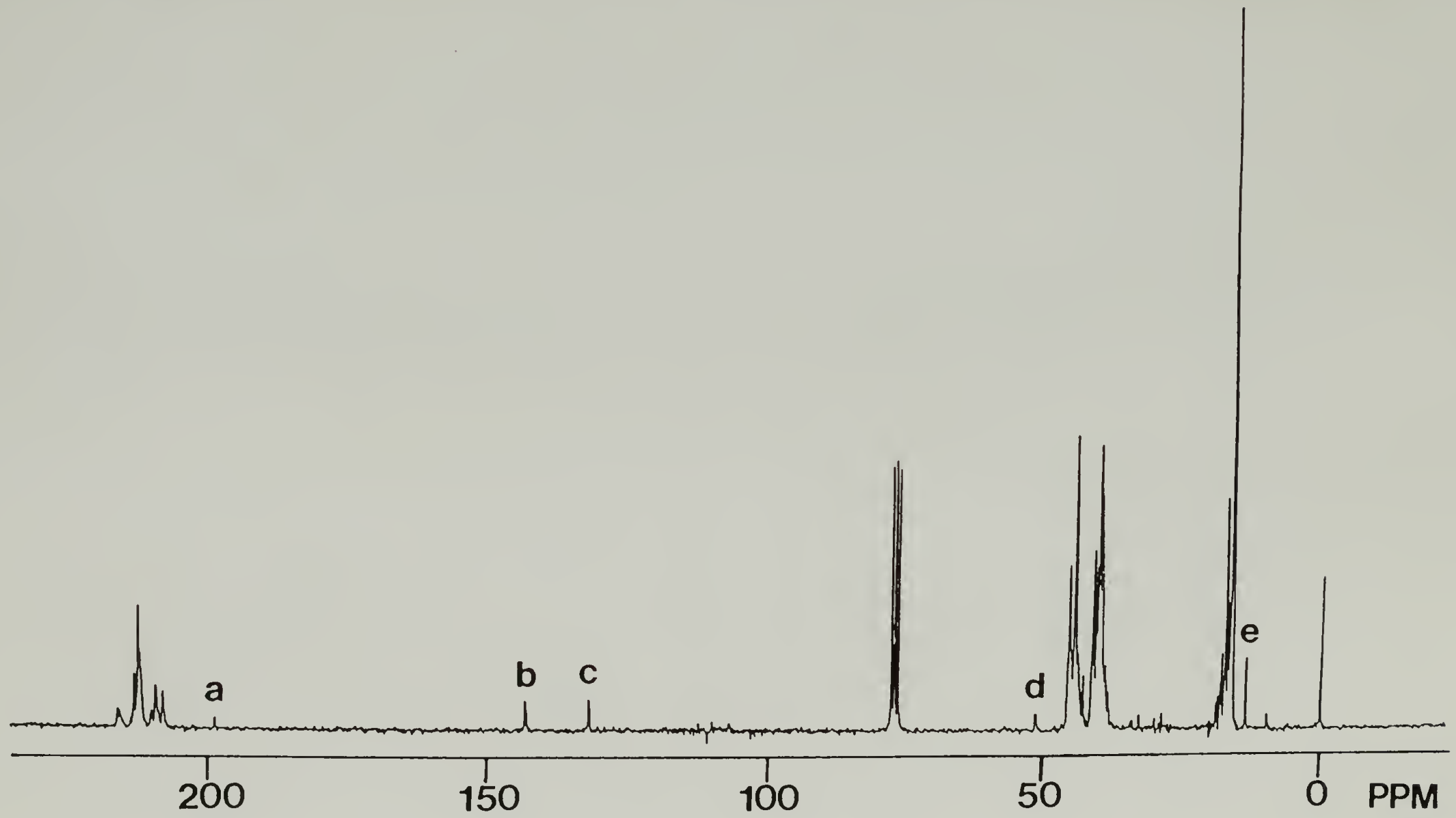

Figure 2.3 ^{13}C-NMR spectrum of the low molecular weight alternating copolymer produced by catalyst **3** at 70 °C. Peaks a, b, c, d, e are attributed to the end group.

insertion) that produces a secondary alkyl group attached to the palladium.[12] According to the conventional notation, one end of propylene unit can be designated as the head (e.g. = $CHCH_3$); the other end is the tail (e.g. = CH_2). Therefore, regiochemically there are head-head (H-H), head-tail (H-T), and tail-tail (T-T) sequences as shown in Figure 2.4 for two consecutive propylene insertions.

Figure 2.2 shows significant chemical shift split within carbonyl groups region of the ^{13}C-NMR spectrum. Using the ^{13}C-NMR empirical addition rules for the substituent effect,[13] we attempted to assign the different regiosequences of the copolymer from carbonyl carbon resonance peaks. Because P-CO alternating copolymer has the back bone structure of the ethylene-CO alternating copolymer, only the substituent effect of methyl side group needs to be considered.

$$\delta = \delta^o + \sum Z \qquad (1)$$

where δ, δ^o are carbonyl chemical shifts for the P-CO (with different regiosequences) and E-CO alternating copolymers, respectively. Solid state NMR result showed the δ^o to be 210.9 ppm.[5] Z is the side chain methyl substituent effects which are 7, 2, and -1 ppm for the methyl substituent α, β, and γ to the carbonyl carbon.[13] Consequently, the three groups of peaks at

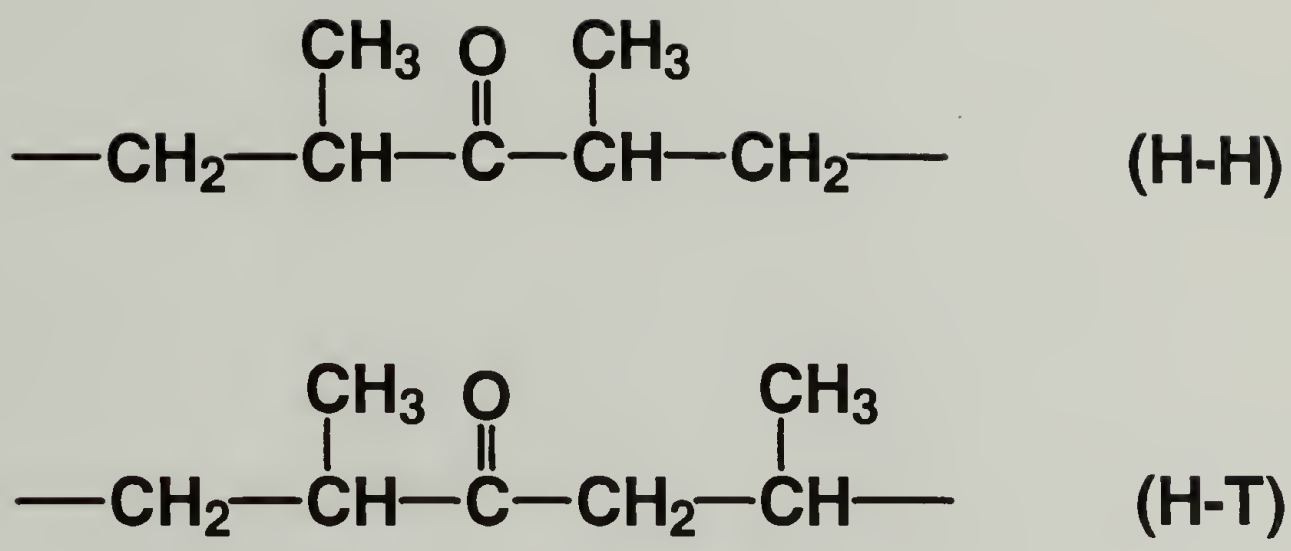

Figure 2.4 Regiosequences of P-CO alternating copolymer.

207-209, 211-213 and 214-216 ppm correspond to the T-T, H-T, and H-H sequences, respectively.

Stereochemically, *meso* enchainment competes against *racemic* enchainment of the prochiral propylene monomer to form different stereo-sequence. The P-CO copolymers have varying degrees of stereoregularity depending upon the relative configuration of the adjacent tertiary carbon atoms of the propylene units. To enable assignment of peaks for stereoconfiguration, it requires the ^{13}C-NMR spectra of completely stereo-random copolymer. The latter can be obtained by epimerization[10] as shown in Figure 2.5.

^{13}C-NMR spectrum of carbonyl carbon region of the regioregular alternating copolymer is depicted in Figure 2.6a. The epimerized alternating copolymer has three ^{13}C-NMR peaks in the carbonyl carbon region (Figure 2.6b) at 212.3 (I), 211.9 (H), and 211.6 ppm (S) with 25 : 50 : 25 observed peak ratio. Resonance H must be the heterotactic triad by virtue of its intensity and chemical shift values. The relative intensity of peak I decreased upon epimerization. Batistini et al.[7] showed that bisphosphine-Pd catalysts of the present type favor the *meso* enchainment of propylene. Consequently, resonance I and S may be attributed to isotactic and syndiotactic triad (Figure 2.7), respectively.

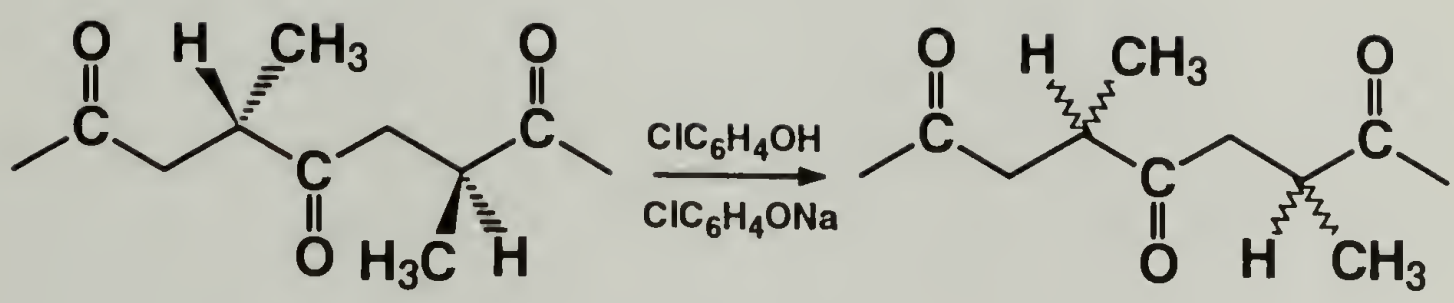

Figure 2.5 Epimerization of stereoregular copolymer.

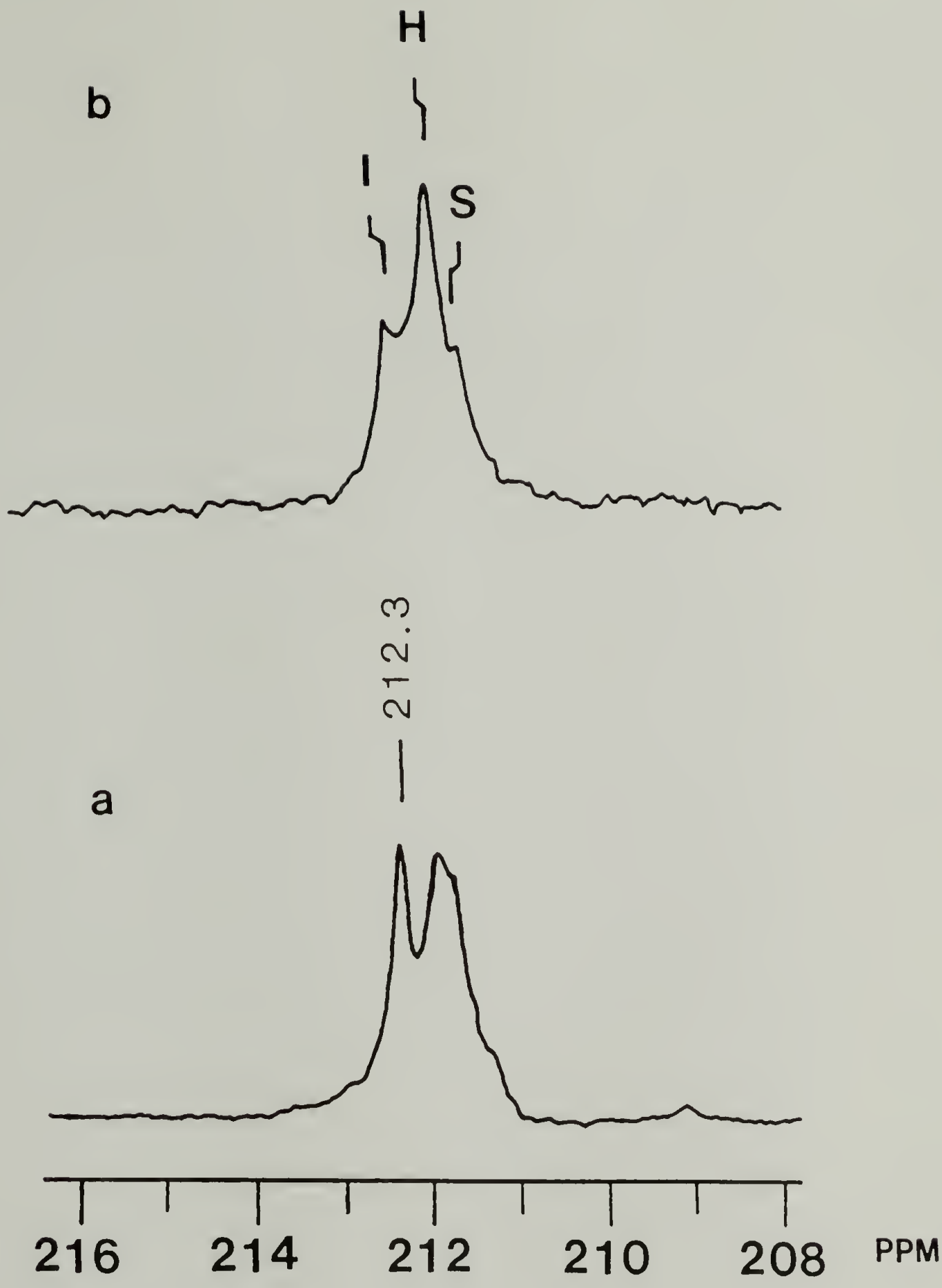

Figure 2.6 ^{13}C-NMR spectra of carbonyl carbon region of the regioregular alternating copolymer: (a) before epimerization, (b) after epimerization.

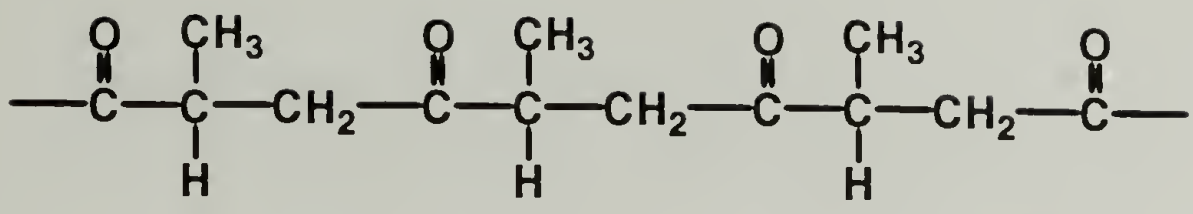

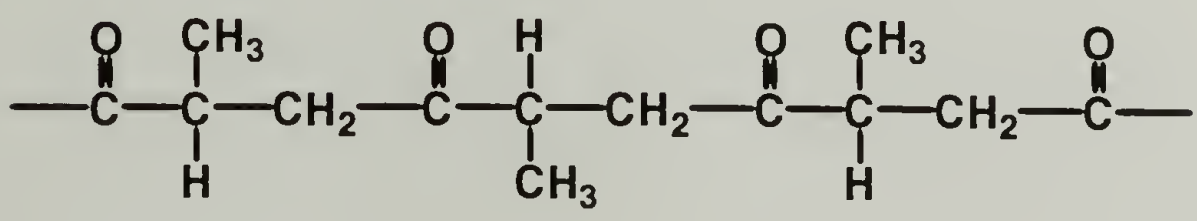

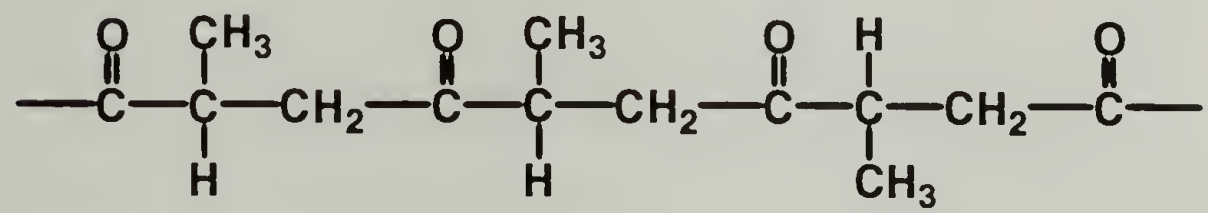

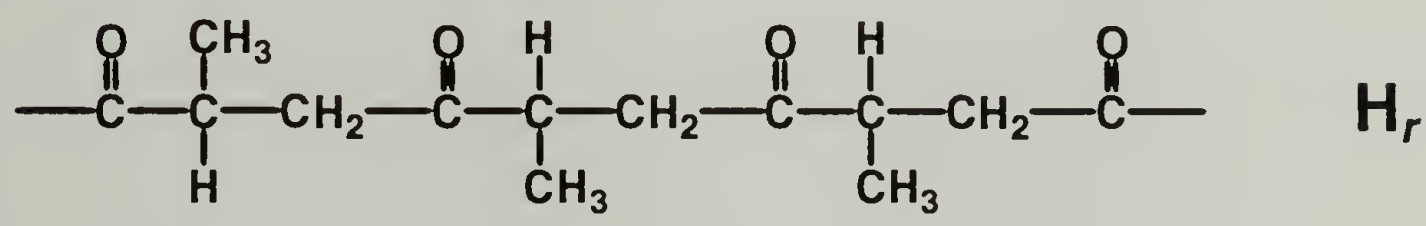

Figure 2.7 The isotactic, syndiotactic, and heterotactic triads of P-CO alternating copolymer.

The two heterotactic triads are distinguishable in principle. However, the epimerized P-CO copolymer contains only a singlet for these two triads. The same magnetic equivalence was noted for poly(oxypropylene). Oguni[14] attributed this phenomenon to the strong magnetic shielding effect of oxygen. In any case the phenomenon does not pose a hindrance to the determination of steric sequence distribution in the P-CO copolymer.

2.3.2 Other Characterization

Figure 2.8 is a typical X-ray diffraction scan of a P-CO copolymer produced with catalyst **4**. The degree of crystallinity was estimated by Ruland analysis to be ca. 39%.

Thermogravimetric analysis was performed on a P-CO copolymer prepared using catalyst **4**. The thermogravimetry (TG) curves obtained for different heating rates are shown in Figure 2.9. Thermolysis commences at 330 °C when the sample was heated at 10 °C/min. This onset temperature was higher when the TG was programmed at a faster heating rate. The data was analyzed by the multiexperimental comparison methods.[15] For a specific conversion,

$$\log_{10}\beta = -0.457E/(RT) + \text{constant} \qquad (2)$$

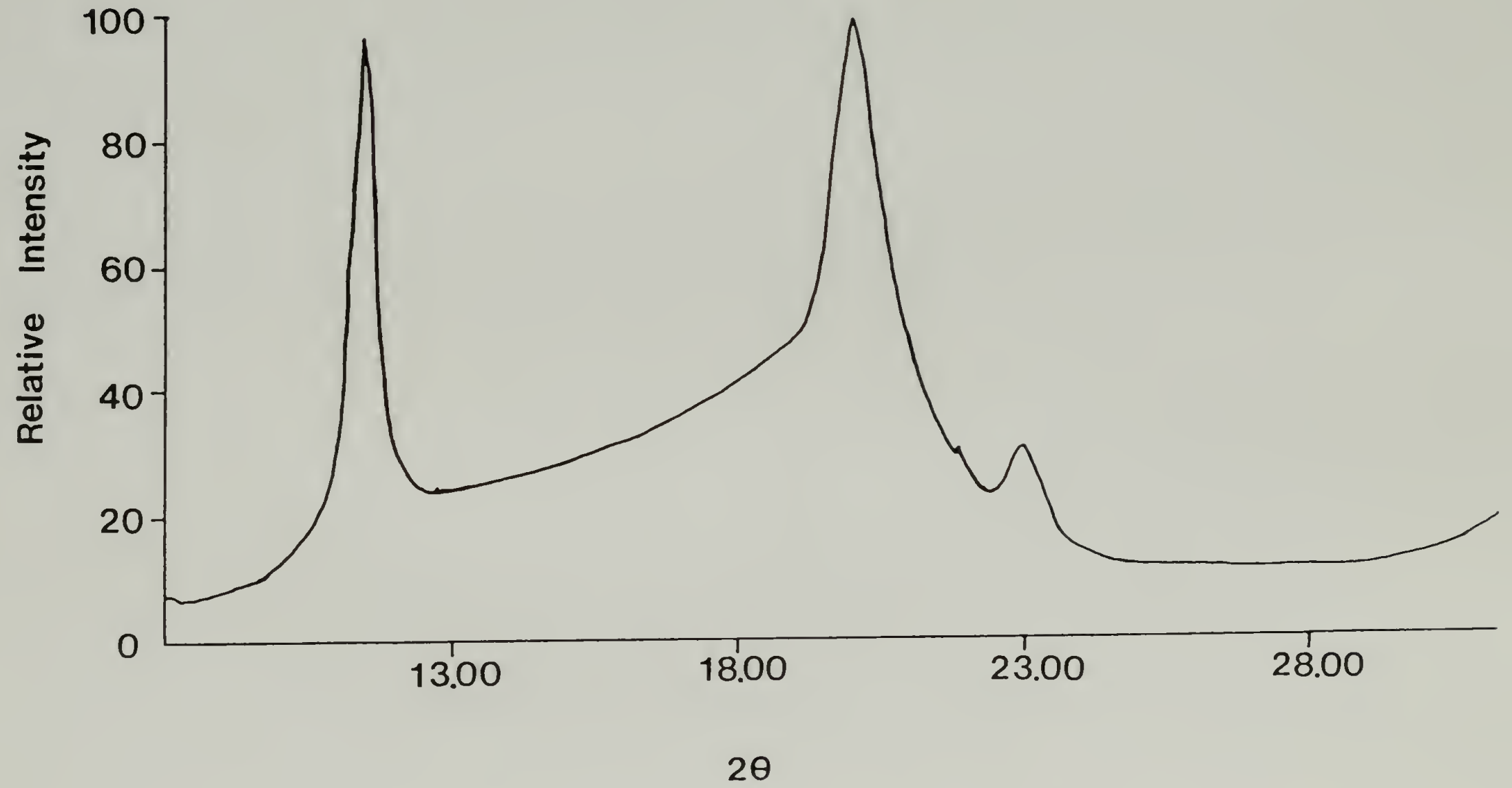

Figure 2.8 X-ray diffraction scan of the P-CO copolymer made by catalyst **4**.

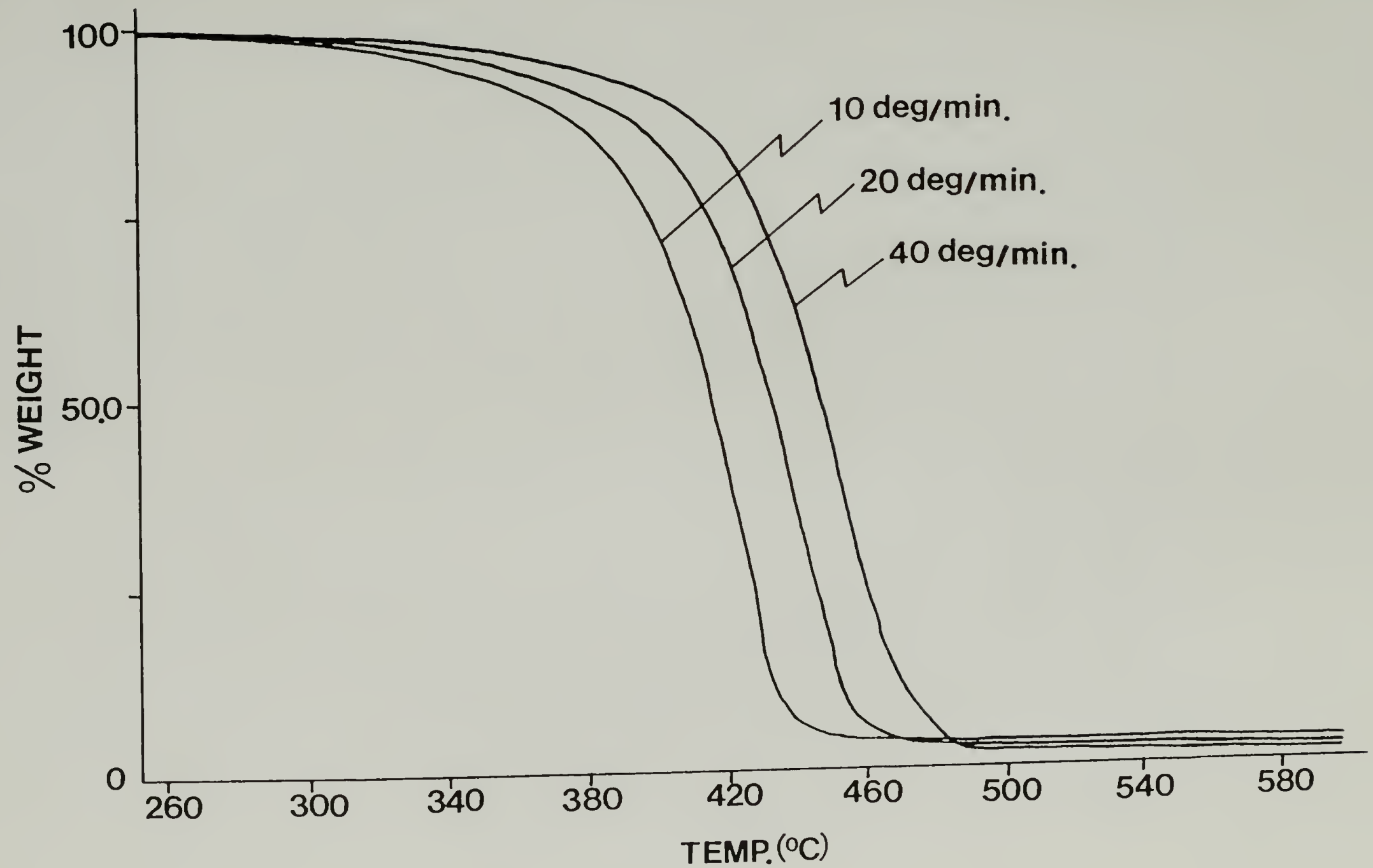

Figure 2.9 TGA curves of the P-CO copolymer made by catalyst **4** under different heating rates as indicated at curves.

where β is the heating rate, T is the corresponding absolute temperature, and R is the gas constant. If the logβ vs. T^{-1} plot is linear, then the slope gives the overall activation energy E of thermal degradation at this conversion. The TGA results of the P-CO copolymer are consistent with a unique activation energy of 29 kcal/mol (121 kJ/mol) independent of conversion. This suggests that P-CO copolymer thermolyzes by one dominant mechanism.

There was a few weight percent of carbonanceous residue remained after thermolysis above 500 °C. The amount of this residue was less at higher heating rate. Apparently it takes time for cyclization and aromatization to occur. In contrast the thermolysis of E-CO copolymer exhibits an increase of activation energy with conversion. The level of carbonaceous residues was much higher for the E-CO copolymer[16] than the P-CO copolymer. The increase of crosslinking, aromatization and charring with conversion could result in the observed increase of TG activation energy.

2.3.3 Chelate Ring Size Effect of Bisphosphine Ligands

A series of catalysts were prepared with bisphosphine ligands containing n number of methylene groups between the phosphine atoms. The value of n lies between two and six, the

resulting chelate ring contains n + 3 atoms (Figure 2.1). They were used to catalyze copolymerizations under identical conditions . The results are summarized in Table 2.2. The regioregularity of the copolymer is taken as the percentage of head-tail sequence. Catalysts **5** and **6** exhibited low to negligible activities. Catalyst **2** has modest activity, and catalyst **3** along with catalyst **4** has high activity for the series of catalyst in Table 2.2. But the polymerization catalyzed by both **2** and **3** were regiochemically random. The products contain only 50 to 58% H-T units, no DSC melting endotherm, and very low glass transition temperature T_g. Catalyst **5** is the most regiospecific in this group but suffers from very low activity. The catalyst in Table 2.2, which has the best balance in activity as well as regio- and stereo-selectivity is compound **4**. It produce semicrystalline P-CO copolymer with the high regioregularity of 79% H-T structure. The melting transition temperature of such copolymer is around 145 ^{o}C by DSC.

Non-chelated catalyst **7**, with monophosphine ligand, is without merit as ligand for Pd in olefin-CO copolymerizations. The combination of diacetopalladium (II), triphenylphosphine (TPP), Bronsted acid in methanol produced predominantly methyl propionate.[3] $[Pd(TPP)_n(CH_3CN)_{4-n}](BF_4)_2$ in CH_2Cl_2 catalyzes E-CO copolymerization with low activity, but only produced oligomers[2b] with degrees of polymerization of 1-5 in

Table 2.2 P-CO copolymerization by catalysts having different chelate ring sizes at 50 °C.

Catalyst	No.	Ring Size	A×10^{-4} (g/mol Pd•h)	T_g (°C)	Regioreg. (H-T %)
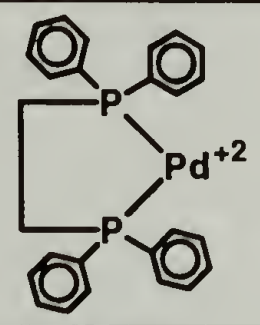	**2**	5	0.21	-11	58 %
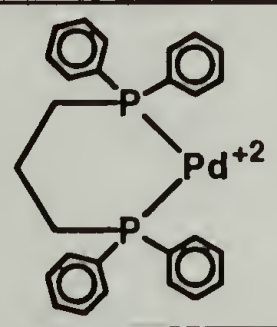	**3**	6	5.2	-8	55 %
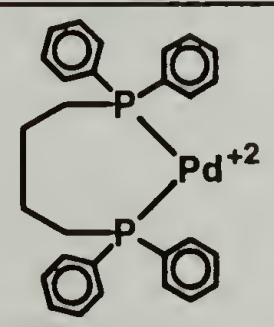	**4**	7	4.8	21	79 %
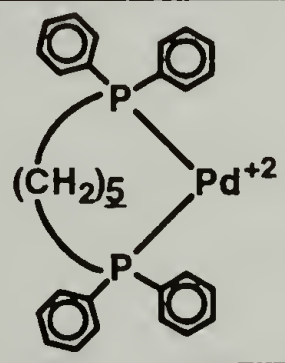	**5**	8	0.07	---	90 %
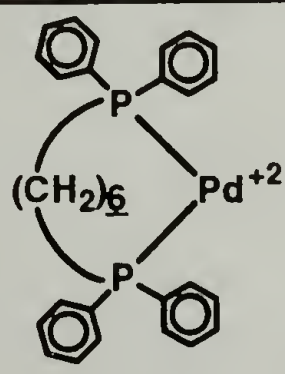	**6**	9 ?	0.01	---	---

the presence of methanol or ethanol. When we copolymerized P-CO under the conditions of $[(TPP)_nPd] = 0.13$ mmol/L without methanol in 1,2-dichloroethane at 50 °C for 24 hours, the oligomers formed exhibit extremely complicated ^{13}C-NMR spectrum (Figure 2.10). The peaks situated between 126-136 ppm are due to TPP without or with Pd. The five resonances from 206 to 216 ppm indicate random regiochemical propylene insertions. Comparison of Figure 2.2 and 2.10 shows the complicity of the latter so that only generic assignments may be proposed. The peaks found in the region 106-118 and 146-160 ppm are due to olefinic carbons of the end groups:

$CH_2=C(CH_3)$-CO-, CH_3-CH=CH-CO-, CH_2=CH-CH_2-CO-

which resulted from primary insertion, secondary insertion, and 1,3-misinsertion,[17] respectively, followed by β-H elimination. If these insertions were followed by protonolysis, they will contribute toward the aliphatic carbon region of 11-15 ppm. The two peaks at about 180 ppm probably arise from -C(O)-OR end groups. There still remain many vinyl and aliphatic carbon resonances with the number greater than it can be accounted for by the above considerations. One explanation can be consecutive propylene insertion. For

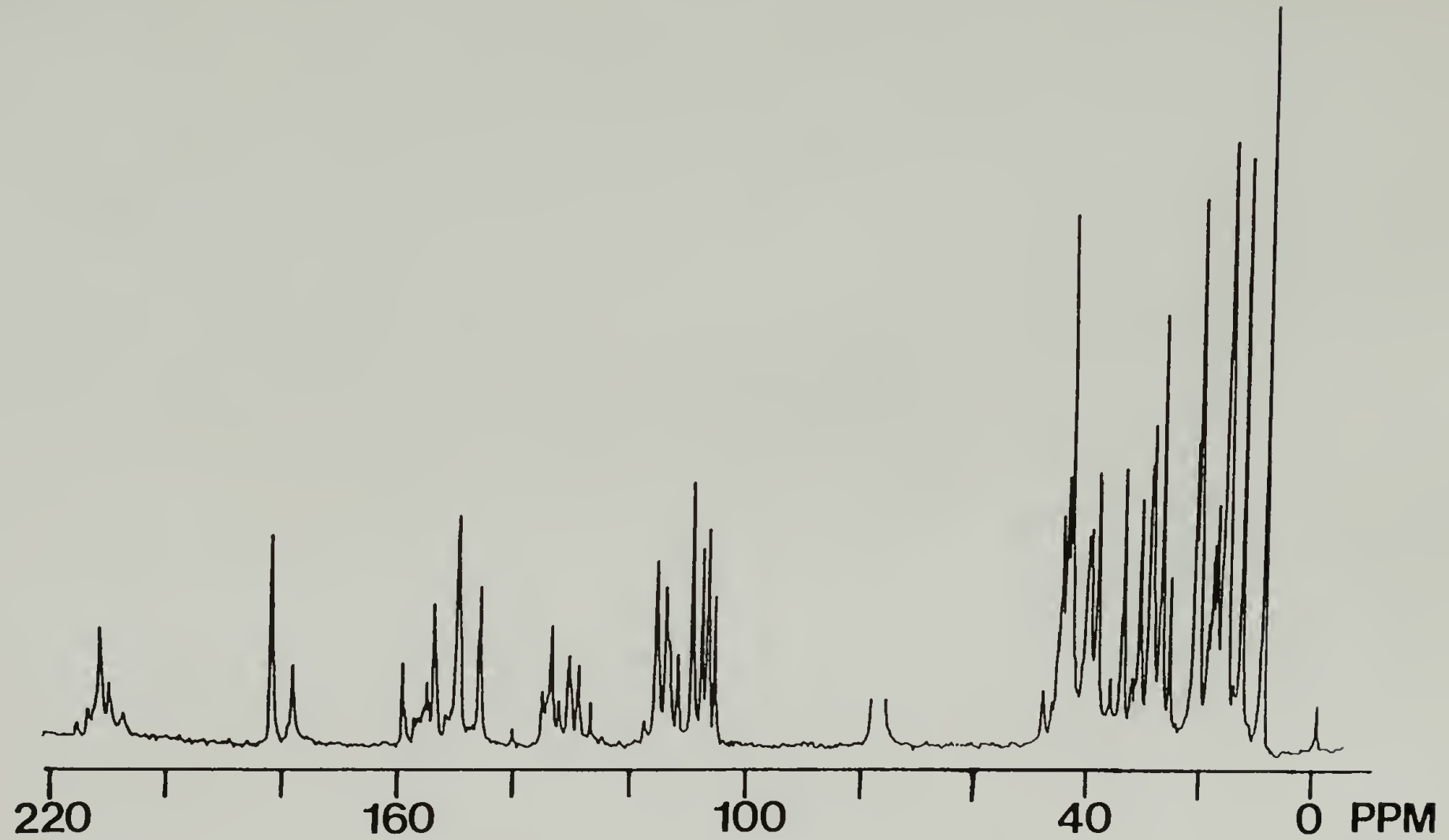

Figure 2.10 ^{13}C-NMR spectrum of the oligomers produced by catalyst **7**.

instance, the insertion of two propylene followed by β-H elimination can produce CH_2=C(CH_3)-CH_2-CH(CH_3)-CO- and CH_2=C(CH_3)-CH(CH_3)-CH_2-CO-, the former by two primary insertions and the latter by a secondary then primary insertion. Taking into consideration of the other possible permutations for consecutive propylene insertion and chain termination processes, the complicated spectrum of Figure 2.10 can be rationalized.

2.3.4 Regio- and Stereo-Control of Catalysts

There are two approaches to improve the regioregularity of the copolymers. First we try to fine tune the structure of aromatic substituted ligands. The catalysts are **3, 4** and **8-11** in Table 2.3. ^{13}C-NMR spectra were used to analyze the regioregularity of the copolymer. Catalysts **3**, **8**, and **9** have none, one and two methyl substituents on the phenyl group, and so do catalysts **4**, **10**, and **11**. The former complexes are trimethylene bisphosphines whereas the latter are tetramethylene analogs. Table 2.3 shows that there are systematic changes in catalytic activity, and the number average molecular weight as well as the regioregularity of the copolymer formed. These properties decrease in the order **3** > **8** > **9** and also **4** > **10** > **11**. The catalysts with

Table 2.3 P-CO copolymerization by aromatic substituted catalysts.

Ligand	Cat. No.	A×10^{-4} (g/mol Pd•h)	M_n	Regioreg. (% H-T)
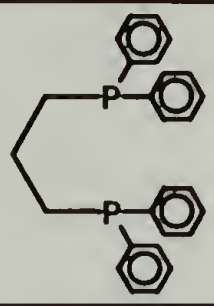	**3**	1.5	17,200	56%
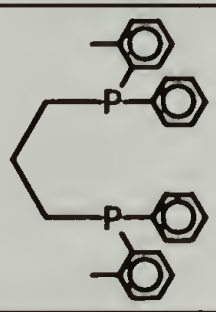	**8**	0.3	13,100	52%
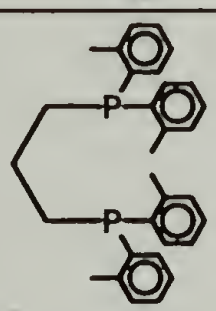	**9**	0.13	4,000	50%
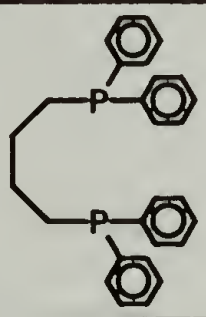	**4**	2.2	11,400	79%
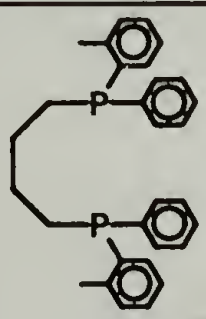	**10**	0.52	9,700	77%
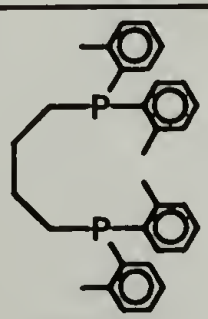	**11**	0.39	4,700	68%

tetramethylene bisphosphine ligands in general perform better in propylene and CO copolymerization than the trimethylene derivatives: **4** > **3**, **10** > **8**, and **11** > **9**. Two effects could be influencing the catalysis: steric or electronic. The former is deemed more significant.

The decrease of M_n and of catalyst activity with increasing number of methyl substituents is consistent with a steric effect. The former indicates the effect of lowering of k_p/k_{tr} ratio, where k_p is the rate constant for propagation and k_{tr} is the rate constant for chain transfer. The dominant mechanism for the latter process is the β-hydride elimination, the transition state of which would require coplanar arrangement for the Pd, C_α, C_β and H_β atoms. This steric demand may be thwarted by the methyl substituent on the phenyl ring of phosphine to decrease k_{tr}. The observed M_n decrease could be attributed to the reduction of k_p by steric hindrance on olefin coordination or insertion.

The *decrease* of regiospecificity with the increase of methyl substituents on the phosphine phenyl ring is counter intuitive, i.e. the more sterically hindered catalyst has less regioselectivity. It will be shown below that electron donation actually increases the regioselectivity of a catalyst. We have performed extensive molecular mechanics calculations on steric energies for stereochemical and regiochemical

selectivities[18,19] of the bisphosphine Pd catalysts and zirconocenium catalysts. This was performed for two systems in Table 2.3. The steric energy for primary propylene insertion in catalyst **4** is 1.0 kcal/mol less than the steric energy for secondary insertion; this is the regiocontrol energy in favor of primary addition. Similarly, catalyst **11** also favors the 1,2-insertion of propylene. However, the regiocontrol energy is 1.5 kcal/mol. These calculations support the expectation but is contrary to observation.

The molecular mechanics calculation employs an initial molecular geometry based on its X-ray crystal structure or of a closely similar analog. This is then optimized for the olefin π-complex and for the transition state[18-21]. It has been found to be generally true that the computed stereo- or regio-preference agrees better with the catalytic selectivities at low polymerization temperature (T_p). In the case of zirconocenium intermediates this is about -60 °C.[22] Raising T_p can cause marked loss in selectivities if the catalyst structure is not sufficiently rigid. We may postulate that dynamic conformational changes occur in the present catalysts as well. The phenyl ring can rotate. One result of such rotation is that the methyl group on it at certain position can inhibit the 1,2-insertion to favor the 2,1-process. Therefore, in average, the

regio-selectivity of the catalyst decreases upon the addition of methyl group on phenyl ring.

Another approach to improve the regioregularity is to alter the ligands' electronic environment by inserting an alkyl group such as methylene group between phosphorus atom and phenyl ring. Table 2.4 shows the regioselectivities of the partially alkyl substituted catalyst **12** and **13** comparing to that of completely aromatic substituted catalyst **4**, **3** and **14**. Catalyst **12** and **13** with the addition of methylene group improve the regioregularity of the copolymers to about 95%. Since this approach works, we further made the ligands more basic by using all alkyl substituent on the phosphorus atoms. The regio- and stereo-selectivity results of the completely alkyl substituted catalyst **14**-**17** comparing to that of completely aromatic substituted catalyst **18**, and **4** are shown in Table 2.5. The stereoregularity is defined by the percentage of the isotactic triad (*mm*). The completely alkyl substituted catalyst **14**, **17**[23], **16**[24] and **15** are 100% regioselective.

The fact that the regioselectivities of catalysts increase in the order of **3, 4** < **13** < **15**, **16** suggests the electronic factor playing a big role in regioregularity control. The alkyl groups in catalyst **13**, **15** and **16** donate electrons via the phosphorous atoms to the catalytic center. Taft[25] suggested a method of separating polar and steric effect in ester

Table 2.4 Comparison of catalysts with partially alkyl substituted ligands to those with completely aromatic substituted ligands.

Ligand	Cat. No.	A×10^{-4} (g/mol Pd•h)	Regioreg. (H-T %)	Stereoreg. (*mm* triad %)
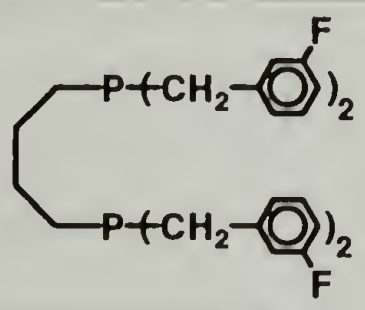	**12**	0.73	> 95 %	30 %
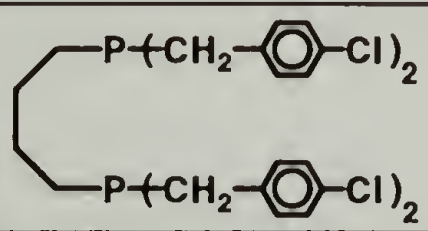	**13**	0.05	> 95 %	34 %
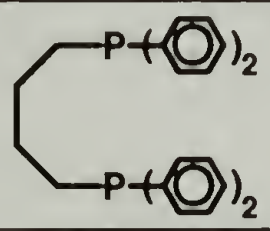	**4**	4.8	79 %	56 %
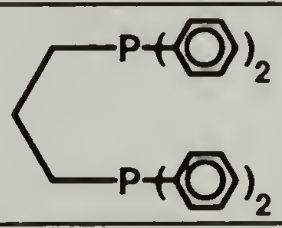	**3**	5.2	58 %	48 %
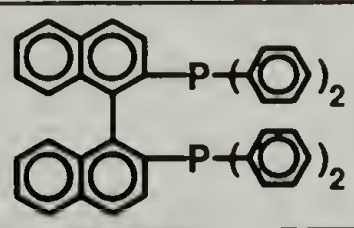	**14**	1.3	61 %	49 %

Table 2.5 Comparison of catalysts with completely alkyl substituted ligands to those with completely aromatic substituted ligands.

Ligand	Cat. No.	Regioreg. (H-T %)	Stereoreg. (*mm* triad %)
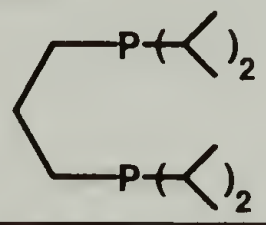	**15**	100 %	48 %
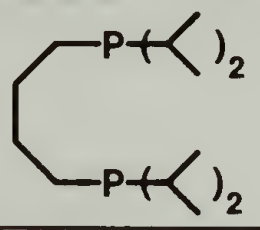	**16**	100 %	65 %
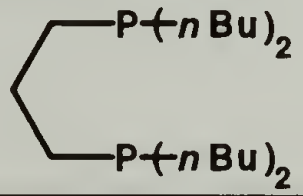	**17**	100 %	---
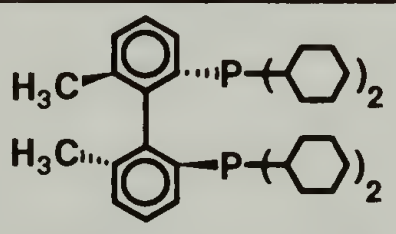	**18**	100 %	80-90 %
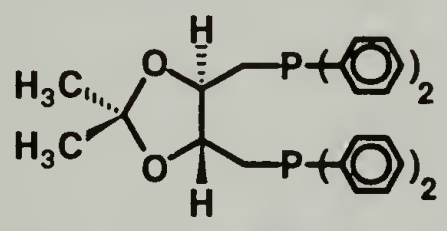	**19**	79 %	55 %
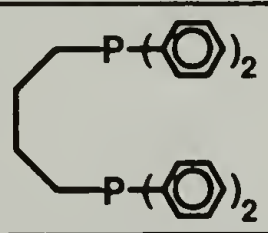	**4**	79 %	56 %

hydrolysis. Similar to the Hammett's σ, he defined the σ* value which represents only polar effect of the substituent group with the electron releasing one having smaller value. The σ*s are 0.60, 0.215, and -0.19 for phenyl, benzyl and isopropyl groups respectively[26]. Therefore the electron donating ability increase in the order of

$$-C_6H_5 < -CH_2C_6H_5 < -CH(CH_3)_2$$

Furthermore, molecular mechanics calculation showed that the steric energies of primary insertion are 0.1 and 1.0 kcal/mol favored over secondary insertion for catalyst **16** and **4**, respectively. The fact that less steric-hindered catalyst **16** has better regio-selectivity confirms that it is the electron releasing of the substituent group on phosphorus atom that improves the regio-selectivity. Electronic factor dominates over steric factor in the regiochemical control of the P-CO alternating copolymerization.

It has been shown above that the chelate ring size of the catalyst plays an important role in both regio- and stereo-control, and the optimal catalyst was found to have the 7-membered ring. Since the 6-membered ring catalyst **15** produces 100% regio-selectivity[23] with low stereo-selectivity, we think the 7-membered ring analog **16** can exhibit better

stereoselectivity. The ligand **16** was synthesized according to the published method.[27] The ^{13}C-NMR spectrum of carbonyl carbon region of P-CO copolymer obtained by catalyst **16** at 50 ^{o}C is shown in Figure 2.11. The missing of peaks at 207-209 and 214-216 ppm proves the polymer is completely regioregular. The peaks around 211-213 ppm refer to the different stereoconfiguration of the head-tail sequence of P-CO copolymer, and the major peak centered at 212.4 ppm is corresponding to the *mm* triad meso configuration. The integration of peak areas gives the *mm* triad content of 62%. We integrated the same ^{13}CNMR peaks for copolymer made by catalyst **15** (the spectrum was taken from reference 23) which gave the *mm* triad content of 48%. The stereo-regularity (*mm* triad percentage) increases about 15% by using 7-membered ring catalyst **16** over the 6-membered ring catalyst **15**. To further improve the stereo-selectivity, chiral ligand is desired. Catalyst **19** does not have better stereo-selectivity than catalyst **4** even though catalyst **19** is chiral. The reason for this is that the chiral center of catalyst **19** may be too far removed from the catalytic center to be effective. Batistini[23] used optical active catalyst **18** to synthesize a rather high stereo-regular P-CO copolymer (88% *mm* triad). There are two major characteristics for this catalyst. First, the chiral center is located very closely to the catalytic center. Second, more

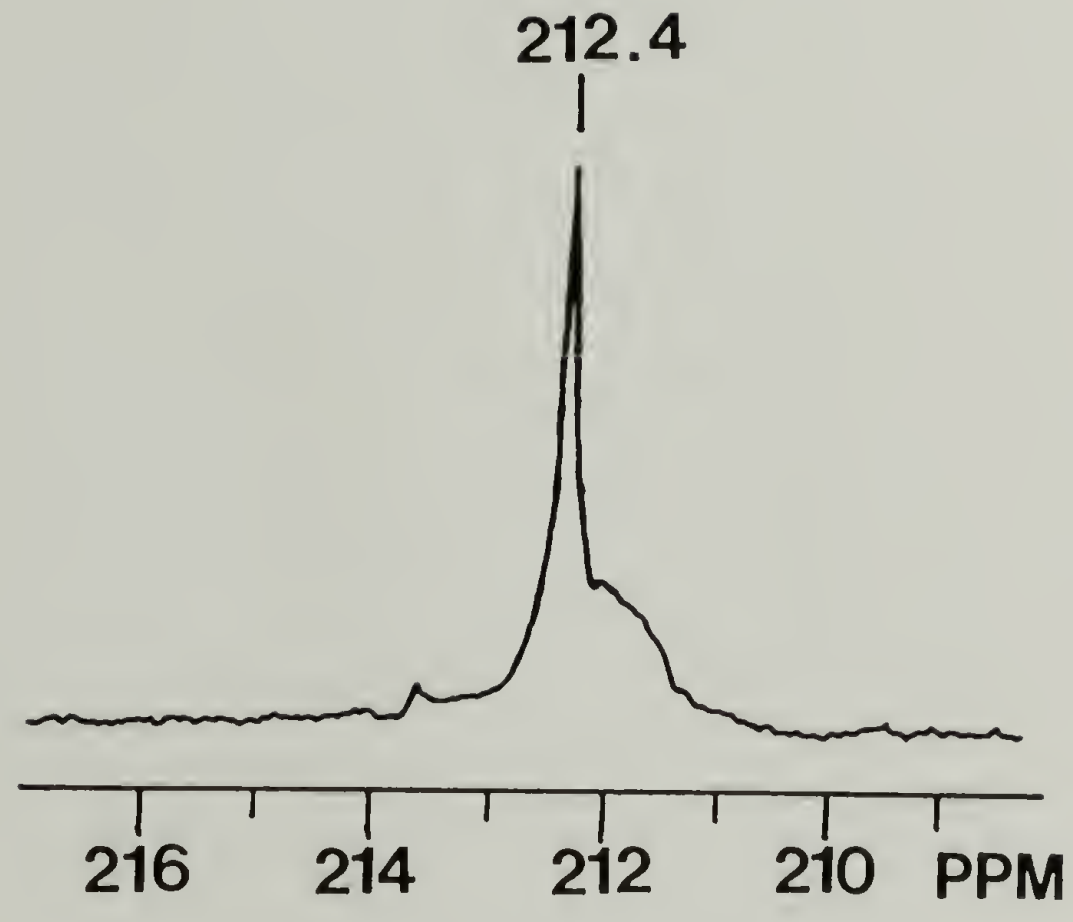

Figure 2.11 ^{13}C-NMR spectrum of carbonyl carbon region of P-CO copolymer obtained by catalyst **16** at 50 °C.

electron releasing cyclohexyl substituent (comparing to phenyl ring) is used.

Overall, alternating copolymers of P-CO with various properties and morphologies were produced by the control of regio- and stereo-regularities which were achieved by using different bisphosphine/palladium catalysts.

References

(1) Reppe, W.; Magin, A. *U.S. Pat.* 2,577,208, **1951**.

(2) a) Sen, A.; Lai, T. W. *J. Am. Chem. Soc.* **1982**, *104*, 3520. b) Lai, T. W.; Sen, A. *Organometallics* **1984**, *3*, 866. c) Sen, A. *CHEMTECH* **1986**, 48. d) Jiang, Z.; Sen, A. *Macromolecules* **1992**, *25*, 880. e) Sen, A.; Jiang, Z.; Chen, J. T. *Macromolecules* **1989**, *20*, 2012. f) Sen, A. *Adv. Polym. Sci.* **1986**, *73/74*, 125.

(3) Drent, E.; van Brockhoven, J. A. M.; Doyle, M. J.; *J. Organomet. Chem.* **1991**, *417*, 235.

(4) a) Fonton, D. M. *U.S. Pat.* 3,530,109, **1970**. b) Nozaki, K. *U.S. Pat.* 3,689,460, **1972**. c) Nozaki, K. *U.S. Pat.* 3,835,123, **1974**.

(5) Zhao, A. X.; Chien, J. C. W. *J. Polym. Sci., Part A: Polym. Chem.* **1992**, *30*, 2735.

(6) Chien, J. C. W.; Zhao, A. X.; Xu, F. Y. *Polym. Bull.* **1992**, *30*, 2735.

(7) Batistini, A.; Consiglio, G.; Suter, U. W.; *PMSE Preprint (Prroceeding of the ACS Division of Polymeric Materials Science and Engineering)* **1992**, *67*, 104.

(8) Jiang, Z.; Dahlen, G. M.; Houseknecht, K.; Sen, A. *Macromolecules* **1992**, *25*, 2999.

(9) Perrin, D. D.; Armarego, W. L. F.; Perrin, D. R. *Purification of Laboratory Chemicals* New York: Pergamon Press, **1980**.

(10) a) Flory, P. J. *J. Am. Chem. Soc.* **1967**, *89*, 1798. b) Park, H. G. *J. Polym. Sci., Part C* **1968**, *16*, 3455. c) Shepherd, L.; Chen, T. K.; Harwood, H. J. *Polym Bull.* **1979**, *1*, 445. d) Suter, U. W.; Neuenschwander, P. *Macromolecules* **1981**, *14*, 528. e) Dworak, A.; Freeman, W. J.; Harwood, H. J. *Polym. J. (Tokyo)* **1985**, *17*, 351.

(11) Ruland, W. *Acta Cryst.* **1961**, *14*, 1180.

(12) Yomamoto, A. *Organotransition Metal Chemistry* New York: John Wiley & Sons, **1986**.

(13) Breitmaier, E.; Voelter, W. *Carbon-13 NMR Spectroscopy* New York: VCH **1987**.

(14) Oguni, N.; Shinohara, S.; Lee, K. *Polym. J. (Tokyo)* **1979**, *11*, 755.

(15) Flynn, J. H. in *Aspect of Degradation and Stabilization of Polymers*, Jellinek, H. H. G. Ed., New York: Elsevier Scientific Publishing Co. **1978**.

(16) Chien, J. C. W.; Zhao, A. X. *Polym. Degrad. Stab.* **1993**, *40*, 257.

(17) a) Soga, K.; Shiono, T.; Takemura, S.; Kaminsky, W. *Makromol. Chem., Rapid Commun.* **1987**, *8*, 305. b) Grassi, A.; Zambelli, A.; Resconi, L.; Albizzati, E.; Mazzochi, R. *Macromolecules* **1988**, *21*, 617. c) Cheng, H. N.; Ewen, J. A.; *Makromol. Chem.* **1989**, *190*, 1931. d) Rieger, B.; Mu, X.; Mallin, D. T.; Rausch, M. D.; Chien, J. C. W. *Macromolecules* **1990**, *23*, 3559.

(18) Xu, F. Y.; Zhao, A. X. and Chien, J. C. W. *Makromol. Chem.* **1993**, *194*, 2579.

(19) Yu, Z.; Chien, J.C.W. *J. Am. Chem. Soc.* submitted.

(20) Kawamura-Kuribayashi, H.; Koga, N.; Morokuma, K. *J. Am. Chem. Soc.* a) **1992**, *114*, 2359. b) **1992**, *114*, 8687.

(21) Castonguay, L. A.; Rappe, A. K. *J. Am. Chem. Soc.* **1992**, 114, 5832.

(22) a) Rieger, B.; Mu, X.; Mallin, D. T.; Rausch, M. D.; Chien, J. C. W. *Macromolecules* **1990**, *23*, 3559. b) Chien, J. C. W.; Tsai, W-M.; Rausch, M. D. *J. Am. Chem. Soc.* **1991**, *113*, 8570. c) Tsai, W-M.; Rausch, M. D.; Chien, J. C. W. *Appl. Organomet. Chem.* **1993**, *7*, 71. d) Chen, Y.; Rausch, M.D.; Chien, J. C. W. *Macromolecules* submitted. e) Tsai, W.-M.; Chien, J. C. W. *Makromol. Chem. Macromol. Symp.* **1993**, *66*, 141. f) Chen, Y.; Rausch, M. D.; Chien, J. C. W. *J. Am. Chem. Soc.* submitted.

(23) Batistini, A.; Consiglio, G.; Suter, U. W. *Angew. Chem. Int. Ed. Engl.* **1992**, *31*, *No. 3*, 303.

(24) Wong, P. K.; van Doorn, J. A.; Drent, E.; Sudmeijer, O.; Stil, H. A. *Ind. Eng. Chem. Res.* **1993**, *32*, 645.

(25) Taft, R. W. in *Steric Effects in Organic Chemistry*, Ed., Newman, M. S. New York: Wiley **1956**.

(26) Shorter, J. *Correlation Analysis of Organic Reactivity*, New York: Research Studies Press, **1982**.

(27) Tani, K.; Tanigawa, E.; Tatsuno, Y.; and Otsuka, S. *J. Organomet. Chem.* **1985**, *279*, 87.

CHAPTER 3

MECHANISM OF THE COPOLYMERIZATION

3.1 Introduction

Ethylene (E) and carbon monoxide (CO) have long been copolymerized by radical initiators.[1] The product is a random copolymer with usually low carbon monoxide content. Shell scientists discovered that group VIII transition element phosphine complexes catalyze strictly alternating E-CO copolymerization to form the poly(ethylene ketone);[2] this catalysis has been extended to P-CO copolymerization.[3-9] With propylene issues other than alternating and nonalternating arose. There are regiochemical modes of insertion, i.e., primary (1,2) versus secondary (2,1); the stereochemistry of added olefin could be *meso* versus *racemic* placement, and P-CO unit can be incorporated as the ketone or spiroketal isomeric structures. ^{31}P-NMR is used to elucidate how the structure of the bisphosphine ligand influences the alternation tendency, regiochemical preference, and stereochemical control of propylene incorporation in the P-CO copolymerization.

Mechanism of E-CO alternating copolymerization have been investigated previously.[10,11] This mechanism may be varied for the P-CO copolymerization. Gas chromatography/ mass spectrometry (GC-MS) of P-CO oligomers leads to the understanding of the chain initiation, propagation, and termination processes of the P-CO copolymerization.

3.2 Experimental

Oligomers were gas chromatographed on DB-5 30 m × 0.21 mm i. d. capillary column with 0.11 μm film of poly(methylphenylsiloxane). The eluent was analyzed with a Hewlett-Packard 5970N mass selected detector. Both ^{31}P-NMR and ^{13}C-NMR were recorded on a Varian XL-300 spectrometer using $CDCl_3$ as solvent. The chemical shift of 85% H_3PO_4 was taken as reference (0 ppm) for all ^{31}P-NMR spectra. Molecular mechanics calculation was carried out on Macintosh *fx* using CAChe Reactivity Modeling Software.

3.3 Results and Discussion

P-CO oligomers were synthesized at 85 °C by using catalyst **4**. They were analyzed by means of GC-MS. The total ion chromatogram of the oligomers is shown in Figure 3.1.

Figure 3.1 The total ion chromatogram of the oligomers produced by catalyst **4** from GC-MS analysis.

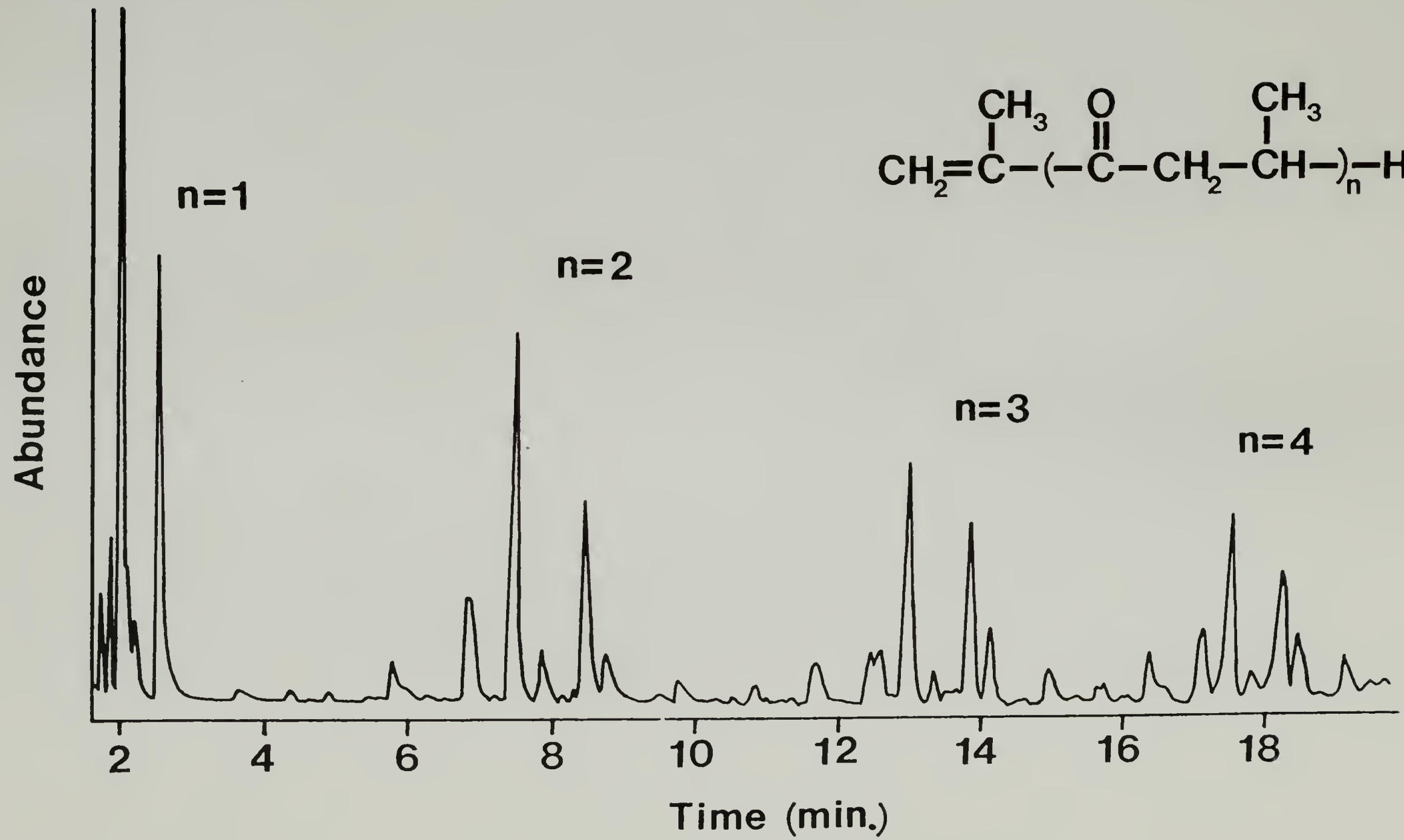
n=1
n=2
n=3
n=4
Abundance
2
4
6
8
10
12
14
16
18
Time (min.)

CH3
O
CH3
CH2=C–(–C–CH2–CH–)n–H

According to their mass spectra, the oligomers have the general structure C_3H_5-(-COC_3H_6-)-$_n$H with n = 1 to 4. The gas chromatograph curve for the n = 1 portion is shown in Figure 3.2. The peaks a, c, e and f all have M^+/z = 112 as shown in Figure 3.3-3.6; they are assigned to the four regioisomeric structures in Figure 3.7 by both their boiling points[12] which are associated with the order of elution and their mass spectra (Table 3.1).

In structures c and f (Figure 3.7) the first propylene was incorporated by primary insertion; it was secondary insertion in the cases of a and e. Based on the relative intensities of (peak c + peak f)/(peak a + peak e), the primary (1,2) insertion is approximately 7.4 times more probable than the secondary (2,1) insertion. After the initial primary propylene insertion and CO incorporation, the next propylene was inserted by either primary or secondary process to produce compound c or f (Figure 3.7), respectively. The intensity ratio peak c/peak f is only 1.2 which is much smaller than the differences of 7.4-fold between the primary and secondary insertions of the first propylene unit. The structures c and f prior to the occurrence of termination by β-H elimination are c' and f ' as shown in Figure 3.8.

The insertion of CO should be much faster with c' than f' according to both steric and electronic considerations. In

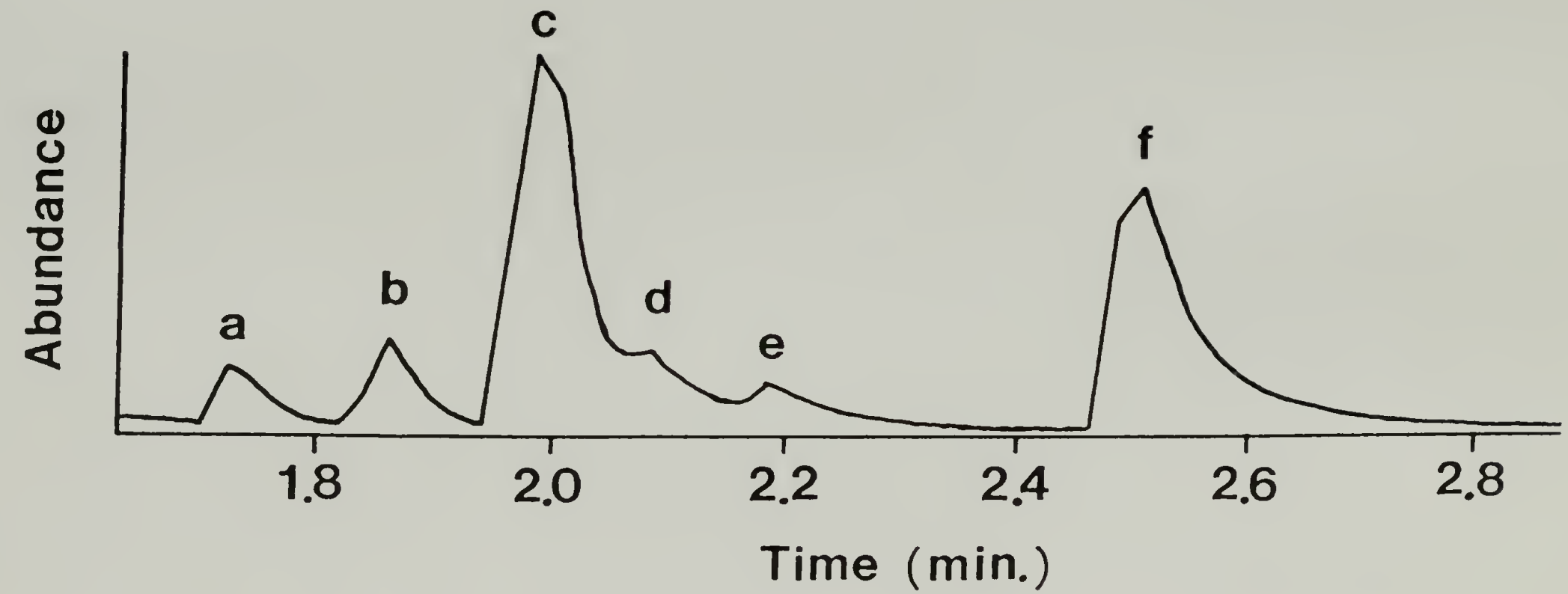

Figure 3.2 Gas chromatography curve of the $n=1$ portion of Figure 3.1.

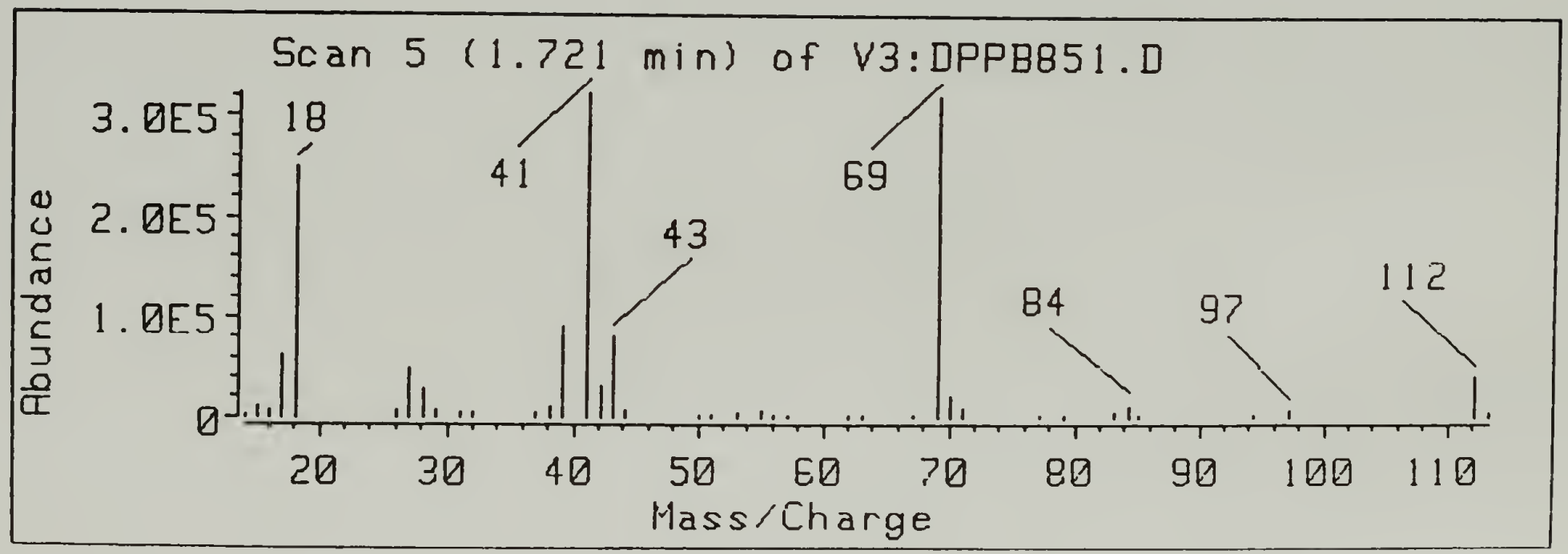

Figure 3.3 Mass spectrum of peak a in Figure 3.2.

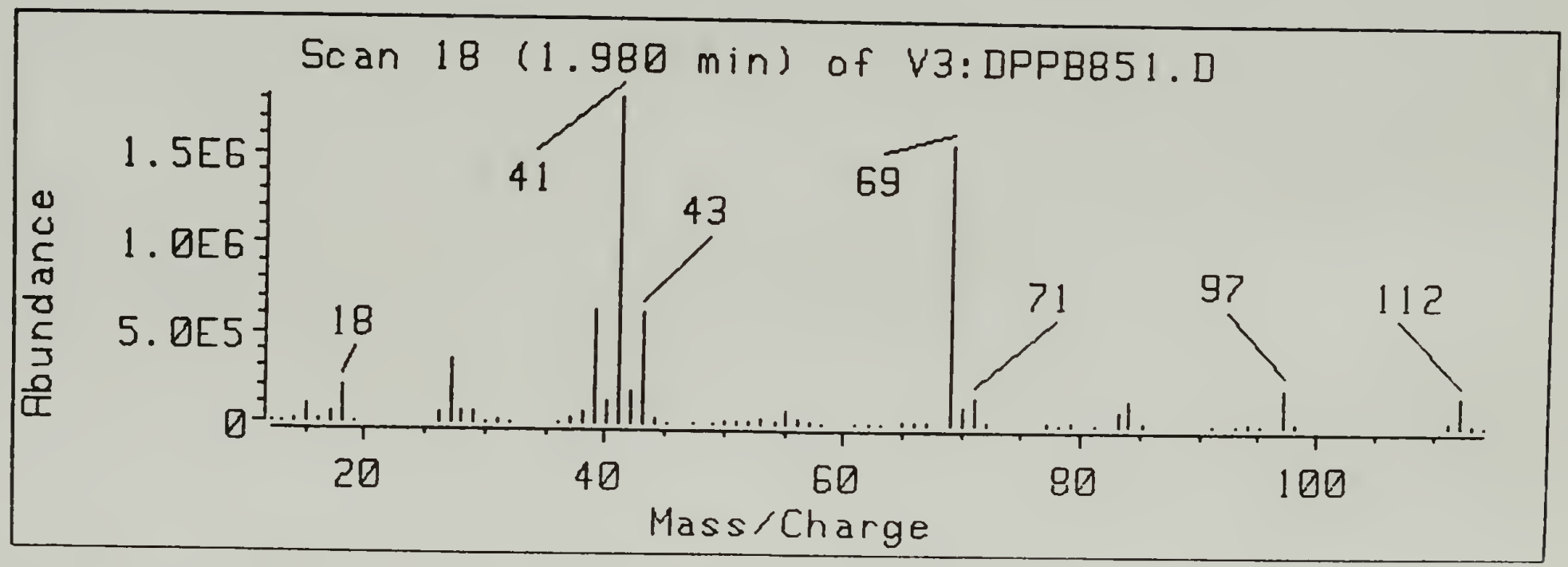

Figure 3.4 Mass spectrum of peak c in Figure 3.2.

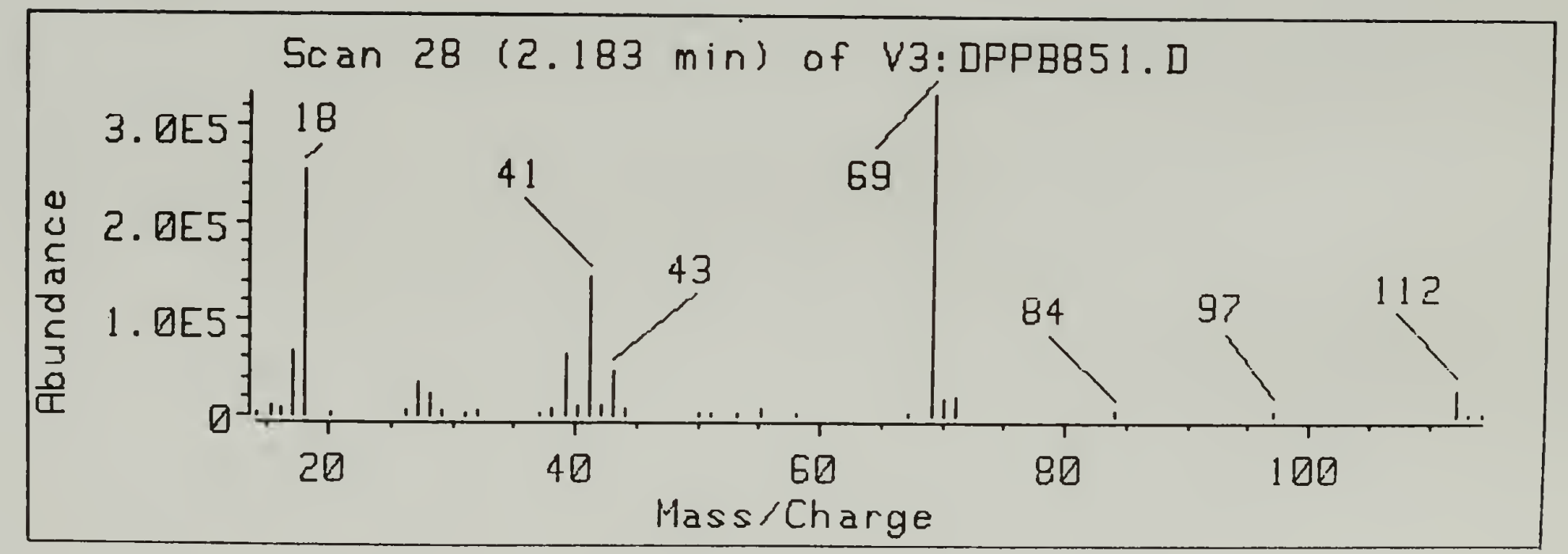

Figure 3.5 Mass spectrum of peak e in Figure 3.2.

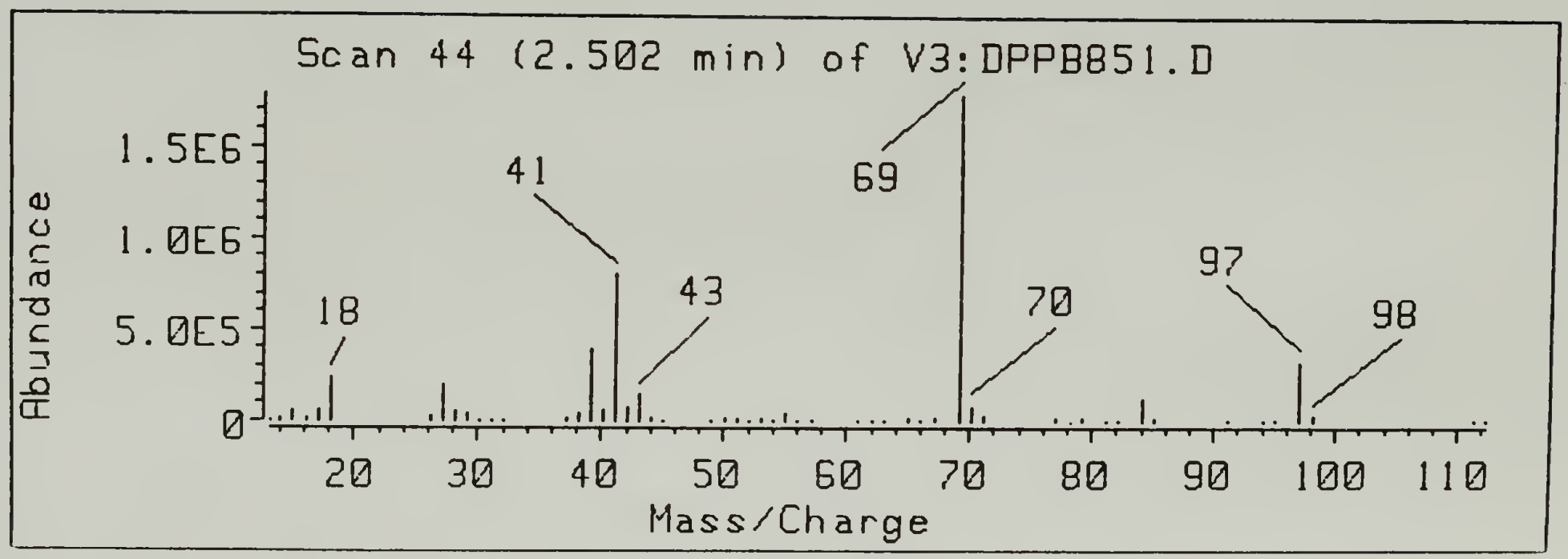

Figure 3.6 Mass spectrum of peak f in Figure 3.2.

a 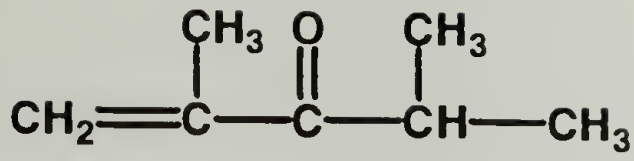

c 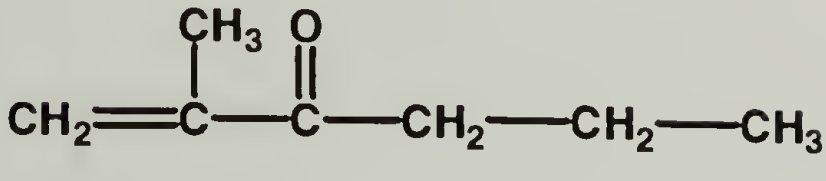

e 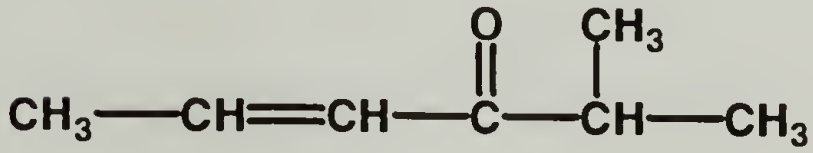

f 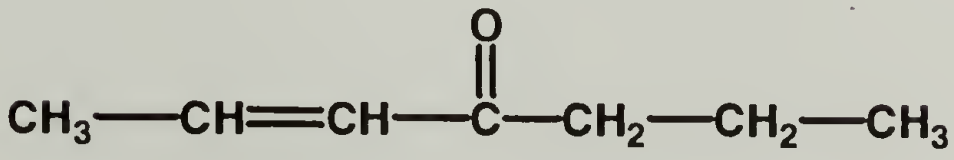

Figure 3.7 Four regioisomeric structures corresponding to the peak a, c, e and f in Figure 3.2.

Table 3.1 Boiling points and relative abundance of mass spectra peaks for peak a, c, e and f in Figure 3.2.

Peak in Figure 3.2	Relative abundance $M^+/z = 41$	Relative abundance $M^+/z = 69$	Boiling point (b.p.) pressure in torr
a	100%	99%	$(52\ ^oC)_{38}$
c	100%	86%	$(140\text{-}141\ ^oC)_{760}$
e	43%	100%	$(147\text{-}148.5\ ^oC)_{739}$
f	44%	100%	$(156\text{-}162\ ^oC)_{740}$

c'

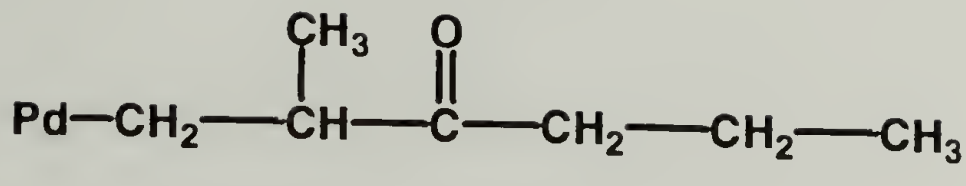

f'

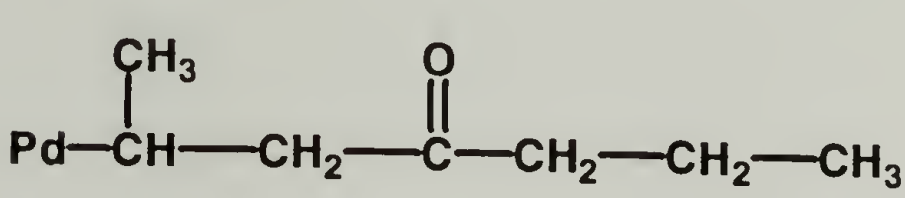

Figure 3.8 Structure c' and f '.

other words the more probable formation of c' than f' is not reflected in a greater yield of c than f because c' is also more favored for a subsequent monomer insertion, where f' undergoes β-H elimination. To test this hypothesis we performed oligomerization by catalyst **4** at 105 °C to produce even shorter chains of mainly n = 1 (see Figure 3.1). The resulting GC-MS (Figure 3.9) has a value of 7.6 for the intensity ratio peak c/peak f. Therefore, primary insertion was also favored in the insertion of the second molecule of propylene. So in general the primary insertion is favored about seven times over the secondary insertion for the polymerization catalyzed by catalyst **4**.

Figure 3.10 shows the gas chromatography curve of the n = 2 portion in Figure 3.1. The compound with methoxycarbonyl terminus is initiated by the Pd-OCH_3 moiety which was produced by the reaction between methanol and the bisphosphine-Pd complex. Its propenyl end group is the result of β-H elimination. Once Pd-H species is thus produced, most of the subsequent chains were initiated by it and terminated by the process regenerating it. This is supported by the large excess of C_3H_5-C(O)-C_3H_6-C(O)-C_3H_7 over C_3H_7-C(O)-C_3H_6-C(O)-C_3H_7.

The simplified propagation steps in the present copolymerization can be written as:

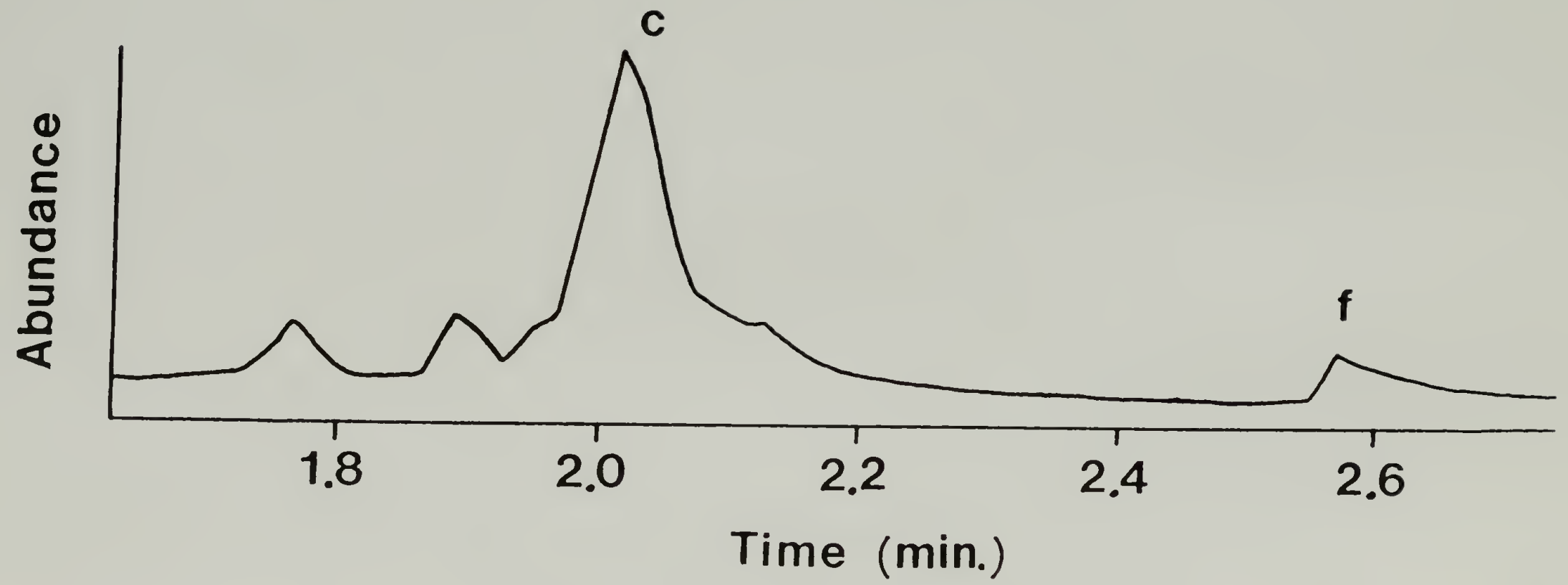

Figure 3.9 The total ion chromatogram of the oligomers produced by catalyst **4** at 105 °C from GC-MS analysis.

Figure 3.10 Gas chromatography curve of the $n = 2$ portion of Figure 3.1.

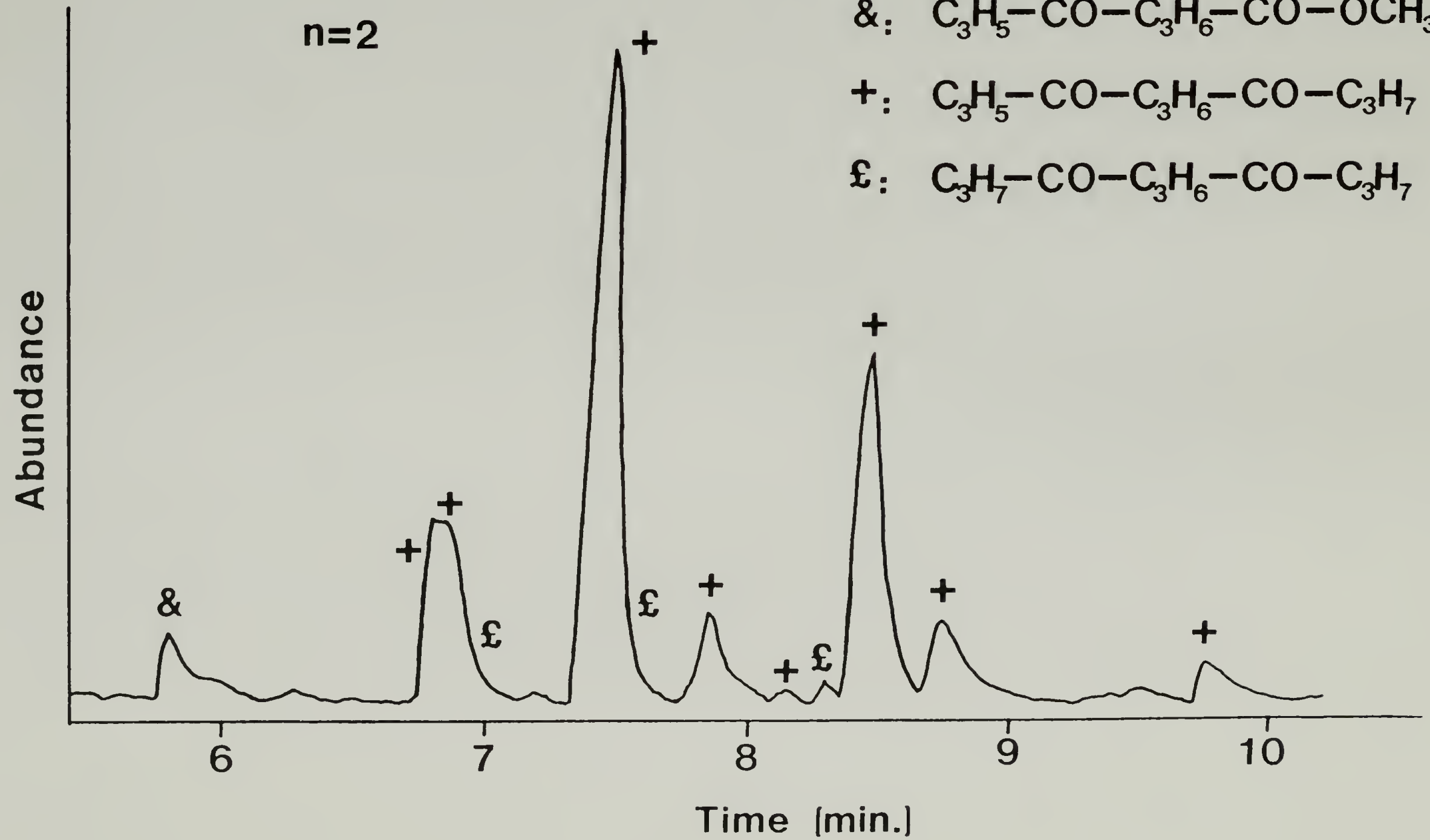
n=2
&: $C_3H_5-CO-C_3H_6-CO-OCH_3$
+: $C_3H_5-CO-C_3H_6-CO-C_3H_7$
£: $C_3H_7-CO-C_3H_6-CO-C_3H_7$
Abundance
Time [min.]
6
7
8
9
10

Pd-R	+	Olefin	----->	Pd-R'		k_{11}
Pd-R	+	CO	----->	Pd-CO-R		k_{12}
Pd-COR	+	CO	----->	Pd-CO-COR		k_{22}
Pd-COR	+	Olefin	----->	Pd-R'		k_{21}

The process is strictly alternating when $k_{11} = k_{22} = 0$. Lai and Sen[13] proposed that the strong tendency toward alternation is due to the greater affinity of Pd for CO than olefin and a greater inherent rate for CO to insert into transition metal bonds when compared to the corresponding insertion of olefin. Therefore, in the absence of CO, catalyst **7** catalyzes rapid dimerization of ethylene into 1-butene, but only alternating copolymerization occurs in the presence of CO. The rate of CO insertion is thought to be extremely fast and $k_{12} >> k_{21}$ because the products arising from a competing β-H abstraction were not observed.[13] This is also true for the copolymerization of propylene and CO. However, consecutive propylene insertions were observed when simple triphenyl-phosphine is the ligand for Pd (*vide infra*). Furthermore, β-H abstraction is the dominant chain termination process in the P-CO copolymerization because of the labile tertiary hydrogen on the β-carbon atom. In contrast, chain transfer involving methanol competes favorably with the elimination of the secondary β-hydrogen in the case of E-CO copolymerization.

In transition metal catalyzed carbonylation reaction, enediolates and other products were identified which could arise from the insertion of CO into a metal-acyl bond.[14] The occurrence of this process is also suggested in the Cp_2ZrCl_2/methylaluminoxane/ethylene polymerization mixture containing radioactive ^{14}CO.[15] However, these reactions are mechanistically very different from the migratory chain insertions. A model compound for the latter process, $PdCOCOPh(Cl)(TPP)_2$, suffers spontaneous decarbonylation at 25 °C which was independent of CO pressure up to 4.82×10^6 Pa.[16]

The chain initiation and termination events can be identified if the end groups are known. We have previously detailed the possible processes[11] as shown in Figure 3.11. GC-MS analysis of the oligomers of this study showed that our P-CO copolymerizations are mostly initiated by Pd-H; initiation by Pd-OCH_3 is far less frequent. Chain termination is mainly via β-H elimination (process 7 in Figure 3.11) and a small fraction by protonolysis (process 6 in Figure 3.11). Two possible mechanisms can be accounted for the chain propagation step. First is the conventional mechanism with monomer forming complex with catalyst, then the migration taking place (Figure 3.12). The second mechanism involves dynamic ring opening which may significantly enhance the

Initiation, head terminus

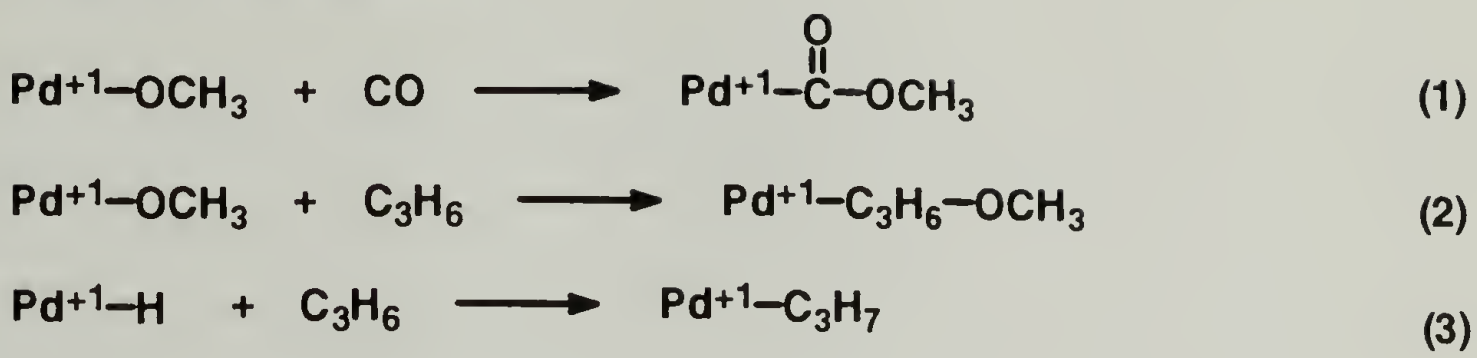

Termination, tail terminus

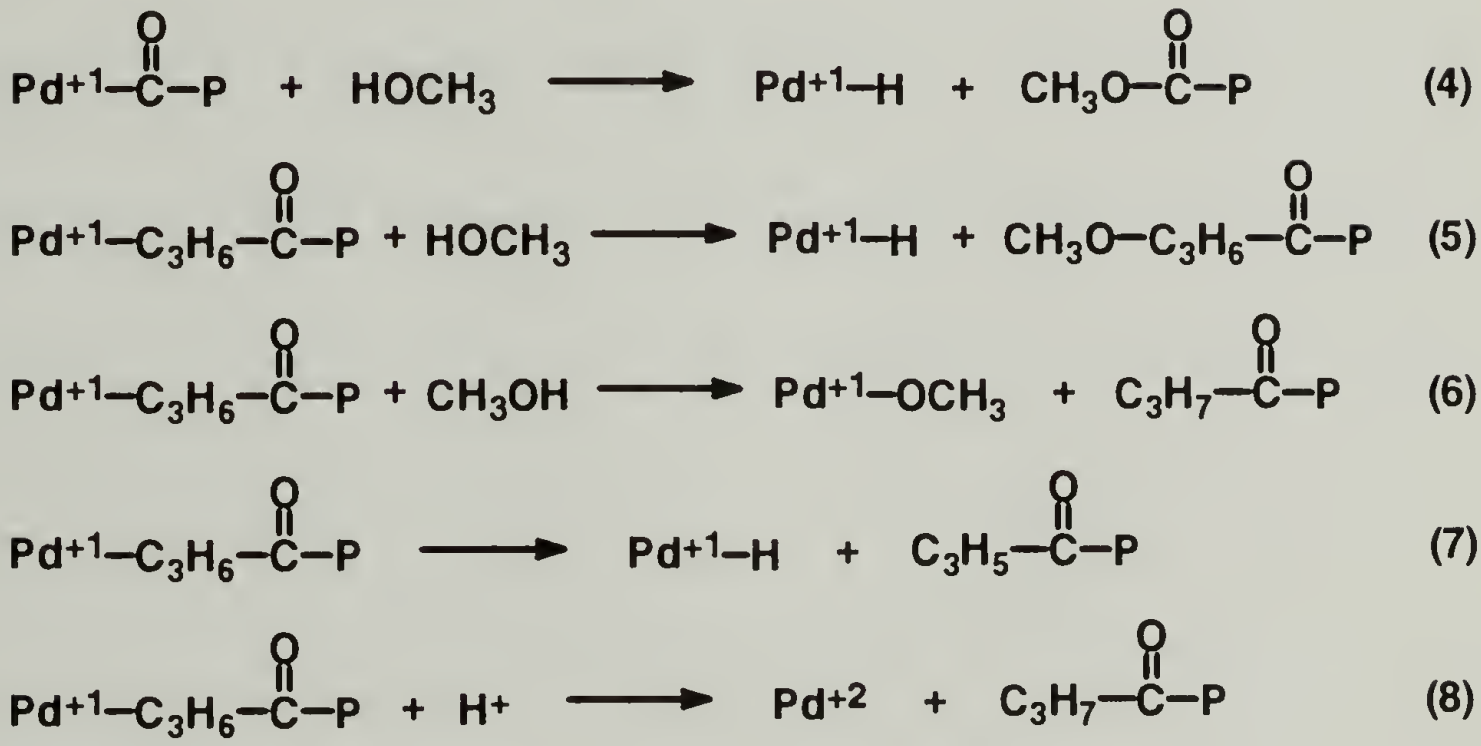

Figure 3.11 Initiation and termination processes of P-CO copolymerization.

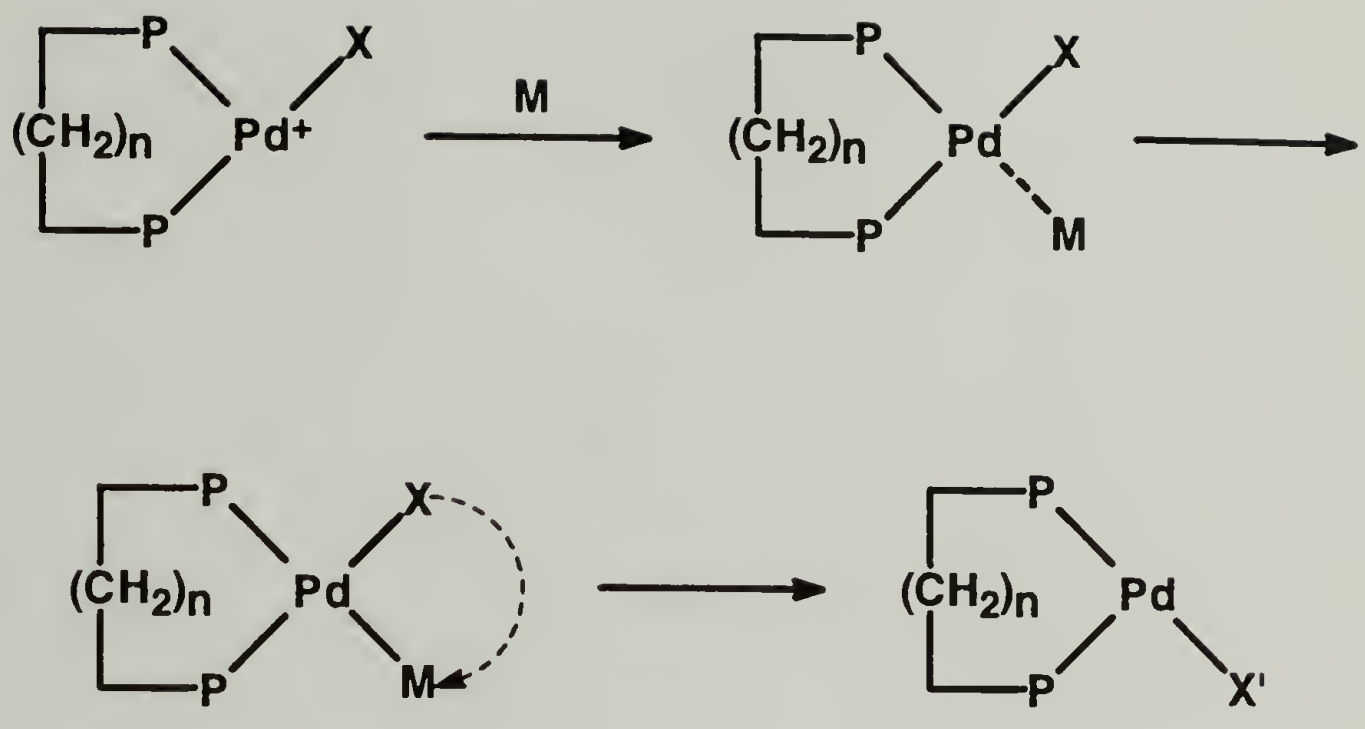

Figure 3.12 Insertion mechanism for the propagation step of P-CO copolymerization.

insertion rates[8,17] as proposed in Figure 3.13. The possible existence of dynamic ring opening was detected by ^{31}P-NMR method (*vide infra*).

To gain further understanding about the mechanism of P-CO copolymerization, ^{31}P-NMR studies of how the structure of the bisphosphine ligand influencing the alternation tendency, regiochemical preference, and stereochemical control of propylene insertion in the P-CO copolymerization were carried out.

Catalyst **4** produced semi-crystalline P-CO alternating copolymer, the ^{13}C-NMR spectrum of which is given in Figure 3.14a. The copolymer obtained with catalyst **4** has a regioregularity of 79%. In contrast the P-CO copolymer produced by catalyst **2** and **3** have regioregularities of only 58% and 55%; these catalysts are nearly non-regioselective.

The product of P-CO copolymerization formed by the TTP catalyst **7** exhibits very complicated ^{13}C-NMR spectra (Figure 3.14b). Even though complete analysis of the spectrum is not presently feasible, the following conclusion are possible. The copolymerization products are low molecular weight oligomers which are not only regiorandom, but also nonalternating. Figure 3.14c shows the ^{13}C-NMR spectrum of the copolymer made by catalyst **5**. The carbonyl carbon peaks, dominated by the ones around 211-213 ppm indicates high regioregularity

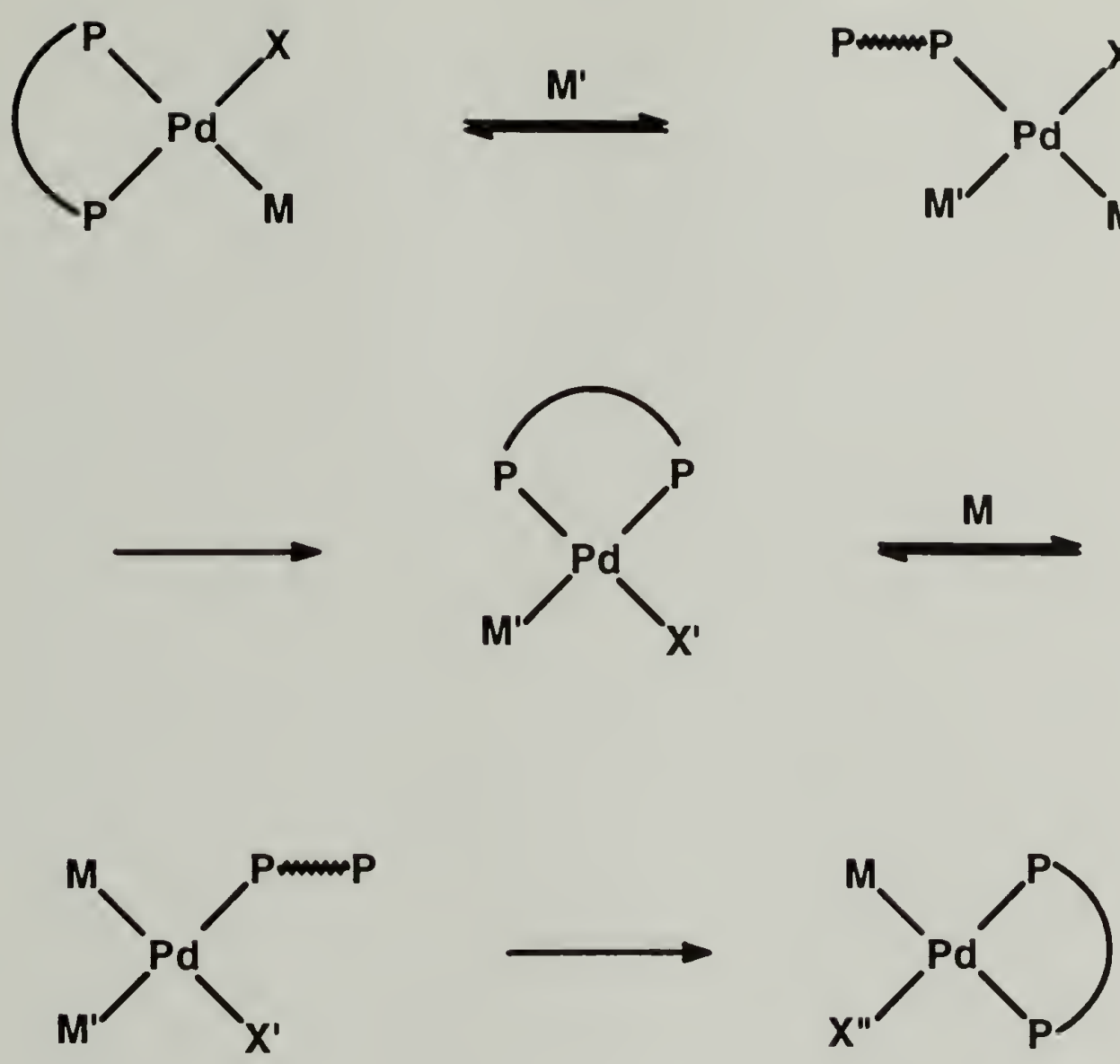

Figure 3.13 Dynamic ring opening mechanism for the propagation step of P-CO copolymerization.

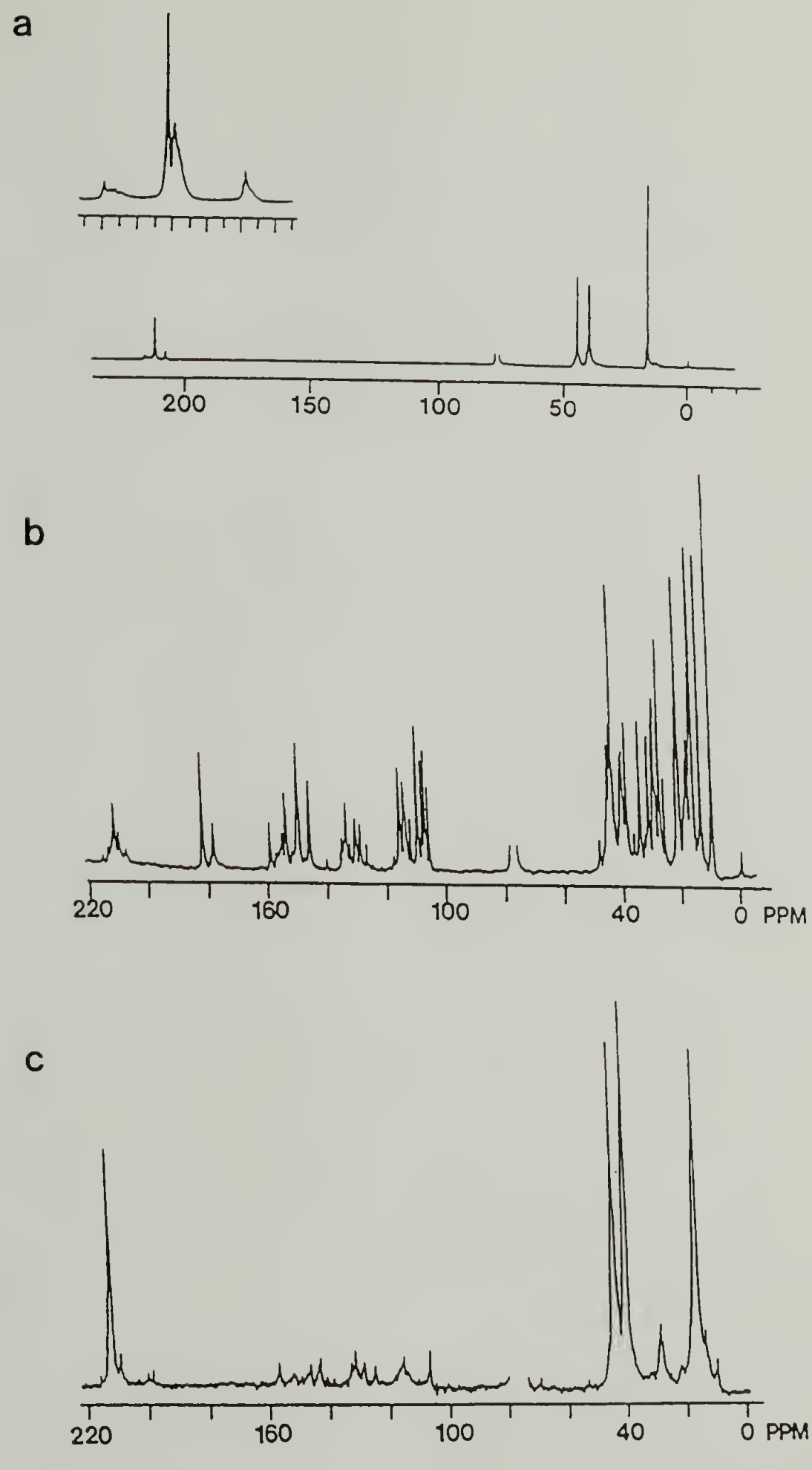

Figure 3.14 ^{13}C-NMR spectra of P-CO copolymers by (a) catalyst **4**, (b) catalyst **7**, and (c) catalyst **5**.

(~90%). However there are also present complicated peaks in the region 100-160 ppm in the ^{13}C-NMR spectrum similar to those generated by monophosphine catalyst **7**.

The above results suggested a definite relationship between the structure of the phosphine ligands in the Pd complex and the microstructure of the polymerization product. Monodente phosphine Pd complex has neither regioselectivity nor chemical control for alternating copolymerization. The catalysts with two and three methylenes bridging the aromatic phosphine moiety are strongly alternating in comonomer incorporation but has only low regioselectivity. Catalyst **4** is the most regiospecific member of this series, and it is strongly alternating in comonomer incorporation as well. On the other hand catalyst **5** produces both regioregular alternating copolymer and non-alternating oligomers.

The ^{31}P-NMR spectra of catalyst **7**, **4** and **5** are shown in Figure 3.15. Catalyst **7** contains two resonances at 34.0 and 22.8 ppm. According to the literature,[18] the low field resonance is assigned to the *trans* structure and the high field peak to the *cis* structure. The two complexes inter-convert slowly at ambient temperature. The value of the equilibrium constant at room temperature is calculated to be $K \approx 0.06$ from the integrated ^{31}P-NMR intensities. The *trans* structure

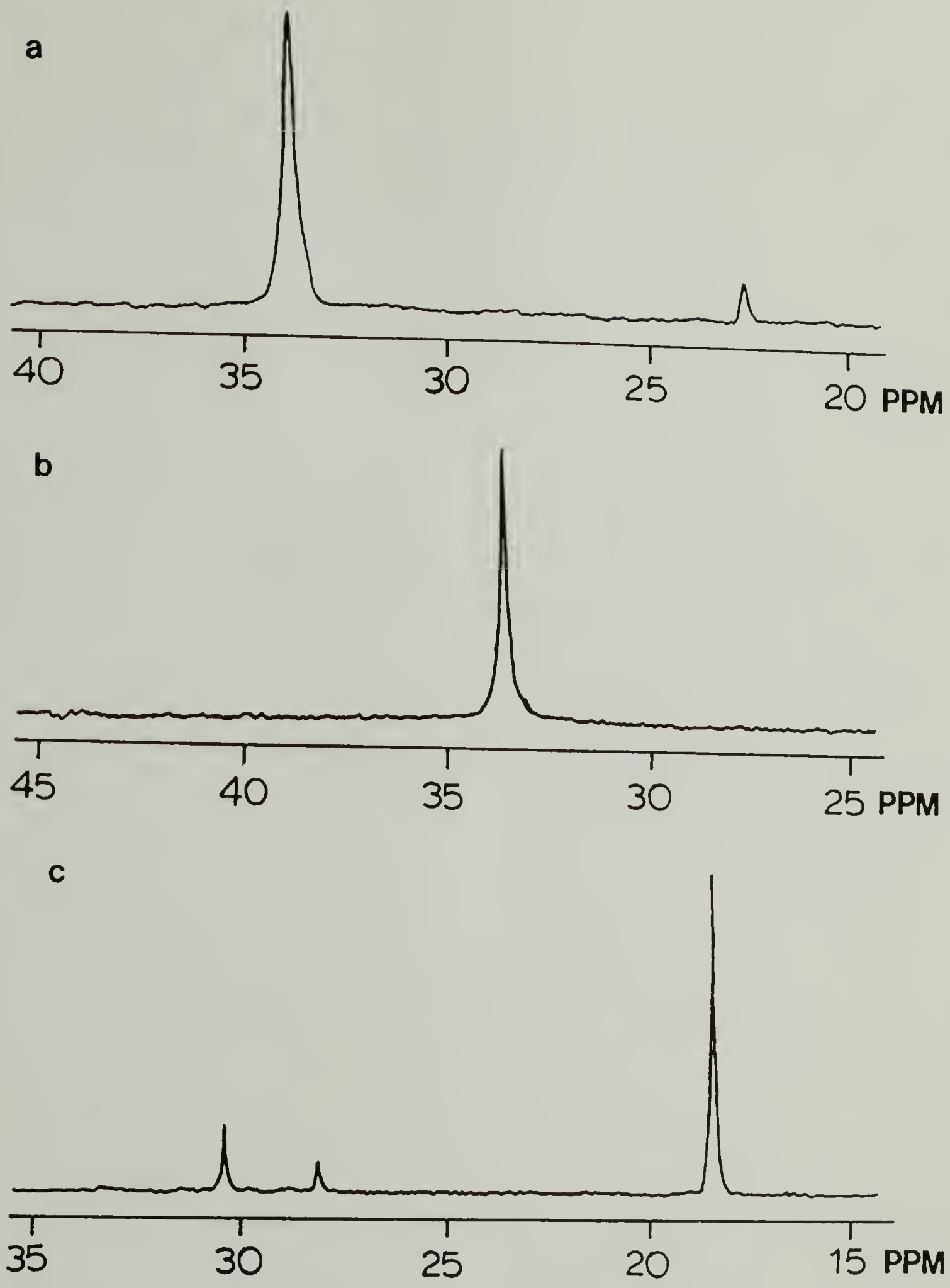

Figure 3.15 ^{31}P-NMR spectra of (a) catalyst **7**, (b) catalyst **4**, and (c) catalyst **5**.

is favored over the *cis* structure by 16-fold due to the *trans*-effect of the TPP ligand.

Catalyst **2**, **3** and **4** all have single ^{31}P resonance at 75.2, 16.0 and 33.7 ppm, respectively. X-ray diffraction of $[(Ph_2P(CH_2)_3PPh_2)Pd](NCS)_2$ showed it to have the *cis* six-membered ring structure.[19] Therefore, catalyst **3** may be assumed to have a *cis* chelated structure with a six member ring as well. Mono- and bidente coordinated bisphosphines have very different ^{31}P-NMR chemical shifts; the values for the present ligands are summarized in Table 3.2. In this table δF is the chemical shift of the free phosphine not complexed to Pd, and δp is the corresponding chemical shift of phosphine complexed to Pd. The difference, $\Delta = \delta p - \delta F$, is the coordination chemical shift. In addition, the ^{31}P-NMR chemical shift of a ligand is different in a chelated ring versus non-chelated analogue.[20] The difference has been referred to as the "ring contribution" (Δ_R). Shaw[21] et al. pointed out that there exists a good linear correlation between the chemical shift of a free tertiary phosphine and the coordination chemical shift, $\Delta = \alpha \bullet \delta F + \beta$. This relationship was used to predict the chemical shift of non-chelated phosphine complexes. However, the relationship was found to be invalid for a number of chelated phosphine complexes[20,22,23] including the catalysts **2**-**5** here. The δp values are directly affected by

Table 3.2 Summary of ^{31}P-NMR chemical shift data.

Cat.	Structure [c]	δp [d]	δF [e]	Δ=δp-δF [f]	$\Delta_R=\Delta-\Delta_{Cat.7}$ [g]
7 [a]	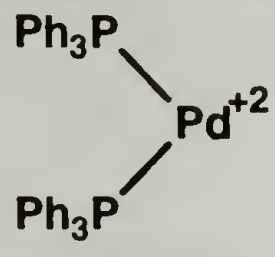	34.0	-4.54	38.5	
2	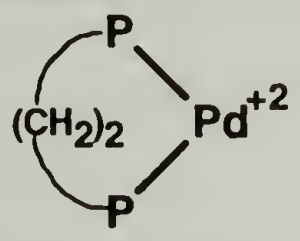	75.2	-13.2	88.4	49.9
3	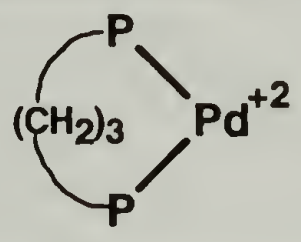	16.0	-16.6	32.6	-5.9
4	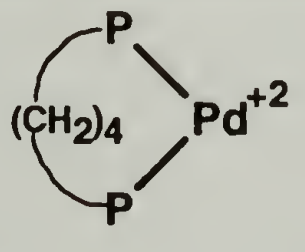	33.7	-15.3	49	10.5
5 [b]	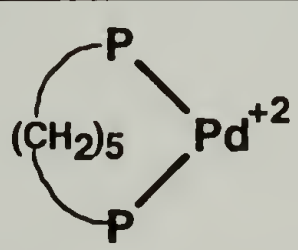	18.5	-15.3	33.8	-4.7

a) Only *cis*-structure is shown here.
b) Only chelated structure is shown here.
c) Two benzene substituents on phosphorus atom are not drawn for catalyst **2**-**5**.
d) Chemical shift of the catalysts in ppm.
e) Chemical shift of the free ligands in ppm.
f) Coordination shift in ppm (see paper text for details).
g) Ring contribution , Δ_R, is the Δ of a chelated catalyst minus the Δ of an equivalent phosphorus in a nonchelated analogue which in this case is catalyst **6**.

the presence of phosphorus in chelate rings of bisphosphine. Garrou[24] and others[22,23,25] suggested that the "ring contribution" is a general phenomenon observed in many complexes; it causes chemical shift to fall outside the range of $\Delta = \alpha \bullet \delta F + \beta$. Our results showed that 5- and 7- membered rings are deshielded comparing to the non-chelated complex, while 6- and 8-membered rings are shielded. Though the theoretical aspects of the Δ_R are not clear,[20] the knowledge of its contribution to the δp value is invaluable when one makes structural assignments in phosphine transition metal complexes.

The ^{31}P-NMR spectrum of catalyst **5** (Figure 3.15) contained three peaks. Catalyst **5** produces both non-alternating oligomers and regioregular alternating copolymer with the later one dominating (Figure 3.14c). This suggests that catalyst **5** is mainly in chelated ring type structure with ^{31}P-NMR peak at 18.5 ppm. The other two resonances are attributed to the non-chelated phosphines.

^{31}P-NMR spectrum of catalyst **4** (Fig. 3.15) shows a single peak at 33.7 ppm corresponding to the *cis* chelating ring structure. However, the great polymerization activity of **4** and regiospecificity over other members of this series suggest the possibility of dynamic opening and closing of chelated ring.[8] The possible dynamic chelation of bisphosphine-Pd complex

has been investigated with ^{31}P-NMR on the model compound **20**,[26] which is obtained by the reaction shown in Figure 3.16. The possible dynamic ring opening process is illustrated in Figure 3.17. Figure 3.18 displays the ^{31}P-NMR spectra of complex **20** and unreacted catalyst **4** at various temperature. Three peaks are observed at low temperature. The phosphorus atoms of unreacted catalyst **4** still resonated at 33.7 ppm. Two phosphorus atoms of complex **20** resonated at 22.0 and 41.3 ppm at -30 ^{o}C. As the temperature increased, these peaks broadened, and coalesced at 40 ^{o}C. These spectral changes can be explained by the dynamic chemical exchange between the two complexes (Figure 3.17). If this exchange occurs for catalyst **4**, its chelate ring will be inevitably dynamically opened.

The catalysts of this investigation contain phenyl phosphines. In the case of $2Ph_3P{\bullet}Pd^{+2}$, the *trans* structure may be considered to be inactive. Migratory insertion of monomer cannot occur in the *trans* complex. Displacement of a phosphine ligand by a monomer has to occur prior to insertion (Figure 3.19). In this figure and elsewhere M is the monomer CO or C_3H_6 and X is the propagating alkyl or acyl group. Qualitatively, one might expect the order of insertion rate constant to be $k_{p,\mathbf{B}} > k_{p,\mathbf{C}} > k_{p,\mathbf{D}}$, In species **B**, X is labilized by the strong *trans* ligand of either comonomer molecule.

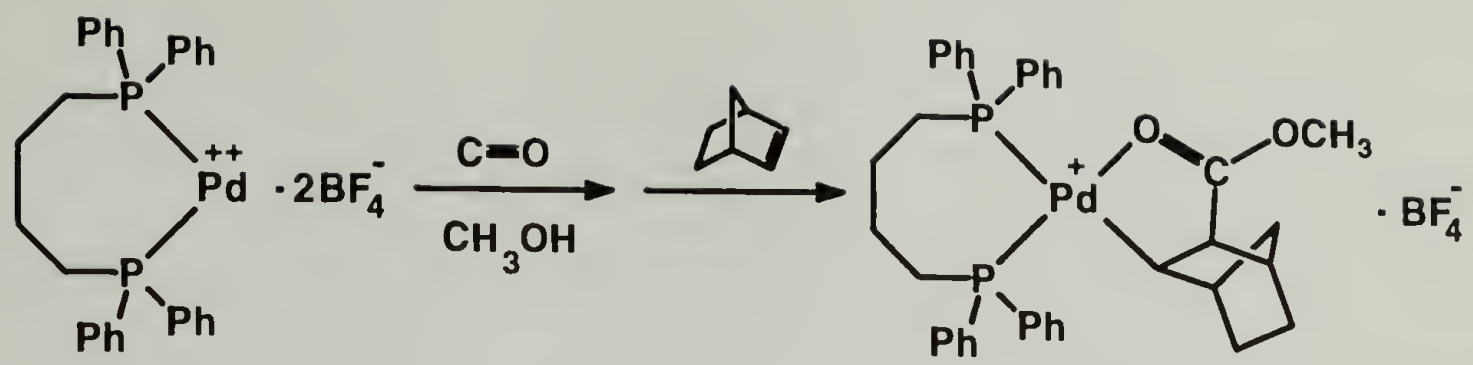

(20)

Figure 3.16 Synthesis route of complex **20**.

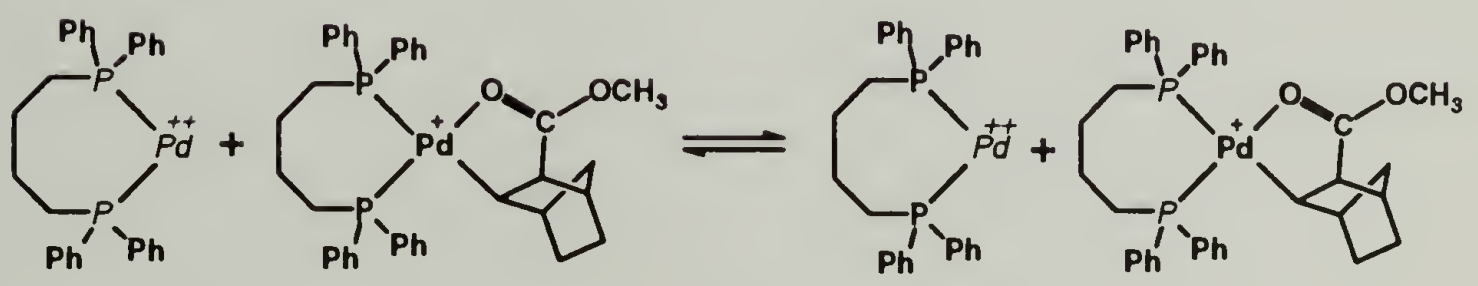

Figure 3.17 Dynamic chemical exchange process.

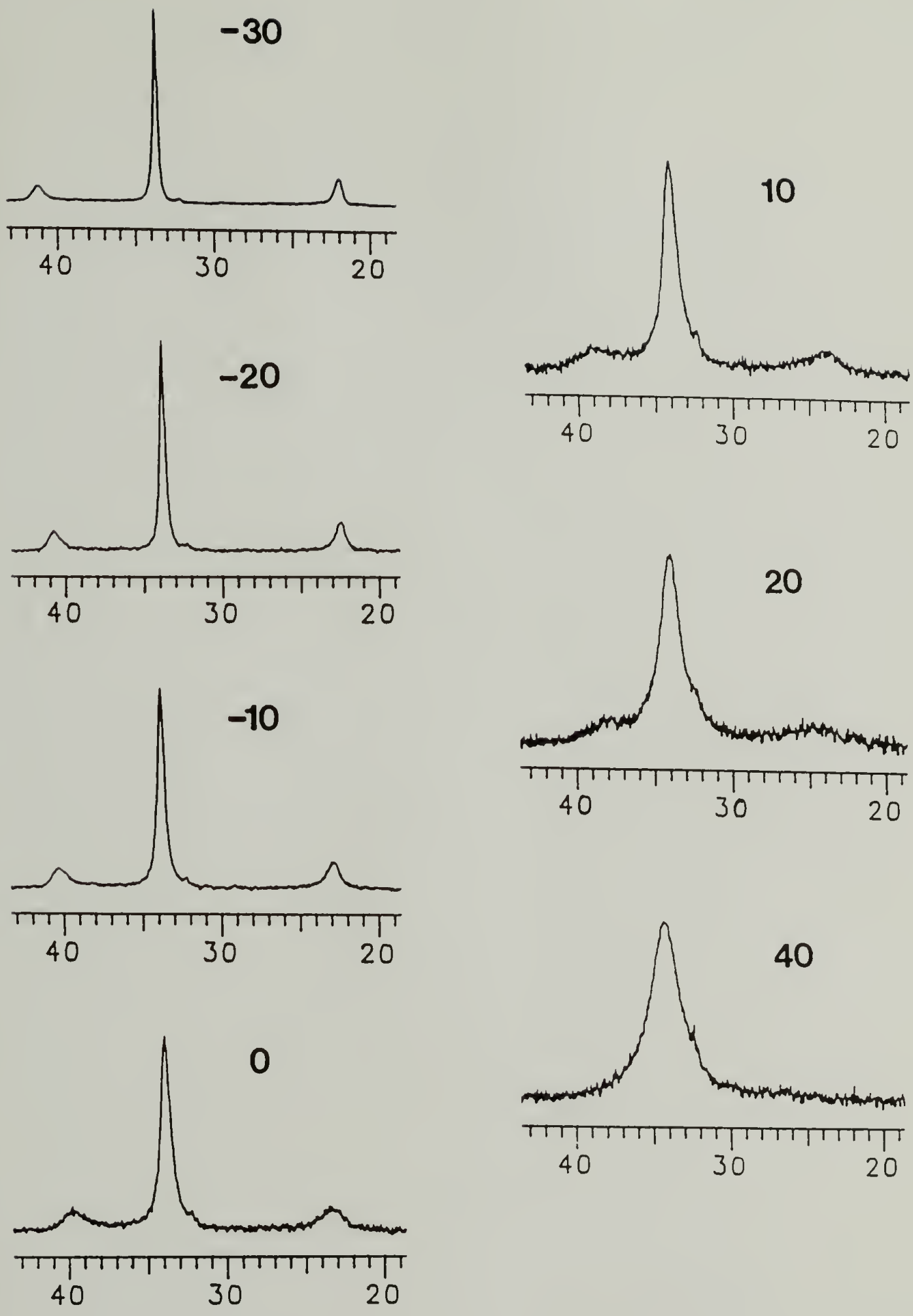

Figure 3.18 VT ^{31}P-NMR spectra of complex **4** and **20** mixture at -30, -20, -10, 0, 10, 20, 40 ^{o}C.

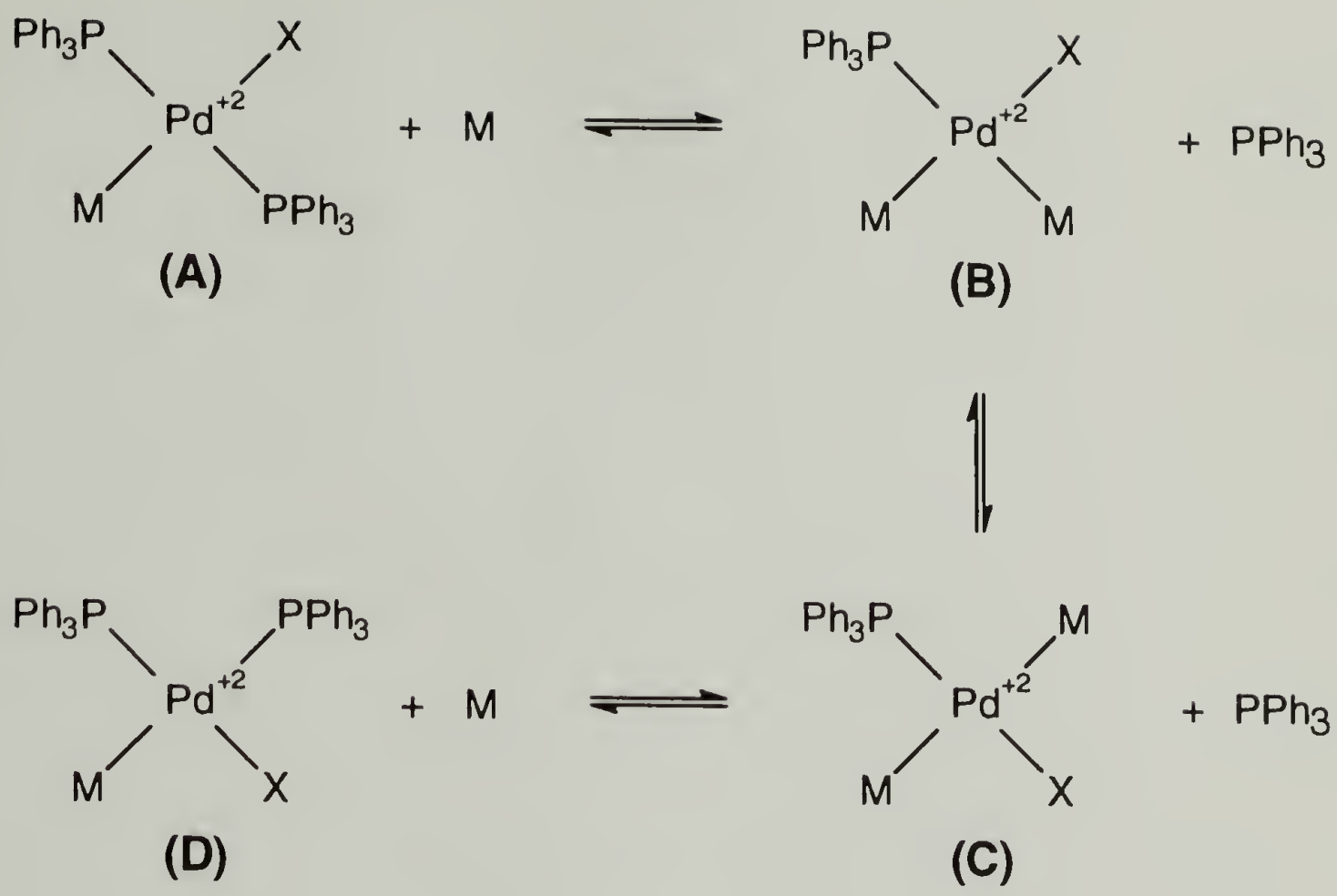

Figure 3.19 Displacement of *trans* catalyst **7** by the monomer.

Species **C** is not benefited by this effect, but there is less steric hindrance having one Ph_3P than **D** which has two Ph_3P ligands. The fact that the active states **B** and **C** have only one Ph_3P ligand may explain for the low regiospecificity.

In the case of **B** and **C** there are two coordinated monomers. Quantum mechanically, one might expect a lower energy if Pd^{+2} is bonded to identical monomer molecules due to the exchange terms. If they are both propylene molecules then non-alternating propagation is likely to occur. This postulation is supported by the ^{13}C-NMR spectrum of Figure 3.14b. Of course if both monomer molecules are carbon monoxide, it will not contribute toward non-alternation since consecutive CO insertion is forbidden.

Catalyst **2** and **3** have low polymerization regiospecificity but there is negligible if any non-alternation. ^{31}P-NMR indicate that the bisphosphine ligands form stable 5- and 6- membered *cis*-chelate ring with Pd^{+2} in catalyst **2** and **3**, respectively. The fact that the alternating copolymers produced by **2** and **3** have regioregularity indices of only 55% to 58% suggests that the steric geometries of the Ph_2P moieties with 2,1 and 1,2 coordinated propylene do not differ appreciably in their steric energies.

Catalyst **4** is the most active and regiospecific of the series. A possible explanation is the dynamic chelation[17,8] for

this complex. The bisphosphine in catalyst **4** forms a 7-membered chelate with Pd^{+2}. It is less stable than the smaller size chelates and dynamic opening and closing of the former ring could occur. In fact this process was shown to occur in the vinylation of chlorobenzene.[17] The investigations determined the structure of $(dippb)_2Pd$, with dippb = 1,4-bis(diisopropylphosphino)butane, to be square-planar chelate in the solid state. The molecule assumes a trigonal structure in solution with one dippb becoming an unidente ligand while the other dippb remaining *cis*-chelated. During the catalysis of vinylation, the *cis*-chelated ring is dynamically opened.

Figure 3.20 depicts the possible mechanism of catalysis by **4**, where M = C_3H_6, X = -C(O)-R, M' = CO, and X' = -C_3H_6-C(O)-R. In the pseudo resting state **E** (or **E'**) the bisphosphine is chelated to Pd^{+2}, and has small dissociation constant. Alternatively, a second monomer can displace one of the phosphine moiety by reaction 1 (Figure 3.20). The complexation of both C_3H_6 and CO invokes σ donation and π* back donation. The migratory insertion (reaction 2 in Figure 3.20) is considered to be accompanied by chelate ring closure nearly simultaneously. The structure **F** (or **F'**) is apparently favorable for the promotion of regiospecific and stereospecific alternating copolymerization of propylene and CO. The chelated structure **E**, in which each phosphorus atom has two

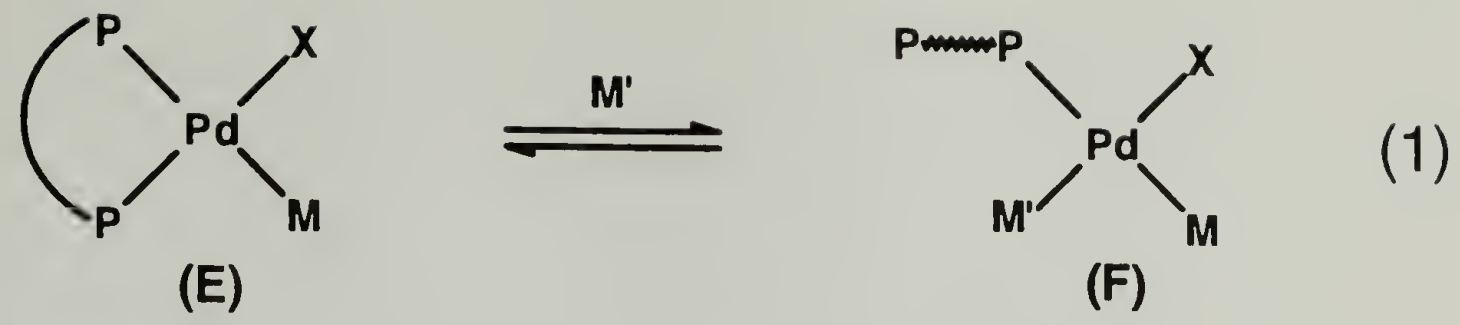

(1)

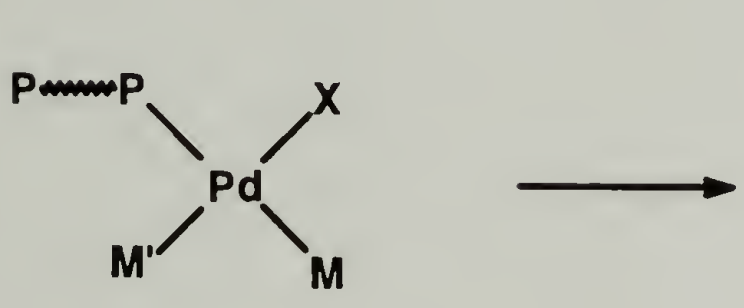

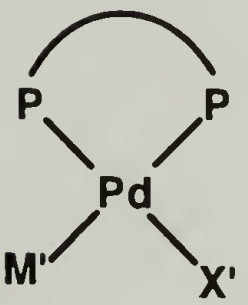

(2)

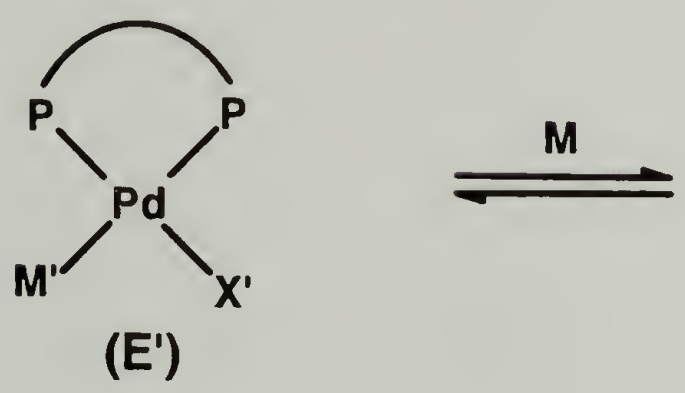

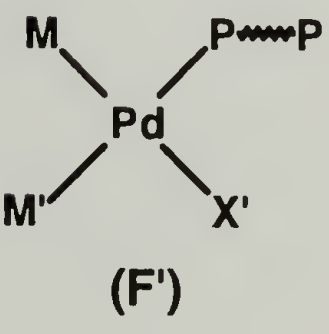

(3)

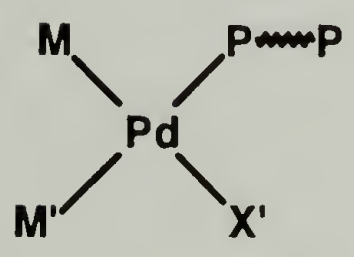

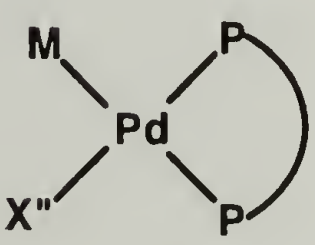

(4)

Figure 3.20 Possible mechanism of catalysis by catalyst **4**.

phenyl substituents, is apparently unfavorable for regiospecific and stereospecific propagation. This is supported by the fact that catalysts $R_2P(CH_2)_nPR_2/Pd^{+2}$, with R = *i*-Pr, *n*-Bu, and cyclohexyl, are 100% regiospecific. This mechanism incorporates two other important features. One is that the second coordinated monomer M' exerts strong *trans* labilizing effect on X to promote migratory insertion. The other is that there is no unidente phosphine intermediates like **D** (*vide supra*).

It is important that chelate opened structure does not exist for any length of time as it will lead to non-alternative insertion. In the case of catalyst **5**, the 8-membered chelate is quite unstable. It has larger ring dissociation constant. Consequently catalyst **5** produced both regioregular copolymer and non-alternating oligomers (Fig. 3.14c).

The chelate structure for catalyst **5** is unknown; both *cis*-chelation and *trans*-chelation are in principle possible because of the long penta-methylene spacer between the two Ph_2P moieties. We have performed molecular mechanics calculation to find out whether *cis*- or *trans*-chelation is more favored. Molecular mechanics calculation has been proven to be very effective in judging the preference among different stereo-isomers.[8,27] The steric energy calculated for *cis*-chelation was about 10 kcal/mol lower than that of *trans*-chelation, which

suggested a preference of *cis*-chelation over the *trans*-chelation. The fact that catalyst **5** produced high regioregular polymer confirmed the existence of *cis*-chelate ring structure. The two remaining ^{31}P-NMR peaks were attributed to the non-chelated bisphosphine Pd fragment.

The presence of poly(spiroketal) structure in P-CO copolymer was first separated by Shell scientists. Subsequently, Batistini et al.[6] used (S)-(6,6'-dimethylbiphenyl-2,2'-diyl)bis(dicyclohexylphosphine) ligand to produce the poly(spiroketal) copolymer and proposed a very elaborate mechanism involving palladium carbene intermediates with the propagating species being alternatingly a Pd-carbene and a Pd-cyclobutane, which is metathesis ring-opening polymerization. In this mechanism for the copolymerization of propylene and CO, the monomer complexed catalytic intermediates would have the impossible five coordinate structures.[8]

Wong et al.[9] used 1,3-bis(di-n-butylphosphino)propane ligand to generate a gel in a mixture of methanol and THF, which displayed poly(spiroketal) structure as well. They suggested a mechanism involving normal insertion of propylene and CO followed by intramolecular polymerization of ketone. On the other hand Sen et al.[3] and us[5,8] did not observe the poly(spiroketal) structure previously. The reason is probably that the copolymers did not have as high regio- and

stereo-regularities and molecular weight as those of Batistini et al.[6] and Wong et al.[9], and are soluble in the reaction solvent such as 1,2-dichloroethane, nitromethane / methanol mixture. Therefore, even the copolymers contained some spiroketal structures initially, they would convert to the polyketone automatically in reaction solvent because the spiroketal structure was thermodynamically unfavored. Batistini et al.[6] observed that their poly(spiroketal) spontaneously converted to polyketone upon dissolve in hexafluoro-2-propanol. Recently we tried the copolymerization with catalyst **3** (*vide infra*) at 0 ^{o}C to increase the molecular weight of the copolymer. The resulted copolymer formed gel in reaction solvent. The solid state ^{13}CNMR spectrum of such copolymer showed peaks around 114 and 211 ppm with the approximately ratio of 7 : 3, which suggested the coexistence of poly(spiroketal) and polyketone structures.

References

(1) Brubaker, M. M.; Coffman, D. D.; Hoehn, H. H. *J. Am. Chem. Soc.* **1952**, *74*, 1509.

(2) Drent, E. *Eur. Pat. Appl.* 121,965, **1984**.

(3) Jiang, Z.; Dahlen, G. M.; Houseknecht, K.; Sen, A. *Macromolecules* **1992**, *25*, 2999.

(4) Batistini, A.; Consiglio, G.; Suter, U. W. *Angew. Chem. Int. Ed. Engl.* **1992**, *31*, *No. 3*, 303.

(5) Chien, J. C. W.; Zhao, A. X.; Xu, F. *Polym. Bull.* **1992**, *28*, 315.

(6) Batistini, A.; Consiglio, G. *Organometallics* **1992**, *11*, 1766.

(7) Batistini, A.; Consiglio, G.; Suter, U. W. *PMSE Preprint*, **1992**, *67*, 104.

(8) Xu, F. Y.; Zhao, A. X.; Chien, J. C. W. *Markomol. Chem.* **1993**, *194*, 2579.

(9) Wong, P. K.; van Doorn, J. A.; Drent, E.; Sudmeijer, O.; Stil, H. A. *Ind. Eng. Chem. Res.* **1993**, *32(5)*, 986.

(10) Drent, E.; van Brockhoven, J. A. M.; Doyle, M. J.; *J. Organomet. Chem.* **1991**, *417*, 235.

(11) Zhao, A. X.; Chien, J. C. W. *J. Polym. Sci., Part A: Polym. Chem.* **1992**, *30*, 2735.

(12) a) Hart, C. *J. Am. Chem. Soc.* **1957**, *79*, 931. b) Kupin, P. *Zh. Obshch. Khim.* **1959**, *29*, 3738. c) Opitz, G.; Adolf, H.; Kleemann, M.; Zimmermann, F. *Angew. Chem.* **1961**, *73*, 654. d) Stutsman, A. *J. Am. Chem. Soc.* **1939**, *61*, 3305.

(13) Lai, T. W.; Sen, A. *Organometallics* **1984**, *3*, 866.

(14) a) Manriquez, J. M.; McAlister, D. C.; Sanner, R. D.; Bercaw, J. E. *J. Am. Chem. Soc.* **1978**, *100*, 2716. b) Marsella, J. A.; Folting, K.; Huffman, J. C.; Caulton, K. G. *J. Am. Chem. Soc.* **1981**, *103*, 5596. c) Kobayashi, T.; Tanaka, M. *J. Organomet. Chem.* **1982**, *233*, C64.

(15) Chien, J. C. W.; Wang, B. P. *J. Polym. Sci., Part A: Polym. Chem.* **1989**, *27*, 1539.

(16) Chen, J. T.; Sen, A. *J. Am. Chem. Soc.* **1984**, *106*, 1506.

(17) a) Ben-David, Y.; Portnoy, M.; Gozin, M.; Milstein, D. *Organometallics* **1992**, *11*, 1995. (b) Ben-David, Y.; Portnoy, M.; Milstein, D. *J. Am. Chem. Soc.* **1989**, *111*, 8742. (c) Ben-David, Y.; Portnoy, M.; Gozin, M.; Milstein, D. *J. Chem. Soc. Chem. Commun.*, **1989**, 1816.

(18) Nakazawa, H.; Ozawa, F.; Yamamoto, A. *Organomet.* **1983**, *2*, 241.

(19) Palenik, G. J.; Mathew, M.; Steffen, W. L.; Beran, G. *J. Am. Chem. Soc.* **1975**, *97*, 1059.

(20) Garrou, P. E. *Chem. Rev.* **1981**, *81*, 229.

(21) a) Mann, B. E.; Masters, C.; Shaw, B. L. *J. Chem. Soc. A*, **1971**, 1104. b) Mann, B. E.; Masters, C.; Shaw, B. L. *J. Chem. Soc., Dalton Trans.* **1972**, 704.

(22) Grim, S. O.; Briggs, W. L.; Barth, R. C.; Tolman, C. A.; Jesson, J. P. *Inorg. Chem.* **1974**, *13*, 1095.

(23) Connor, J. A.; Day, J. J.; Jones, E. M.; McEwen, G. K. *J. Chem. Soc., Dalton Trans.* **1973**, 347.

(24) Garrou, P. E. *Inorg. Chem.* **1975**, *14*, 1435.

(25) Connor, J. A.; McEwen, G. K.; Rix, C. J. *J. Chem. Soc., Dalton Trans.* **1974**, 589.

(26) Brumbaugh, J. S.; Whittle, R. R.; Parvez, M.; Sen, A. *Organometallics*, **1990**, *9*, 1735.

(27) Yu, Z.; Chien, J. C. W. *J. Am. Chem. Soc.* submitted.

CHAPTER 4

MOLECULAR MECHANICS CALCULATION OF REGIO- AND STEREO-CONTROL ENERGIES

4.1 Introduction

Molecular mechanics is basically a computational realization of the ball-and-stick models of molecules that are familiar to every chemist.[1] It is based on the Born-Oppenheimer separation of the electronic and nuclear motion. The electrons are not considered explicitly. They provide an effective potential, which is experienced by the nuclei. Molecular mechanics treats the interactions between the nuclei and the effective potential generated by the electrons according to the laws of classical mechanics. Molecular mechanics calculation, in comparison with quantum chemical technique, can be performed quickly and effectively, and they permit quite large systems to be investigated.

The origin of regiochemical and stereochemical control by palladium/bisphosphine complex is of great interest to scientists engaged in olefin-carbon monoxide catalysis research. Molecular mechanics calculation has been proven to

be very effective in judging the preference among different stereo-isomers, and it has been successfully applied to investigate the regio- and stereo-control of Ziegler-Natta catalysis.[2-6] The purpose of this portion of work is to use molecular mechanics calculation method to predict the regio- and stereo-selectivity of the palladium/bisphosphine catalyst in propylene-carbon monoxide alternating copolymerization. The six-membered ring catalyst **3** and seven-membered ring catalyst **4** were chosen for the calculation. The structures of these two catalysts are displayed in Table 2.2 on page 35.

4.2 Computational Method

The program used to perform the molecular mechanics calculation was Allinger's MM2.[7] The potential energy function used to calculate the total steric energy (E_s) of the catalytic precursors as a function of the relative positions of the atomic coordinates by successive iterations with a block-diagonalized Newton-Raphson least-squares algorithm is given in following eq. 1 with the *main* components defined in eq. 1a-1d.

$$E_s = \sum (E_r + E_\theta + E_\phi + E_{nb}) \qquad (1)$$

$$E_r = \frac{1}{2} K_r (l - l_o)^2 + K_r' (l - l_o)^3 \qquad (1a)$$

$$E_\theta = (0.043828) \frac{1}{2} K_\theta (\theta - \theta_o)^2 + K_\theta' (\theta - \theta_o)^4 + K_\theta'' (\theta - \theta_o)^6 \qquad (1b)$$

$$E_\phi = \frac{1}{2} [\, V_1 (1 + \cos\phi) + V_2 (1 - \cos 2\phi) + V_3 (1 + \cos 3\phi)] \qquad (1c)$$

$$E_{nb} = \varepsilon^* \{\, 2.9 \times 10^5 \exp[-12.5(\frac{r}{r^*})] - 2.25(\frac{r^*}{r})^6 \,\} \qquad (1d)$$

By *main*, we mean that the numerous cross terms including stretch-bend, stretch-torsion, and bend-bend are not listed in the equation above. Here E_r represents the bond deformation energies (stretching term), K_r is the derived stretching force constant (mdyn/Å), K_r' is the anharmonic correction stretching force constant (2.0 mdyn/Å, default value), while l and l_o are the actual and ideal bond length (Å), respectively. E_θ accounts for the angle deformation strain contributions (bending term), where 0.043828 is a conversion factor (mdyn Å/rad²/molecule to kcal/deg²/mole), K_θ' and K_θ'' are the angle bending force constants (7×10^{-8} mdyn Å/rad² default value), where θ and θ_o are the actual and ideal bond angle (deg), respectively. E_ϕ is the strain energy contribution from each torsional angle deformation, with V_1, V_2, and V_3, the 1-, 2-, and 3-fold torsional constants (kcal/mol) that determine the variation in torsional strain energy as a function of the dihedral angle ϕ.

The nonbonded (van der Waals) energy for the interactions of all atom pairs ij is given by E_{nb}, where $\varepsilon^* = (\varepsilon_i\varepsilon_j)^{1/2}$ with ε_i and ε_j representing the "hardness" of atoms i and j (kcal/mol), $r^* = r_i+r_j$, the sum of the van der Waals radii of atoms i and j (Å), and r is the distance between the two atoms (Å). When $r^*/r > 3.311$, eq. 1d reduces to $E_{nb} = \varepsilon^*(336.176)r^*/r$ to prevent two atoms fusing when they come very close together. This augmented MM2 force field provides good approximation for the transition metal compounds.[8]

The molecular structure of $(Ph_2P(CH_2)_3PPh_2)Pd(NCS)_2$ from X-ray diffraction[9] provides the initial model geometries. We input this structure into the computer and performed energy minimization. This resulted in negligible changes in any of the bond angles or distances. Certain bonding parameter was altered by 10%; energy minimization of this arbitrary structure returns the parameter to the X-ray value. These exercises lend confidence to the calculation.

4.3 Results and Discussion

The steric energies were computed for the Pd catalytic species having a propagating chain and a coordinated propylene, which is referred to as the activated complex (AC). This was done by replacing one NCS moiety with $-C(O)-C_3H_6-$

C(O)-CH_3, which simulates a propagating chain, while the other NCS moiety was substituted by a π-complexed propylene. The structure of the AC resulted after energy minimization is shown in Figure 4.1 for the catalyst **4** system with 1,2-insertion of propylene in the *R* configuration. Steric energies were computed for all sixteen cases of AC: 1,2- or 2,1-insertion and *R* or *S* configuration for the penultimate propylene and the monomer just inserted. The results are given in Table 4.1. In the case of the seven-membered ring catalyst, its crystal structure is not available. The computation began by inserting a methylene unit into the $(Ph_2P(CH_2)_3PPh_2)Pd(NCS)_2$ structure. This structure was refined by energy minimization. The steric energies were obtained as above; the results are also given in Table 4.1.

The regioselectivity is reflected in the difference between the steric energies of AC having the 1,2 or the 2,1 coordinated propylene. The energy differences for different configurations are shown in Table 4.2. Two important conclusions can be derived from Table 4.2: (a) *R* configuration is favored over *S*, especially when the previous insertion is in *S* configuration; (b) 1,2 insertion is favored over 2,1 insertion, especially when the previous insertion is in 2,1 mode. Therefore we define the regiocontrol energy, $\Delta E_s'$, for 1,2-insertion as $|E_{1,2R} - E_{2,1R}|$ with penultimate propylene inserted in 1,2 *R* configuration; and

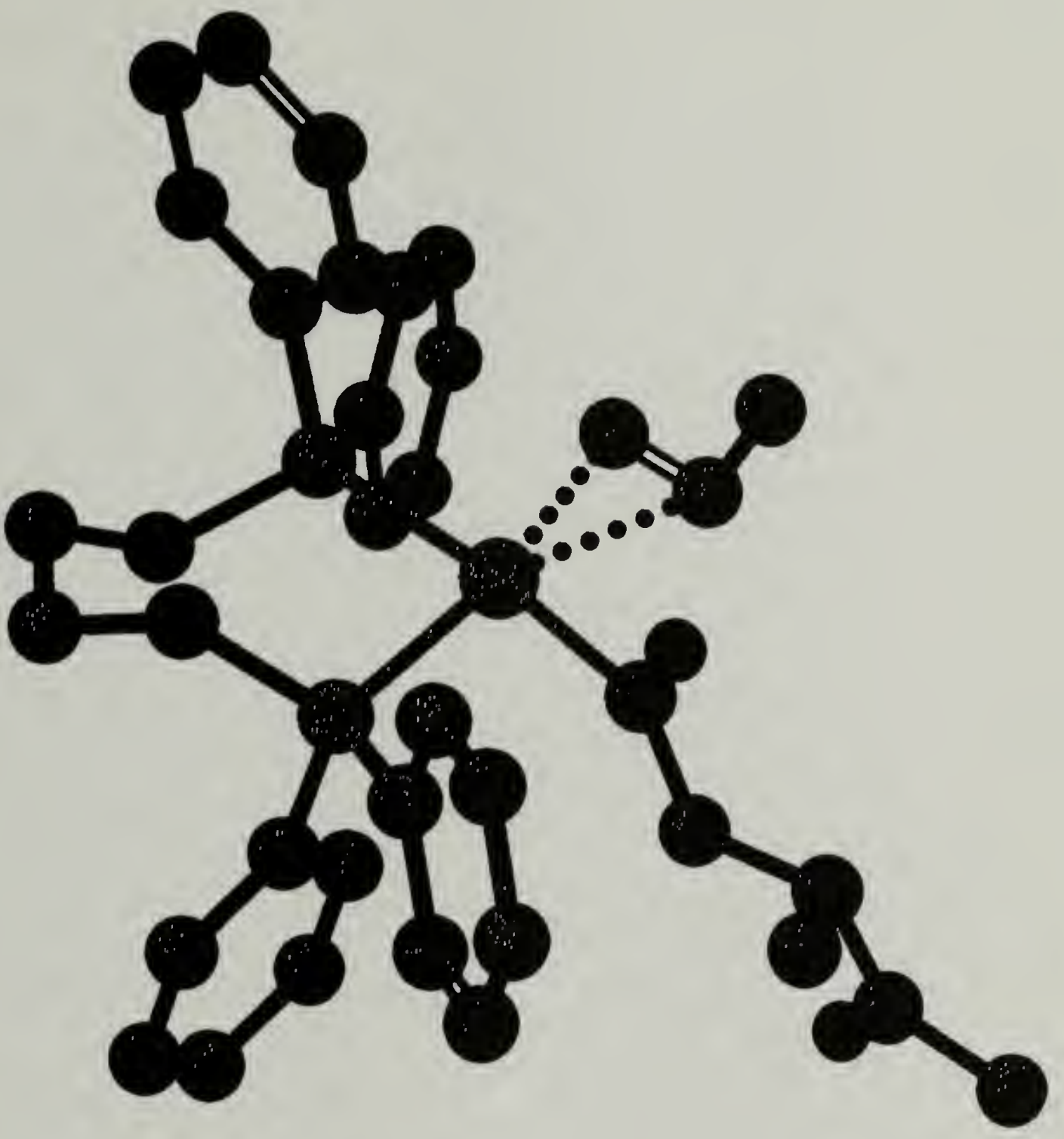

Figure 4.1 Molecular mechanics modeling result of the structure of catalyst **4** system with a growing polymer chain and an inserting propylene. Structure with chain-end propylene and inserting propylene both in *R* configuration and primary insertion mode has the overall lowest energy, which is shown here.

Table 4.1 Molecular mechanics calculation of steric energies for P-CO copolymerization with catalyst **3** and **4**.

Configuration	E_{steric} (kcal/mol) catalyst **4**	E_{steric} (kcal/mol) catalyst **3**
1,2 *R** (1,2 *R*)**	30.58	21.29
1,2 *S* (1,2 *R*)	31.65	21.84
2,1 *R* (1,2 *R*)	31.57	21.86
2,1 *S* (1,2 *R*)	33.17	22.52
1,2 *R* (1,2 *S*)	29.98	21.13
1,2 *S* (1,2 *S*)	32.61	23.31
2,1 *R* (1,2 *S*)	31.17	21.92
2,1 *S* (1,2 *S*)	32.54	22.6
1,2 *R* (2,1 *R*)	29.12	20.27
1,2 *S* (2,1 *R*)	31.54	22.17
2,1 *R* (2,1 *R*)	31.06	22.1
2,1 *S* (2,1 *R*)	31.47	21.32
1,2 *R* (2,1 *S*)	32.08	22.31
1,2 *S* (2,1 *S*)	34.98	25.53
2,1 *R* (2,1 *S*)	34.25	23.41
2,1 *S* (2,1 *S*)	35.64	24.97

* Configuration of inserting propylene
** Configuration of penultimate propylene unit

Table 4.2 Steric energy differences for various configuration.

Penultimate propylene	Difference for insertion	ΔE (kcal/mol) catalyst **4**	ΔE (kcal/mol) catalyst **3**
1,2 *R*	$E_{1,2R} - E_{1,2S}$	-1.1	-0.6
1,2 *R*	$E_{2,1R} - E_{2,1S}$	-1.6	-0.7
1,2 *R*	$E_{1,2R} - E_{2,1R}$	-1.0	-0.6
1,2 *R*	$E_{1,2S} - E_{2,1S}$	-1.5	-0.7
1,2 *S*	$E_{1,2R} - E_{1,2S}$	-2.6	-2.2
1,2 *S*	$E_{2,1R} - E_{2,1S}$	-1.4	-0.7
1,2 *S*	$E_{1,2R} - E_{2,1R}$	-1.2	-0.8
1,2 *S*	$E_{1,2S} - E_{2,1S}$	≈ 0	0.7
2,1 *R*	$E_{1,2R} - E_{1,2S}$	-2.4	-1.9
2,1 *R*	$E_{2,1R} - E_{2,1S}$	-0.4	0.8
2,1 *R*	$E_{1,2R} - E_{2,1R}$	-1.9	-1.8
2,1 *R*	$E_{1,2S} - E_{2,1S}$	≈ 0	0.8
2,1 S	$E_{1,2R} - E_{1,2S}$	-2.9	-3.2
2,1 S	$E_{2,1R} - E_{2,1S}$	-1.4	-1.6
2,1 S	$E_{1,2R} - E_{2,1R}$	-2.2	-1.1
2,1 S	$E_{1,2S} - E_{2,1S}$	-0.7	0.6

stereocontrol energy, ΔE_s", for *meso* enchainment of prochiral propylene as $|E_{1,2R} - E_{1,2S}|$ with penultimate propylene inserted in 1,2 *R* configuration. These values are summarized in Table 4.3. The ΔE_s' values are bigger for catalyst **4** than catalyst **3** is consistent with the high regioregularity observed for the copolymers produced with the catalyst **4**. Similarly ΔE_s" values predict higher stereo-selectivity for catalyst **4** which agreed with the experimental results. Therefore molecular mechanics calculations on the π-olefin complex showed that the non-bonded interaction between propylene and the ligands on Pd is both regio- and stereo-selective.

Table 4.3 Regio- and stereo-control energies for catalyst **3** and **4**.

Catalyst	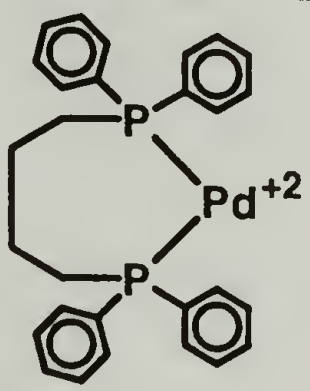 **4**	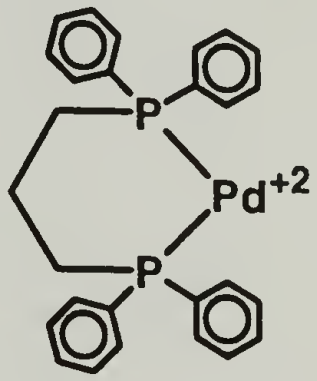 **3**
$\Delta E_s' = \lvert E_{1,2R} - E_{2,1R} \rvert$ (kcal/mol)	1.0	0.6
Regioreg.	79 %	55 %
$\Delta E_s'' = \lvert E_{1,2R} - E_{1,2S} \rvert$ (kcal/mol)	1.1	0.6
Stereoreg.	56 %	48 %

References

(1) Wilson, S. *Chemistry by computer* New York: Plenum Press, **1986**.

(2) Cavallo, L.; Guerra, G.; Vacatello, M.; Corradini, P. *Macromolecules* **1991**, *24*, 1784.

(3) a) Kawamura-Kuribayashi, H.; Koga, N.; Morokuma, K. *J. Am. Chem. Soc.* **1992**, *114*, 8687. b) Kawamura-Kuribayashi, H.; Koga, N.; Morokuma, K. *J. Am. Chem. Soc.* **1992**, *114*, 2359.

(4) a) Castonguay, L. A.; Rappe, A. K. *J. Am. Chem. Soc.* **1992**, *114*, 5832. b) Hart, J. R.; Rappe, A. K. *J. Am. Chem. Soc.* **1993**, *115*, 6159.

(5) a) Apellmeyer, D. C.; Houk, K. N. *J. Org. Chem.* **1987**, *52*, 959. b) Dorigo, A. E.; Houk, K. N. *J. Org. Chem.* **1988**, *53*, 1650.

(6) Yu, Z.; Chien, J. C. W. *J. Am. Chem. Soc.* in press.

(7) Allinger, N. L. *J. Am. Chem. Soc.* **1977**, *99*, 8127.

(8) Brubaker, R. G.; Johnson, W. D. *Coord. Chem. Rev.* **1984**, *53*, 1.

(9) Palenik, G. L.; Mathew, M.; Steffen, W. L.; Beran, G. *J. Am. Chem. Soc.* **1975**, *97*, 1059.

CHAPTER 5

CRYSTAL STRUCTURE OF PROPYLENE-CARBON MONOXIDE ALTERNATING COPOLYMER

5.1 Introduction

The propylene-carbon monoxide alternating copolymer is a relatively new polymer. There is no literature report on its crystal structure yet. Ethylene-carbon monoxide copolymer was reported to have the zig-zag structure with an orthorhombic unit cell (a=7.97 Å, b=4.76 Å, and c=7.57 Å).[1] With the presence of additional methyl group in P-CO copolymer, a helical structure is expected.

X-ray diffraction is useful in distinguishing ordered from disordered states of solid substances.[2] Amorphous materials produce X-ray patterns of a diffuse nature consisting of one or more halos, whereas well-crystallized substances yield patterns of numerous sharp circles or spots. This capacity to reveal the degree of ordering in solid substances makes X-ray diffraction well suited to the investigation of polymers.

The crystal structure of polymers can be derived from the X-ray diffraction pattern based on three statements:[3] (i) In

linear crystalline polymers the axis of the macromolecule runs parallel to a crystallographic axis of the crystal. Moreover, in all known structures all the monomeric units have been found to occupy geometrically equivalent positions with regard to this axis (equivalence postulate); (ii) The conformation of the chain in a crystal approaches the one of minimum potential energy, that should be assumed by an isolated chain oriented along an axis, with the restrictions contained in the equivalence postulate. This means that lateral packing contacts (between neighboring chains) generally play a secondary role in determining the conformation of the chain on comparison with the internal contacts in the chain. Thus, lateral packing contacts cause only slight deviations of the form of the chain from the one foreseeable only on the basis of the above consideration; (iii) The chains approach themselves parallel each other at intermolecular distances similar to those realized in low molecular weight compounds, to fill possibly any hole between themselves. With this restriction, as many as possible elements of symmetry of the isolated chain are maintained in the lattice. That is, equivalent atoms of different monomeric units along an axis tend to assume equivalent positions in regard to the atoms of neighboring chains. The repetition of these equivalent units is done through the operation of a translation c/p along z, accompanied by a rotation $2\pi(P/p)$ in a

plane perpendicular to *z*. A helix is thus generated which contains *p* monomeric units and *P* pitches within the period *c*. Therefore a 5_2 fold helix suggests that the period *c* contains 5 monomer units (or motifs) and 2 turns of the helix.

5.2 Experimental

The polymer was prepared as previously described. The oriented fibers were obtained by elongating a strip of a film at 80 °C, and were annealed under stress in order to achieve a good crystallization.

X-ray diffraction pattern of copolymer sample was recorded on a Siemens Station camera using a Ni filtered Cu-K α radiation excited at 40 kV. The *d* spacing of the crystal is calculated by following formula,

$$n\lambda = 2d\sin\theta \qquad (1)$$

Where λ is the X-ray wavelength which is 1.54 Å here; *d* is the interplanar spacing; θ is one-half the angle of deviation of the diffracted rays from the incident x-rays; and *n* is integer which is usually 1. Computer simulation was carried out on a Silicon Graphics workstation by using POLYGRAF software supplied by Molecular Simulation Incorporated.

5.3 Results and Discussion

Depending on the configuration of the molecular chains and their arrangement with respect to one another, any given structure can be assigned to one of six crystal systems characterized by the ratios of the lengths of its unit cell edges- *a*, *b*, and *c* and the three angles defined by those edges-α, β, and γ.[2] The powder and fiber X-ray diffraction patterns of the crystalline copolymer are shown in Figure 5.1. Many diffraction layers have weak intensities, and they didn't show well in Figure 5.1. To illustrate all the diffraction layers, the schematic draw of the fiber pattern is shown in Figure 5.2. Three meridian layers (not counting the *hk*0 layer) are observed in the fiber pattern, which suggests that the copolymer has the 3_1 fold helix structure. The computer simulation result of such 3_1 fold helix is shown in Figure 5.3. The C_3 symmetry is nicely preserved. Figure 5.4 displays this single chain structure in the direction of perpendicular to the *c* axis. The unit cell structure of crystalline copolymer is hexagonal. The *d* spacing of a hexagonal unit cell can be calculated by following formula,

$$d_{hkl} = \frac{1}{\sqrt{\frac{4(h^2+hk+k^2)}{3a^2}+\frac{l^2}{c^2}}} \qquad (2)$$

a

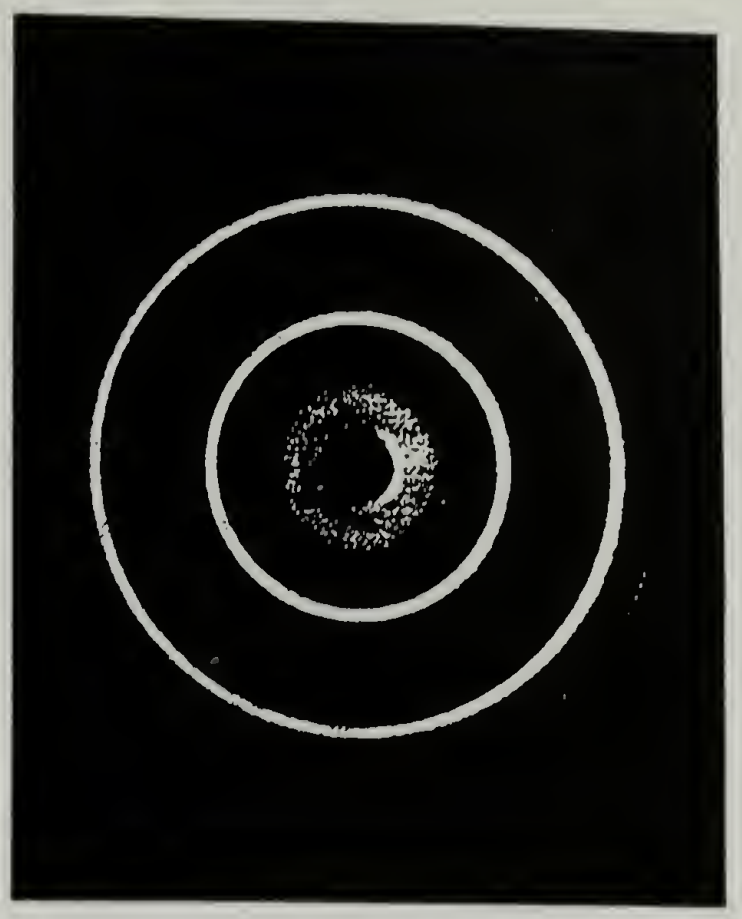

b

Figure 5.1 X-ray diffraction patterns of the crystalline copolymer in (a) powder, (b) fiber.

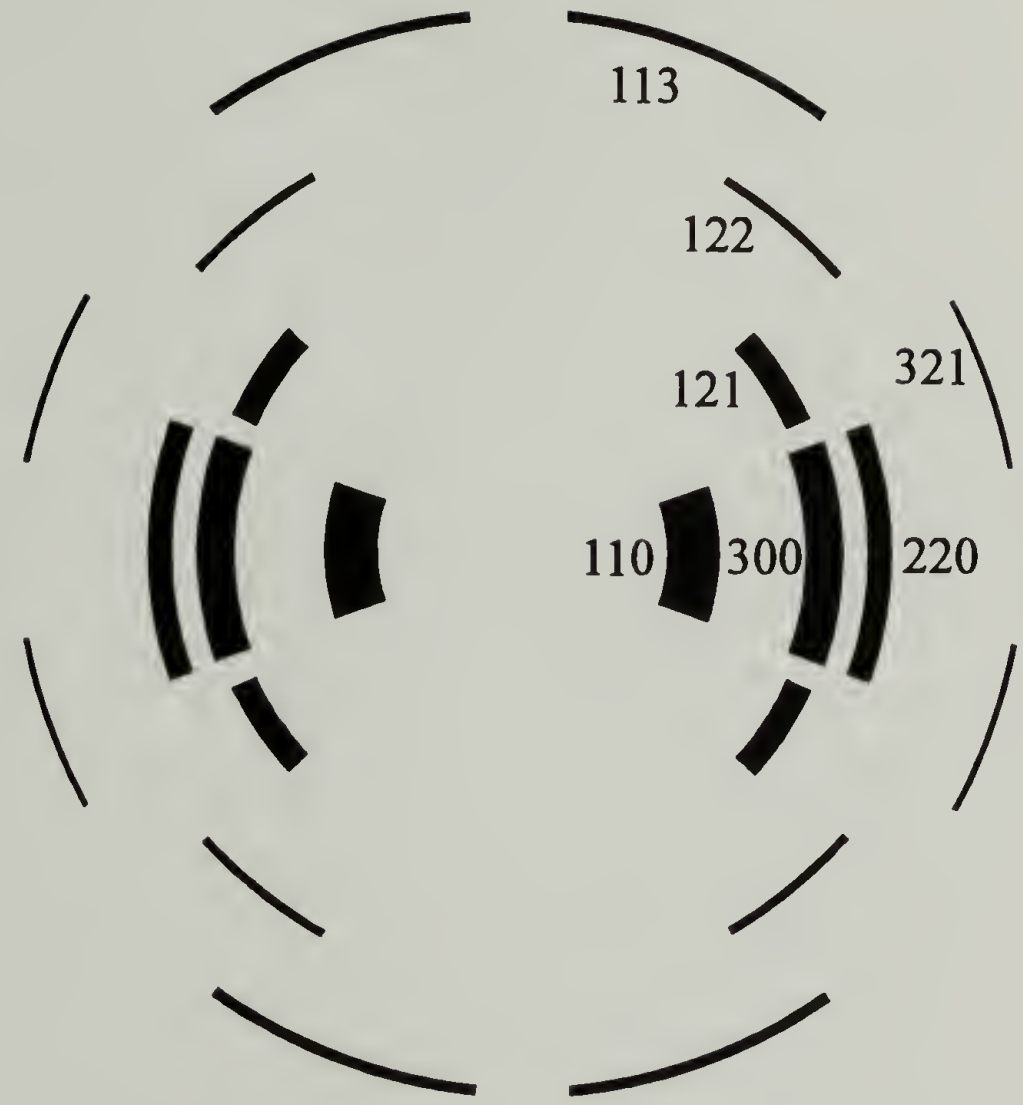

Figure 5.2 The schematic draw of the fiber pattern.

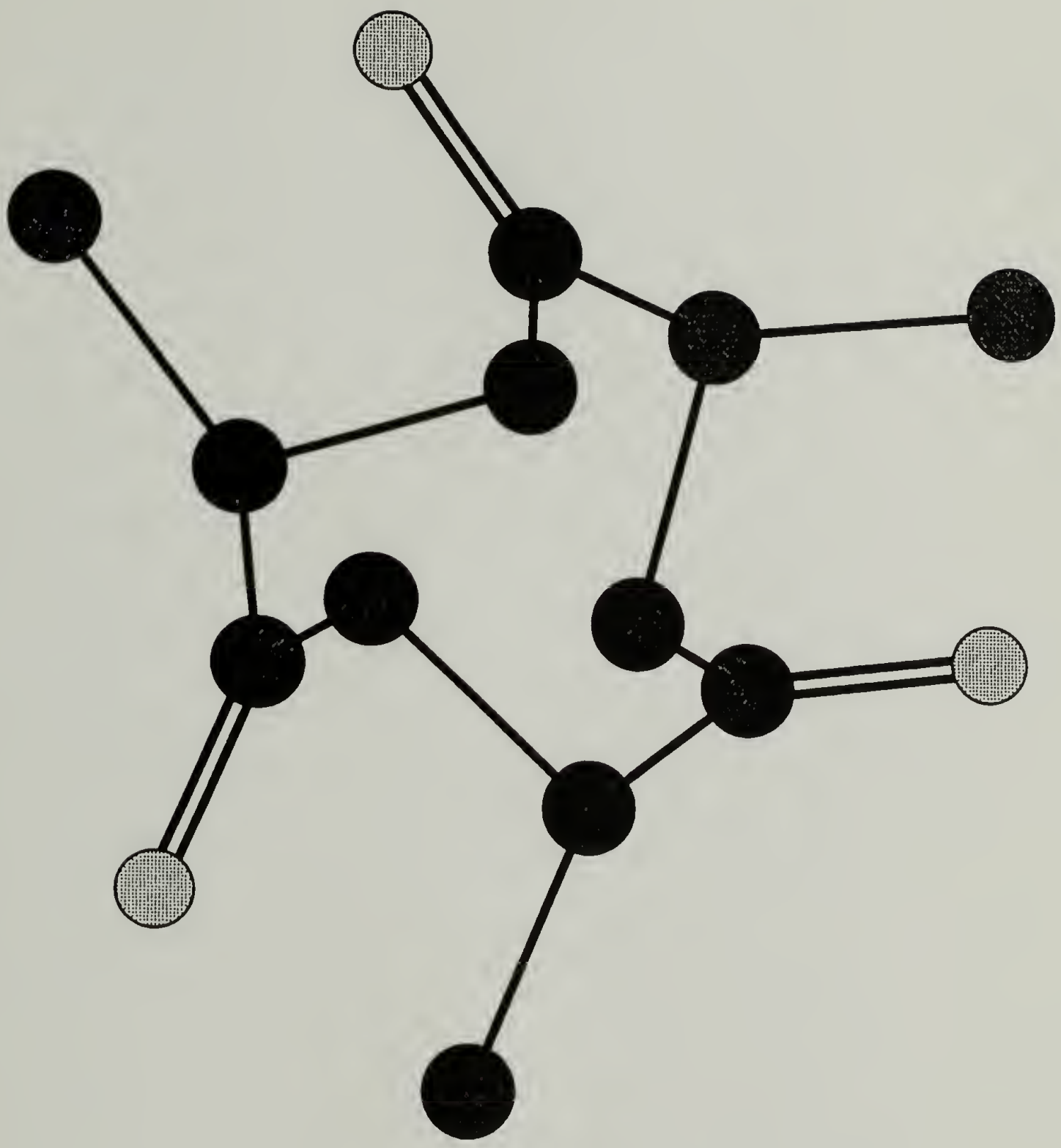

Figure 5.3 The 3_1 fold helix structure of the copolymer by computer simulation. The lightly shaded balls represent oxygen atoms; the darkly shaded balls represent carbon atoms.

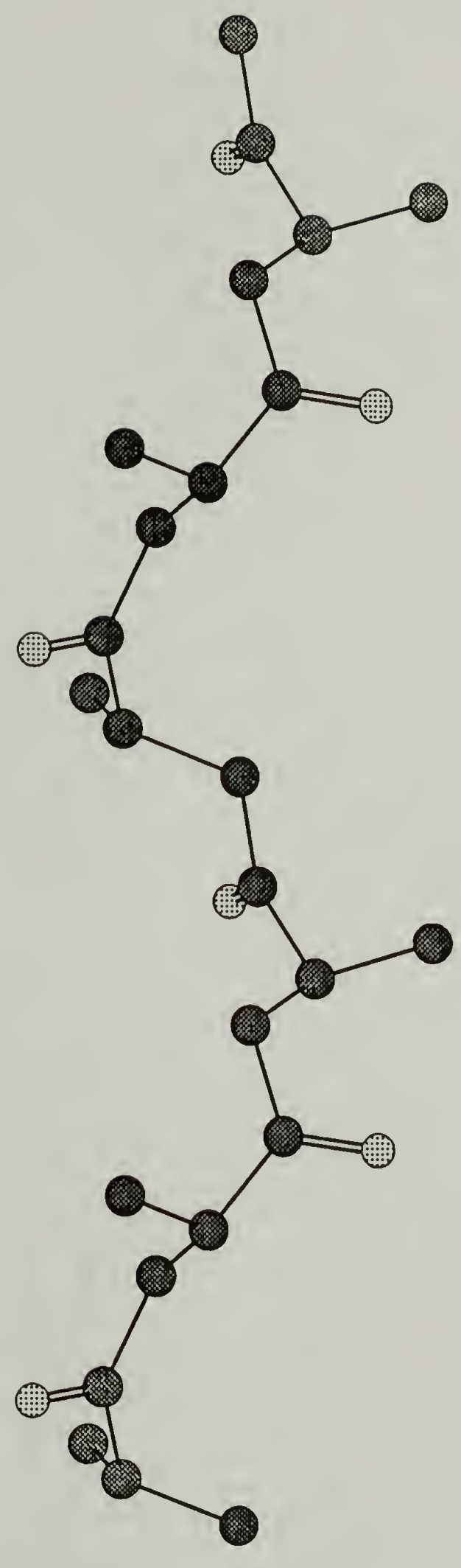

Figure 5.4 The 3_1 fold helix single chain structure viewing in the direction of perpendicular to the *c* axis.

where h, k, and l are the Miller indices. Table 5.1 shows the comparison of calculated and observed d spacing for the hexagonal unit cell with $a = b = 15.50$ Å, $c = 8.97$ Å, $\alpha = \beta = 90$, and $\gamma = 120$. The calculated and observed d spacing values match very well. Each unit cell contains 6 polymer chains, and the possible interchain packing is shown in Figure 5.5. The measured density is 1.11 which is in good agreement with the calculated value of 1.121.

Table 5.1 Comparison of calculated and observed *d* spacing for the hexagonal unit cell.

h k l	**Obs.** (angstrom)	**Calc.** (angstrom)
1 1 0	7.75	7.75
2 2 0	3.88	3.88
3 0 0	4.47	4.47
1 2 1	4.44	4.42
1 2 2	3.36	3.36
1 1 3	2.79	2.79
3 2 1	2.93	2.91

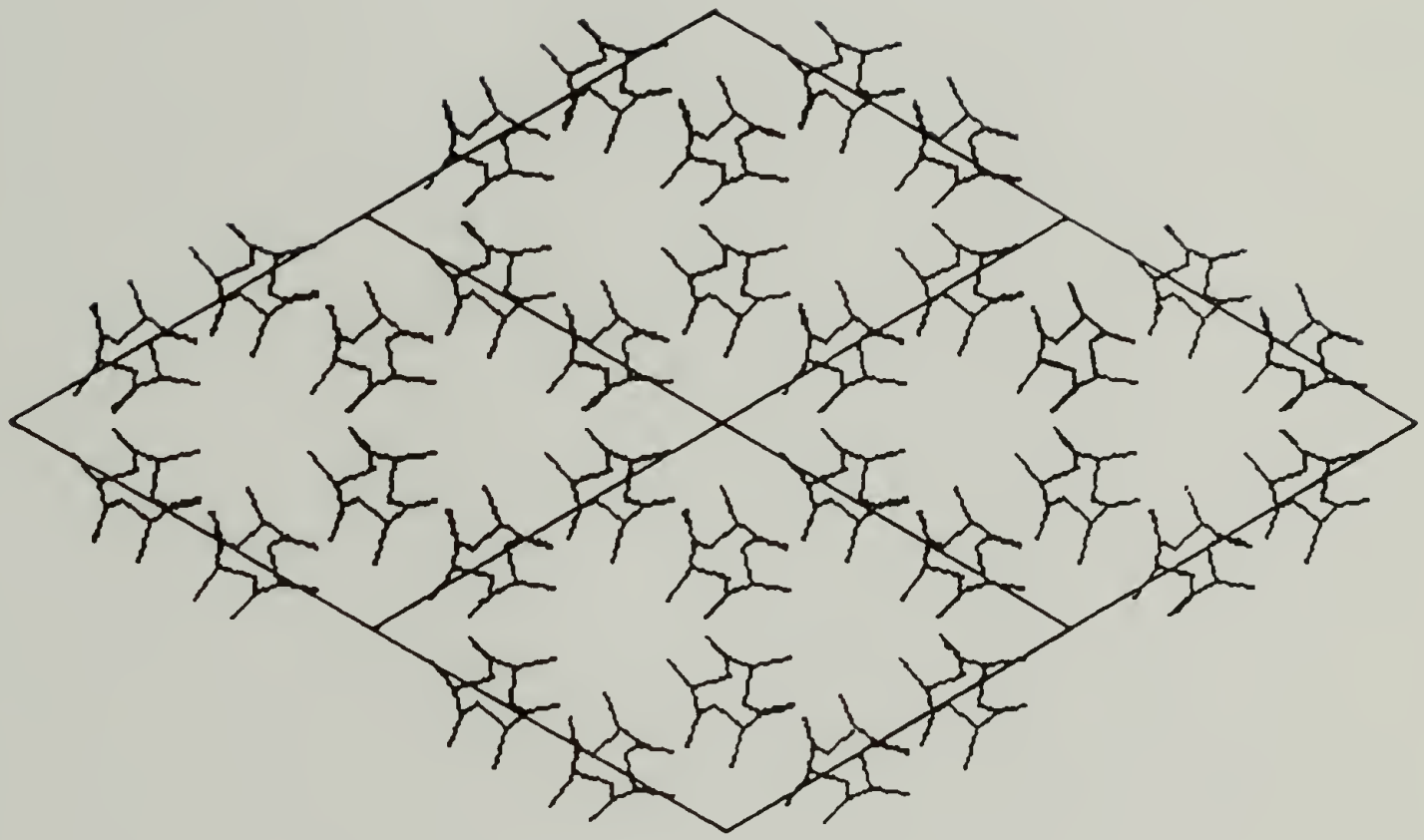

Figure 5.5 The possible interchain packing of the hexagonal structure.

References

(1) Chatani, Y.; Takizawa, T.; Murahashi, S.; Sakata, Y.; Nishimura, Y. *J. Polym. Sci.* **1961**, *55*, 811.

(2) Alexander, L. E. *X-ray Diffraction Methods in Polymer Science* New York: John Wiley & Sons, Inc., **1969**.

(3) Natta, G.; Corradini, P. *Nuovo Cimento, Supplemento* **1960**, *15*, 1.

CHAPTER 6

PHOTODEGRADATION OF α-OLEFIN-CARBON MONOXIDE ALTERNATING COPOLYMER

6.1 Introduction

One possible application of the α-olefin-carbon monoxide (CO) alternating copolymers is that they can serve as photo-degradable materials. The ketone group C=O contained in the olefin-CO alternating copolymer is a photoactive chromophore. Packing material fabricated from a bio- or photodegradable polymer[1] is deemed more friendly to the environment. Non-alternating E-CO copolymer of low CO content such as the 0.99-0.01 E-CO material had been marketed as Ecoplastics. It has been shown that ketones in polymeric materials undergo some of the same photochemical reactions as low molecular weight ketone.[2-6] Norrish type I and type II reaction (Figure 6.1a, b) are the main pathways. A third primary process, which produces a cyclobutanol product (Figure 6.1c),[7] had been identified for a few ketones. Extensive studies have also been carried out on photodegradation behaviors of polymers containing ketonic pendant groups.[6]

Figure 6.1 Photodegradation pathways of propylene-carbon monoxide alternating copolymer: (a) Norrish type I, (b) Norrish type II, (c) cyclization.

(a) Norrish Type I

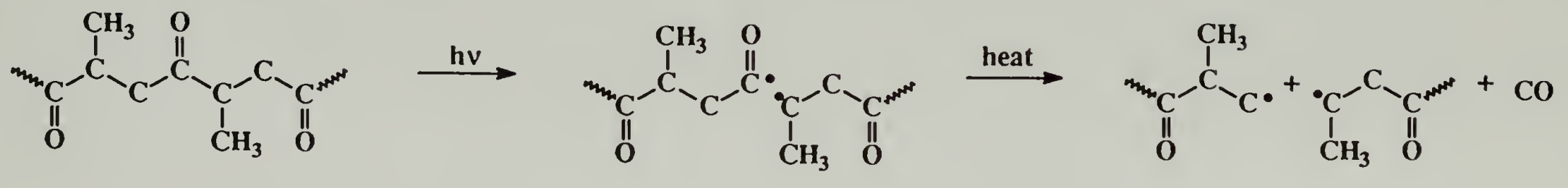

(b) Norrish Type II

(c) Cyclization

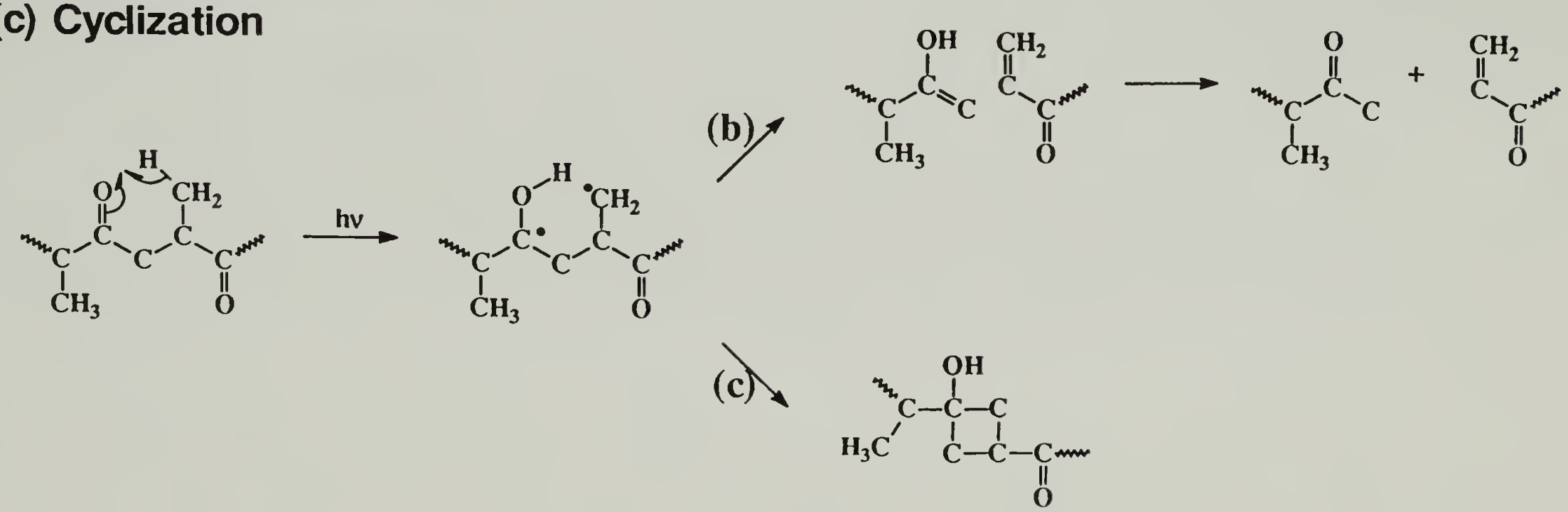

The purpose of this study is to investigate the photolysis mechanisms of ethylene and propylene carbon monoxide alternating copolymers. Significant differences were found between the two materials.

6.2 Experimental

6.2.1 Materials

The alternating copolymers were prepared by polymerizations of α-olefin and CO catalyzed by catalyst **3** as described previously. Most chain end groups of P-CO alternating copolymer are -C(O)OCH_3 types, with a small proportion of chain end groups being CH_3CH=CHCOP and CH_2=C(CH_3)COP. They are different from the Norrish type II photolysis product which is CH_2=CHCOP (*vide infra*).

6.2.2 Polymer Characterization

The molecular weight of the degraded polymer was determined by Water GPC using $CHCl_3$ as solvent. The GPC column used was Jordi 500 Å which was specifically designed for low molecular weight (100-25,000) measurement. Infrared spectra of the polymers, both before and after photolysis, were

run on a Nicolet IR/32 FTIR spectrometer, using the thin films (vide infra). DSC was performed on a Du Pont 2000 thermoanalysis system with a 20 °C/min heating rate. The ultraviolet spectra were taken on a Perkin-Elmer Lambda Array 3840 UV spectrophotometer.

6.2.3 Photolysis

A RPR-100 Rayonet photochemical chamber manufactured by the Southern New England Ultraviolet Co. was used in this study. The intensity of the 2537 Å light was measured by using uranyl oxalate actinometry.[8] The result of the light intensity calibration was in close agreement with the intensity reading supplied by the company.

A thin film of alternating copolymer was photolyzed. P-CO copolymer film was prepared by solvent casting of copolymer (10.5 mg) dissolved in chloroform onto a 25×4 mm NaCl salt and dried to constant weight. E-CO copolymer film was made by compression molding.

A quartz cell, 3.5 cm in diameter and 5 cm high, was constructed to enable measurement in the absence of oxygen. The cell was purged with argon in all the photochemical reactions. The ultraviolet spectrum of each sample was

recorded before photolysis to determine the optical density of the alternating copolymer film.

6.3 Results and Discussion

Photolysis of the P-CO copolymer results in a decrease in molecular weight and weight loss. NMR was found to be unhelpful in monitoring the photodegradation. ^{13}C-NMR is too low in sensitivity. Each P-CO copolymer film weighs only 10.5 mg. Forty films have to be irradiated and combined for NMR spectral analysis. The meaningfulness of such measurements is questionable. ^{1}H-NMR is in principle a useful technique. The copolymer is known to have $CH_3CH=CHC(O)$- (I) and $CH_2=C(CH_3)CO$- (II) end groups. The Norrish type II product will have the end group $CH_2=CHCO$- (III). In the virgin polymer neither I or II was detectable with 50× sensitivity. After 20 min of UV exposure, weak resonances at 5.1-5.6 ppm were detected with high gain. The S/N ratio is so poor that measurement has no quantitative value.

The intense carbonyl IR band of P-CO copolymer was located around 1700 cm^{-1} (Figure 6.2). The infrared spectrum of the degraded polymer shows an increase in the absorbance at 11.0 μm (912 cm^{-1}, Figure 6.3), which was also observed by Hartley and Guillet[9] in the photolyzed 0.99-0.01 E-CO

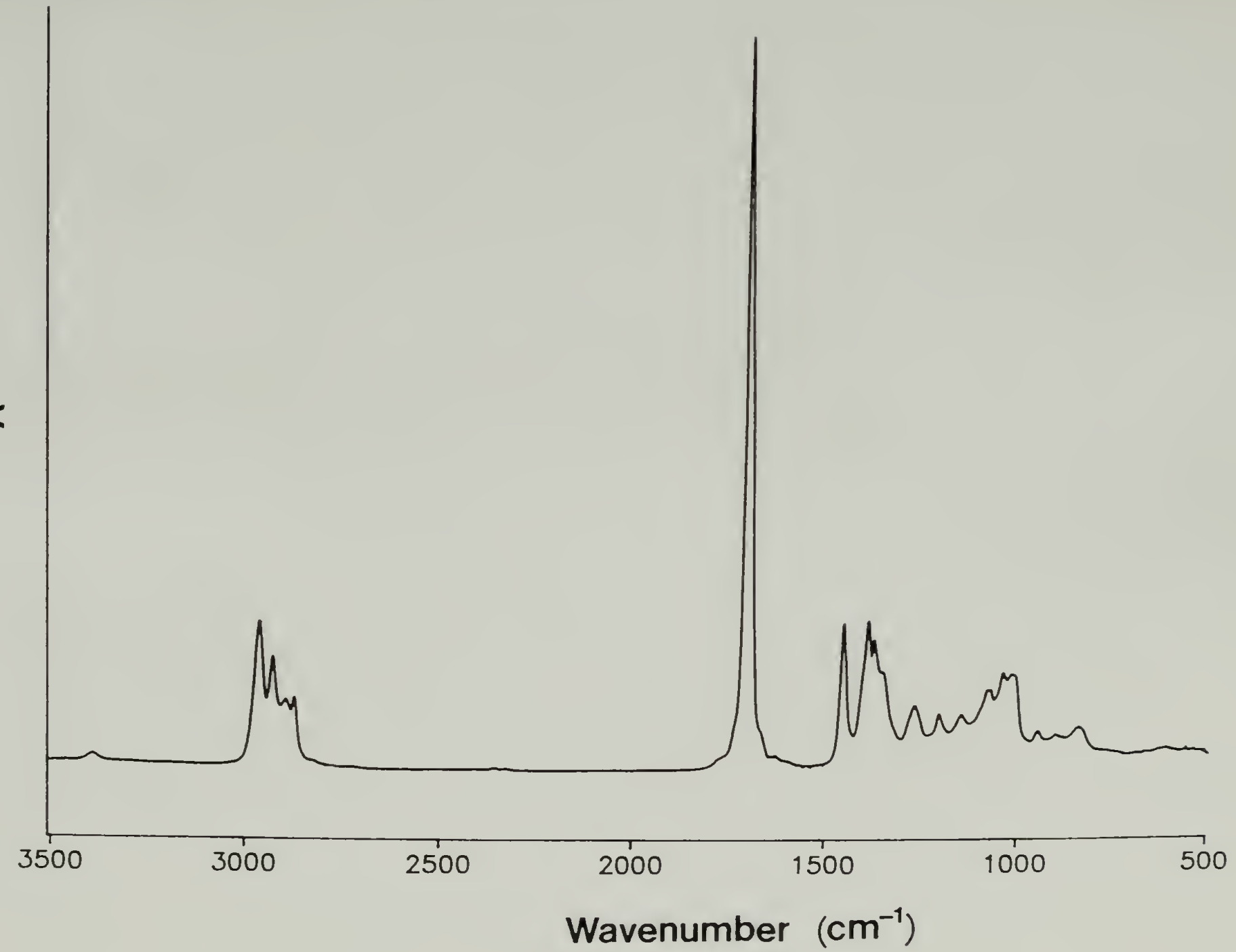

Figure 6.2 IR absorbance spectrum of P-CO alternating copolymer.

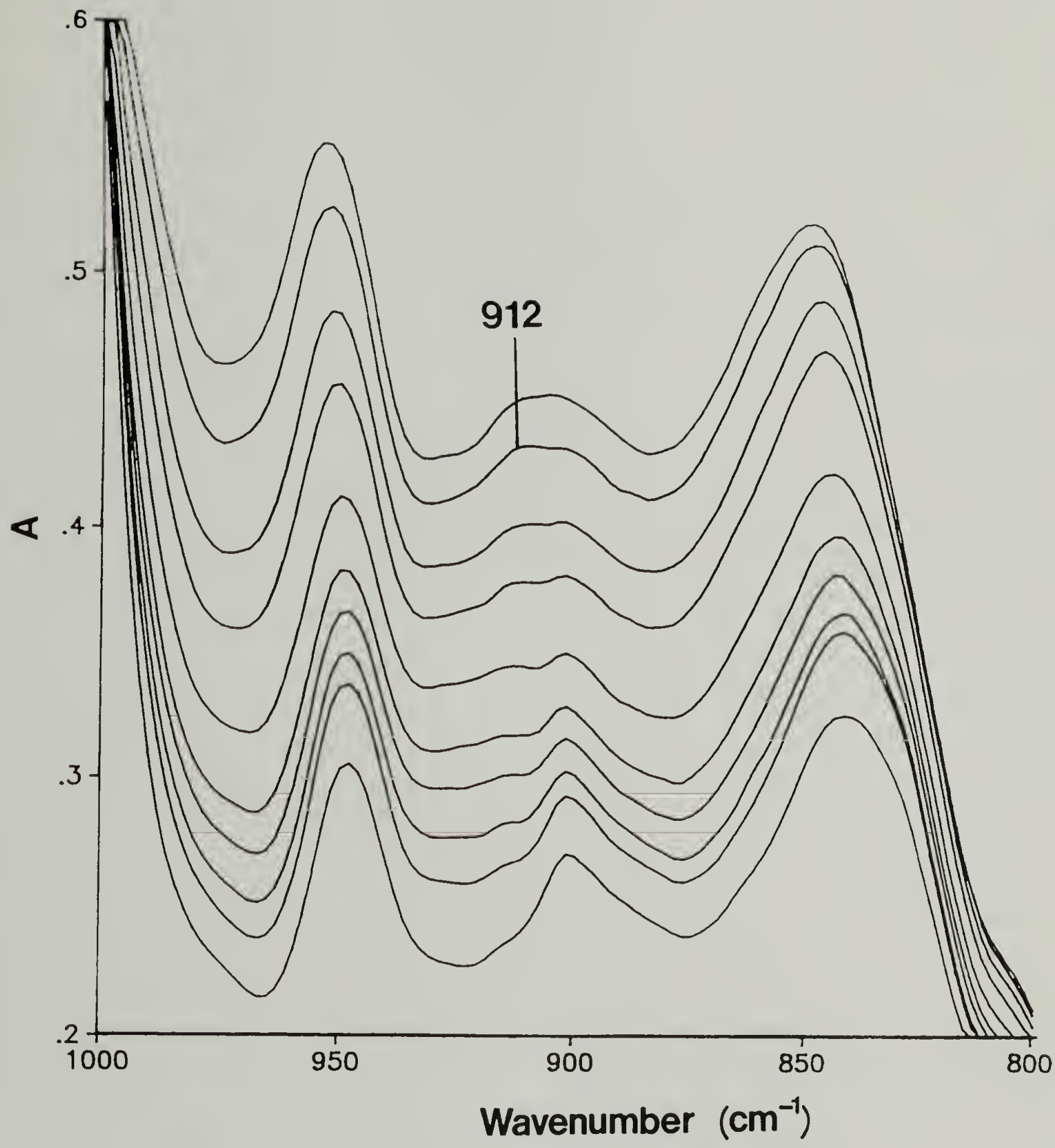

Figure 6.3 IR absorbance spectra (800-1000 cm^{-1} region) of degraded P-CO alternating copolymers. The curves from bottom to top represent the spectra of the polymer having 0, 10, 20, 30, 40, 60, 90, 120, 180, and 240 min of UV exposure.

copolymer. They assigned this band to terminal vinyl double bonds $RCH=CH_2$. There was also an increase in the absorbance around 3480 cm^{-1}, characteristic of the -OH group as depicted in Figure 6.4. The absorbance at 3400 cm^{-1} is assigned to the overtone of the C=O stretching frequency. The photolyzed P-CO copolymer has a UV spectrum shifted to long wavelength as compared to the virgin material (Figure 6.5). This red shift may be attributed to the formation of an α, β-unsaturated ketone, $CH_2=CHC(O)P$.

The above results are consistent with the degradation mechanism for the P-CO copolymer based on the Norrish type I and type II reaction (Figure 6.1). The former produces radicals (Figure 6.1a) and evolves carbon monoxide, whereas the latter (Figure 6.1b) yields a ketone and a terminal vinyl group. Both processes cause main chain scission and reduction of MW. The weight loss is mainly due to the elimination of CO following the Norrish type I process.

If $(M_n)_o$ is the number average molecular weight of the starting material, and M_n is the number average molecular weight of the degraded polymer, then $[(M_n)_o/M_n - 1]$ is equal to the average number of polymer bonds severed per initial polymer molecule. Therefore, the quantum yield of chain scission (ϕ_{sc}) can be calculated by using eq. 1.

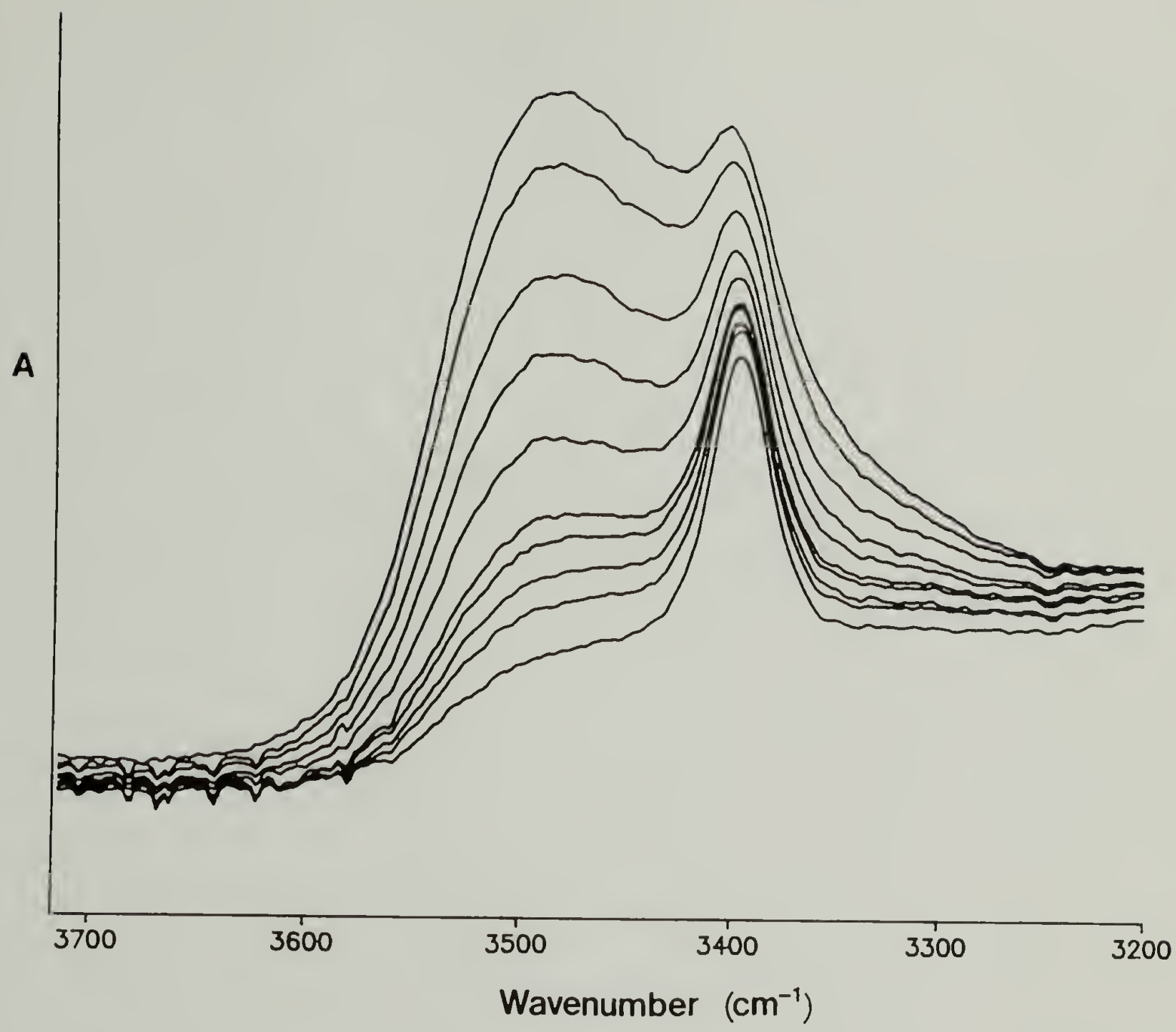

Figure 6.4 IR absorbance spectra (3200-3750 cm^{-1} region) of degraded P-CO alternating copolymers. The curves from bottom to top represent the spectra of the polymer having 0, 10, 20, 30, 40, 60, 90, 120, 180, and 240 min of UV exposure.

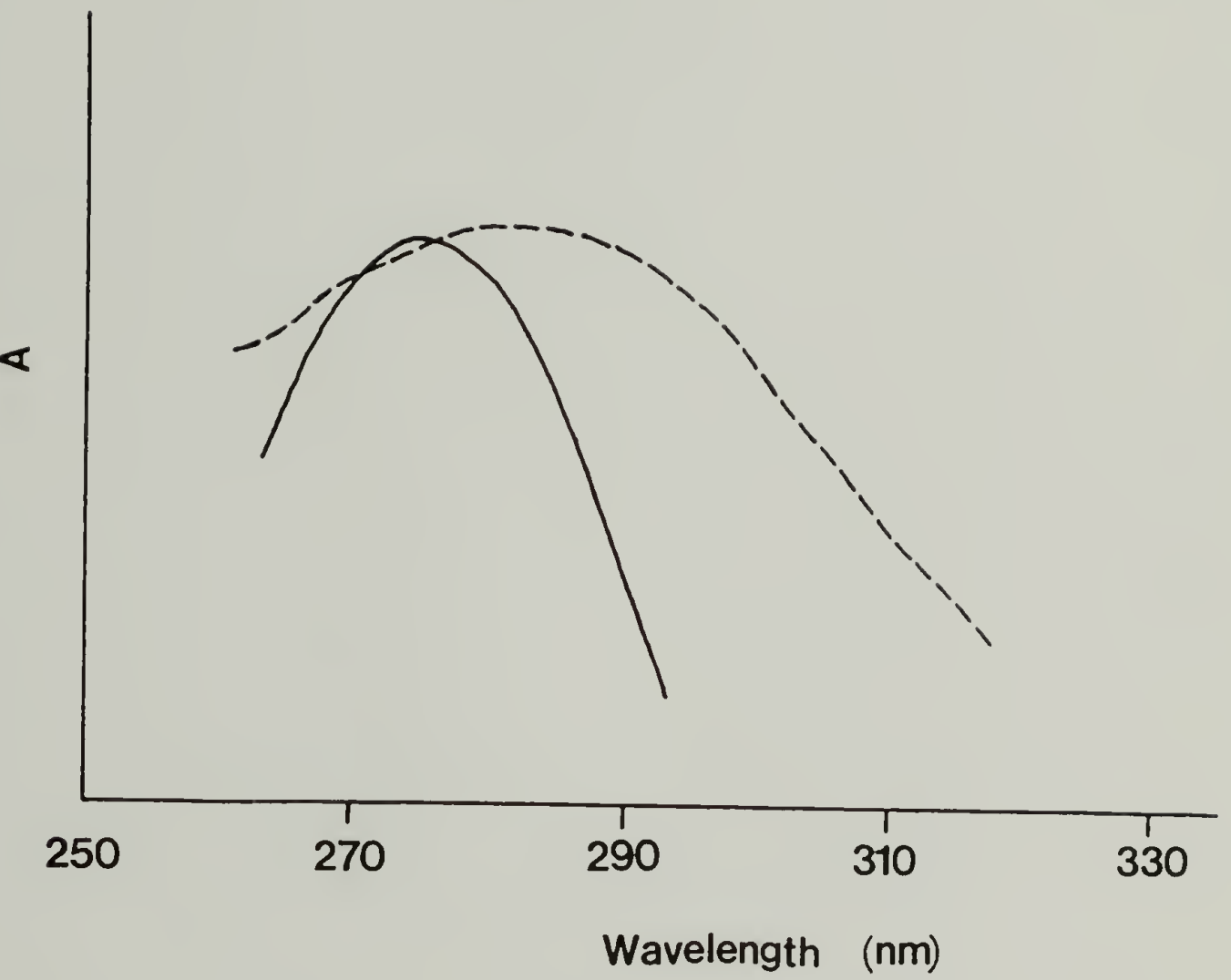

Figure 6.5 UV spectra of P-CO polymers having 0 (solid line) and 120 (dotted line) min of UV exposure.

$$\phi_{sc} = \frac{d\left[\frac{(M_n)_o}{M_n} - 1\right]}{d(I_a t)} \times \frac{W}{(M_n)_o} \qquad (1)$$

where I_a is absorbed light intensity per second, t is time in seconds, and W is the initial weight of the polymer. Figure 6.6 shows the increase in $[(M_n)_o/M_n - 1]$ as the photolysis progresses. It can be seen that the rate of bond breaking is initially linear but slows down as the reaction proceeds. Knowing the amount of light absorbed by calibration and using the initial slope of the curve in Figure 6.6, we calculated the quantum yield of chain scission for bulk P-CO copolymer to be 0.015 ± 0.002 at ambient temperature.

Hartley and Guillet[9] had proposed an explanation for the observed decrease in the rate of chain scission with the progress of photolysis. One of the Norrish type II reaction products is a polymer chain which terminates in a $CH_3C(=O)$- group. The concentration of these groups increases as the photolysis proceeds; the photo reaction of these groups by either type I or type II reaction would produce no detectable change in the molecular weight. Besides this apparent reason, we can offer another explanation which is probably more important here. The radicals generated by type I reaction will cause crosslinking in the copolymer which in turn will slow

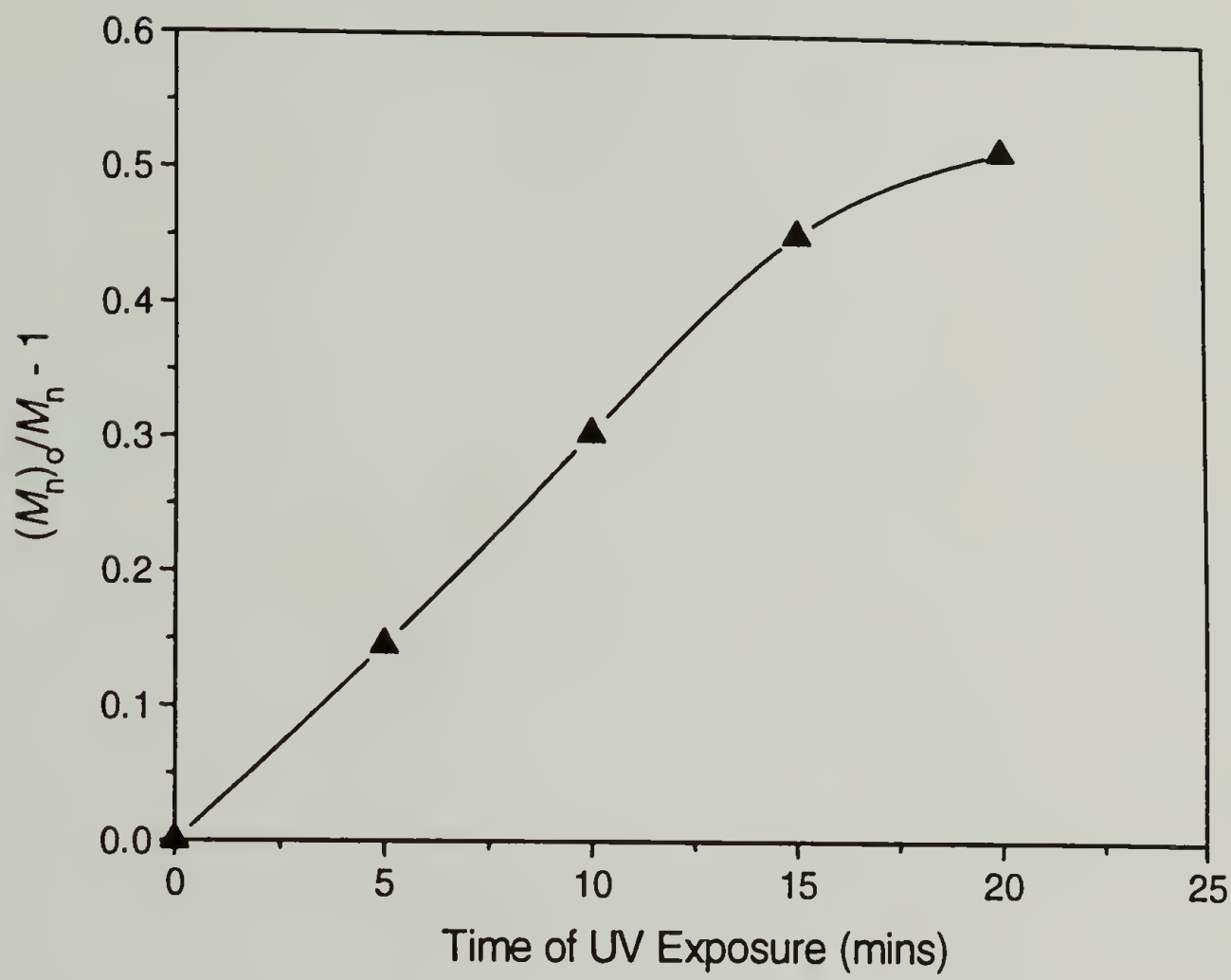

Figure 6.6 Number of backbone chain scissions as a function of the UV exposure time during photolysis of bulk P-CO alternating copolymer at ambient temperature: 10.5 mg of polymer was cast on the 25×4 mm NaCl plate; film thickness = 1.8×10^{-3} cm; intensity of light absorbed = 8.0×10^{6} einstein/g•s or 1.7×10^{-8} einstein/cm²•s. $(M_n)_o$ = 4170.

down the depression of molecular weight. In the later stage of the photolysis, the molecular weight will even increase. This explanation was evidenced by the fact that the P-CO thin film became partially insoluble in any organic solvent after 30 min of UV exposure, while the films irradiated for 5, 10, 15 and 20 min could be easily dissolved in the chloroform.

The infrared absorbance of the degraded polymers at 912 cm^{-1} (11.0 μm), characteristic of vinyl double bonds, is expressed as the absorbance, *A*, in eq. 2,

$$A = \varepsilon bc \qquad (2)$$

where *b* is the film thickness, *c* is the concentration of the terminal vinyl double bond in bulk P-CO copolymer, and ε is the extinction coefficient for the vinyl double bond produced in type II reaction. We can further write

$$\frac{\Delta A_1}{\Delta A_2} = \frac{b_1 c_1}{b_2 c_2} \qquad (3)$$

Figure 6.7 is the plot of ΔA versus time of UV exposure; the data are taken from Figure 6.3. The curve shows an increase in the absorbance at 912 cm^{-1} with the progress of photolysis. Using the initial rate and a set of *A*, *b*, and *c*,[9] a value of c_2 for

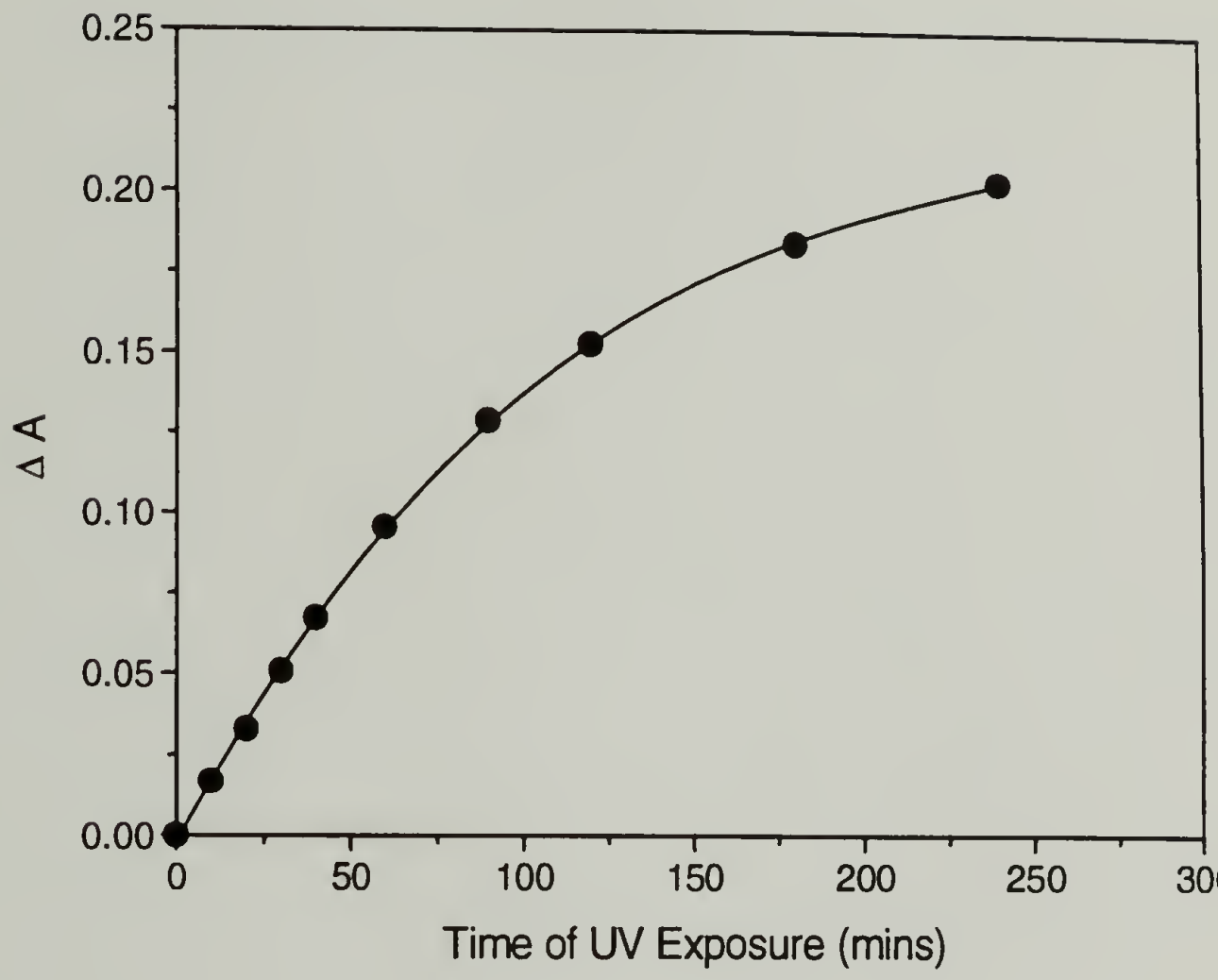

Figure 6.7 Increase in the absorbance at 912 cm-1 (11.0 μm) as a function of the UV exposure time during photolysis of bulk P-CO alternating copolymer. The data are taken from Figure 6.3.

the vinyl double bond molar concentration in P-CO polymer at a given time of UV exposure could be calculated. The quantum yield for vinyl double bond production or Norrish type II reaction, ϕ_{II}, was thus determined to be 0.011 ± 0.002 in solid phase at ambient temperature.

Similar to the rate of chain scission, the rate of vinyl double bond production slows down in the later stage of the photolysis, possibly due to the reaction of the olefinic species with radicals generated in the type I reaction.[9]

The similarity of the values of ϕ_{II} and ϕ_{sc} for P-CO copolymer indicates that most of the chain scissions are the result of the Norrish type II process. Norrish type I reaction contributes very little (< 25%) to the backbone scission. The low quantum efficiency of the latter can be explained by the "cage effect".[10,11] Radical pairs produced by photolysis or thermolysis either can recombine within the cage at the site of their formation, which is about one molecular diameter in dimension or can be separated by diffusion. The fraction of the former event, "cage recombination", increase with an increase in the viscosity of the medium. Therefore, the efficiency of cage recombination of the radical pair generated by Norrish type I is higher in bulk P-CO copolymer than in liquid medium and is even greater in highly crystalline E-CO copolymer (*vide infra*).

Conversely, the quantum efficiencies of chain scission following the Norrish type I process decrease in this order.

It is interesting to compare the ϕ_{II} of P-CO alternating copolymer to the ϕ_{II} of 0.99-0.01 E-CO copolymer studied by Hartley and Guillet. Their result showed $\phi_{II} = 0.025 \pm 0.003$ for the 0.99-0.01 E-CO copolymer in the solid phase. Both materials have T_g much lower than the ambient temperature; The T_g of P-CO copolymer was measured to be -8 °C. So, at the ambient temperature, as was shown for the 0.99-0.01 E-CO copolymer,[9] ϕ_{II} is independent of temperature provided it is higher than T_g. A possible explanation for higher ϕ_{II} of 0.99-0.01 E-CO copolymer than that of the P-CO copolymer may be due to the difference between the two types of γ-hydrogen atoms abstracted in their photolysis. The type II reaction involved abstraction of hydrogen to form a biradical (Figure 6.1a); the relative reactivities would be expected to be sensitive to the substitution at the γ-carbon atoms.[12] Ausloos[13] found that there is a 13/1 preference for attack on the secondary position in 4-methyl-2-hexanone for the type II reaction. Nicol and Calvert[14] showed that ϕ_{II} involving secondary γ-carbon is 7 times higher than that involving primary γ-carbon atom for the 4-octanone. They also showed that the total ϕ_{II} of 4-octanone is 1.8 times larger than the total ϕ_{II} for 4-heptanone. Wagner and Hammond[12] performed quenching experiments which

demonstrated that the abstraction of a secondary γ-hydrogen atom was easier than the abstraction of a primary γ-hydrogen. In the 0.99-0.01 E-CO copolymer, each carbonyl group was separated on the average by 200 methylenes. Therefore, it is a secondary γ-hydrogen being abstracted by the carbonyl carbon in type II reaction. For P-CO copolymer, however, the primary γ-hydrogen will be abstracted due to the alternating structure. The above argument justifies the higher ϕ_{II} of 0.99-0.01 E-CO copolymer than that of the P-CO alternating copolymer. There is another trivial factor which may contribute to difference between the two ϕ_{II}'s. The P-CO copolymer was irradiated by a 253.7 nm lamp, while the 0.99-0.01 E-CO copolymer was photolyzed by 313.0 nm light.

The observance of the -OH group (Figure 6.4) during the photolysis of P-CO copolymer may be attributed to the formation of several types of alcohol. An alternative pathway for the Norrish type II process is the combination of radicals following H abstraction. Cyclobutanol could be formed as the result of the cyclization (Figure 6.1c). Figure 6.8a and 6.8b show other pathways which may produce an alcohol. Radicals produced in the type I reaction can attack a carbonyl carbon; the resulting alkoxy radical subsequently abstracts a hydrogen atom to form tertiary alcohol (Figure 6.8a). The major difference between these two processes is that the one in

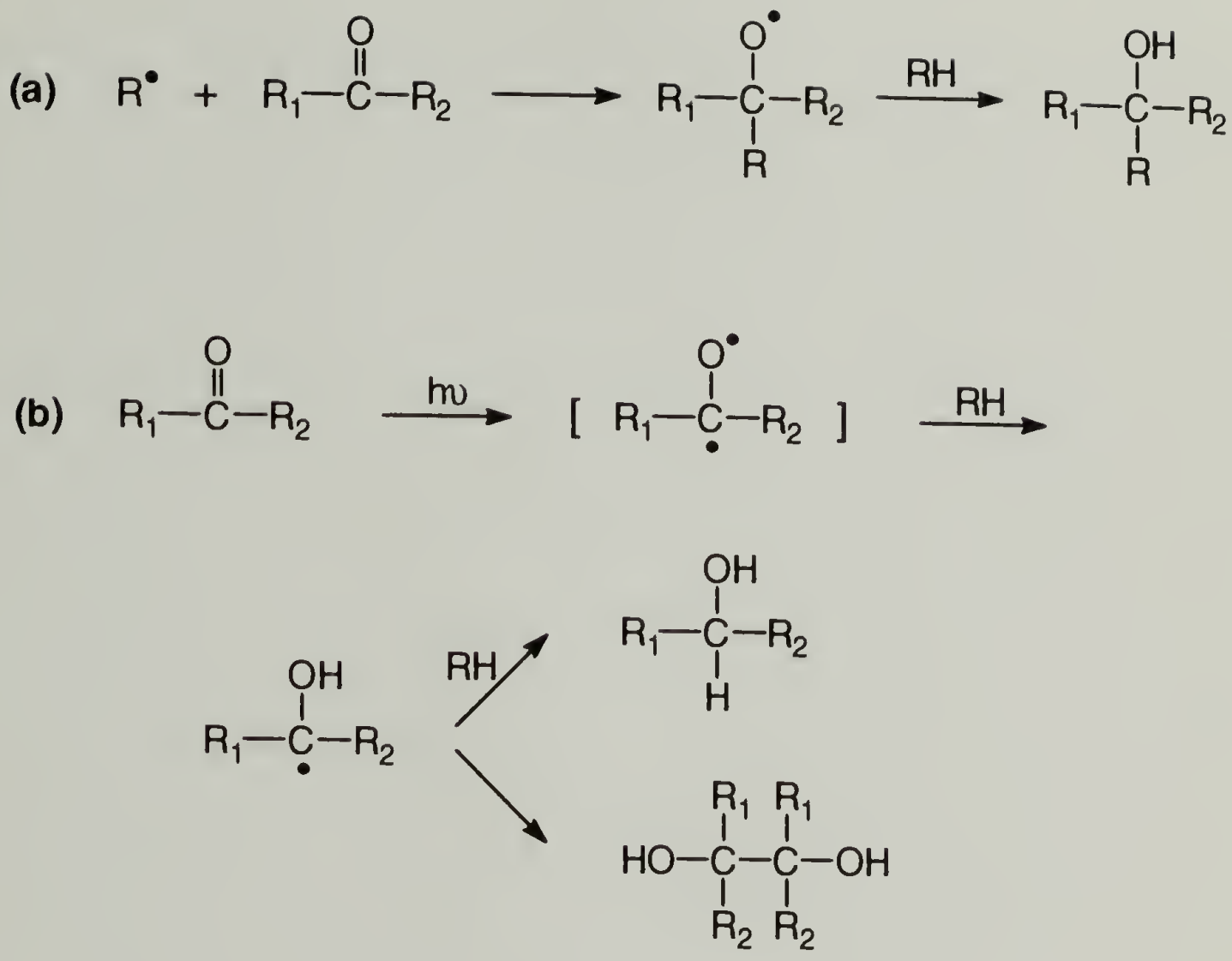

Figure 6.8 Alternative pathways which may produce an alcohol.

Figure 6.1c is intramolecular, while the one in Figure 6.8a is intermolecular. The necessary condition for the process illustrated in Figure 6.8b to occur is the presence of good hydrogen donors. If the keto radicals are present at high enough concentrations or have long lifetimes, they may combine to form pinacols.[8] The relative contributions of these three processes may be revealed by studying the photolysis of E-CO alternating copolymer.

The absence of the IR absorption peak around 900 cm^{-1} for the E-CO copolymer after 1 hour of UV irradiation indicates no vinyl double bonds were formed; therefore, Norrish type II reaction did not occur. This is expected because there is no γ-hydrogen in the polymer. Figure 6.9 shows that there is an increase of absorbance around 3480 cm^{-1} for E-CO polymer with 1 hour of UV exposure, which indicates the formation of an -OH group. Since the E-CO alternating copolymer lacks a γ -hydrogen, the process shown in Figure 6.1c is not suitable for accounting for the formation of an -OH group. Furthermore, the biradical generated in Figure 6.8b would prefer to undergo radiationless relaxation because the polymer is a poor hydrogen donor. Therefore, the -OH group in E-CO copolymer is more likely to be produced by the process given in Figure 6.8a. If P-CO copolymer behaves similarly, we expect the process described in Figure 6.8a to be the source for the -OH

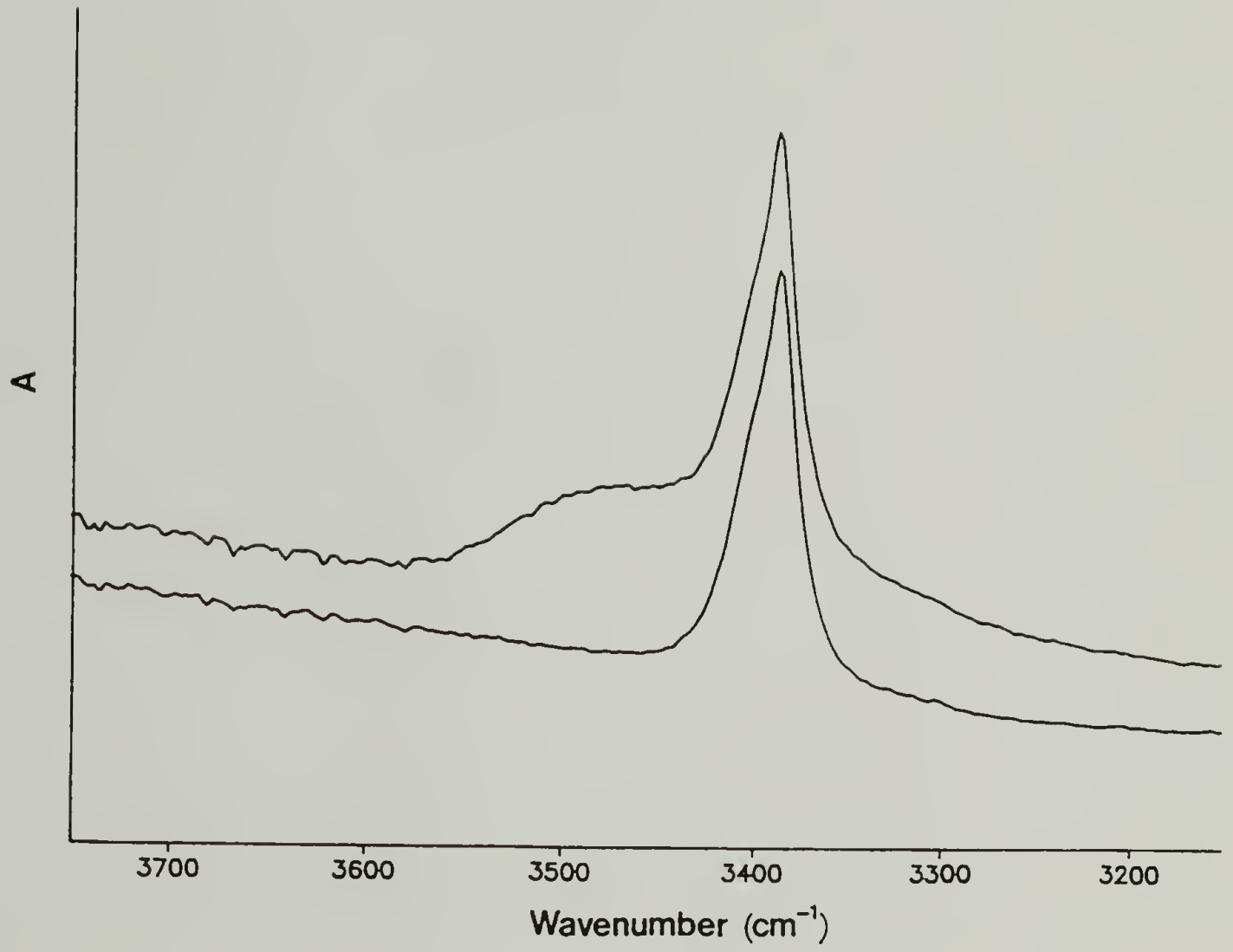

Figure 6.9 IR absorbance spectra (3150-3750 cm-1 region) of the E-CO alternating copolymers having 0 (bottom curve) and 60 (top curve) min of UV exposure.

production in P-CO as well. Obviously, more rigorous proof is needed to make a firm conclusion.

The weight loss behaviors of P-CO and E-CO copolymers are shown in Figure 6.10 by plotting (W_o/W_n - 1) versus time of UV exposure (W_o, original weight; W_n, degraded polymer weight). The rate of weight loss for the P-CO copolymer is about 3 times as fast as that for E-CO copolymer, which suggests that the Norrish type I reaction rate for P-CO is faster than that for E-CO. There is a ready explanation for this phenomenon. The type I reaction of E-CO copolymer generates primary radicals, situated in strong cages of a crystalline E-CO copolymer environment. Cage recombination is more probable than a similar event in the P-CO copolymer. Therefore, the net quantum yield of type I reaction for E-CO copolymer is lower than that for the P-CO copolymer.

Some Pd complexes are photoactive. It is not possible to remove all catalyst residues from the alternating copolymers. The effect of these residues on photolysis has been considered. We used 0.02 mmol of Pd catalyst to produce 5.7 g of P-CO copolymer. Therefore, the mole ratio of the repeat unit $-CH_2CH(CH_3)C(O)-$ to the Pd catalyst is 4.1×10^3 : 1 (the actual ratio is greater than this because some catalysts may dissolve in the methanol when the polymer was precipitated with it). The Pd catalyst may absorb the light and therefore, reduce the

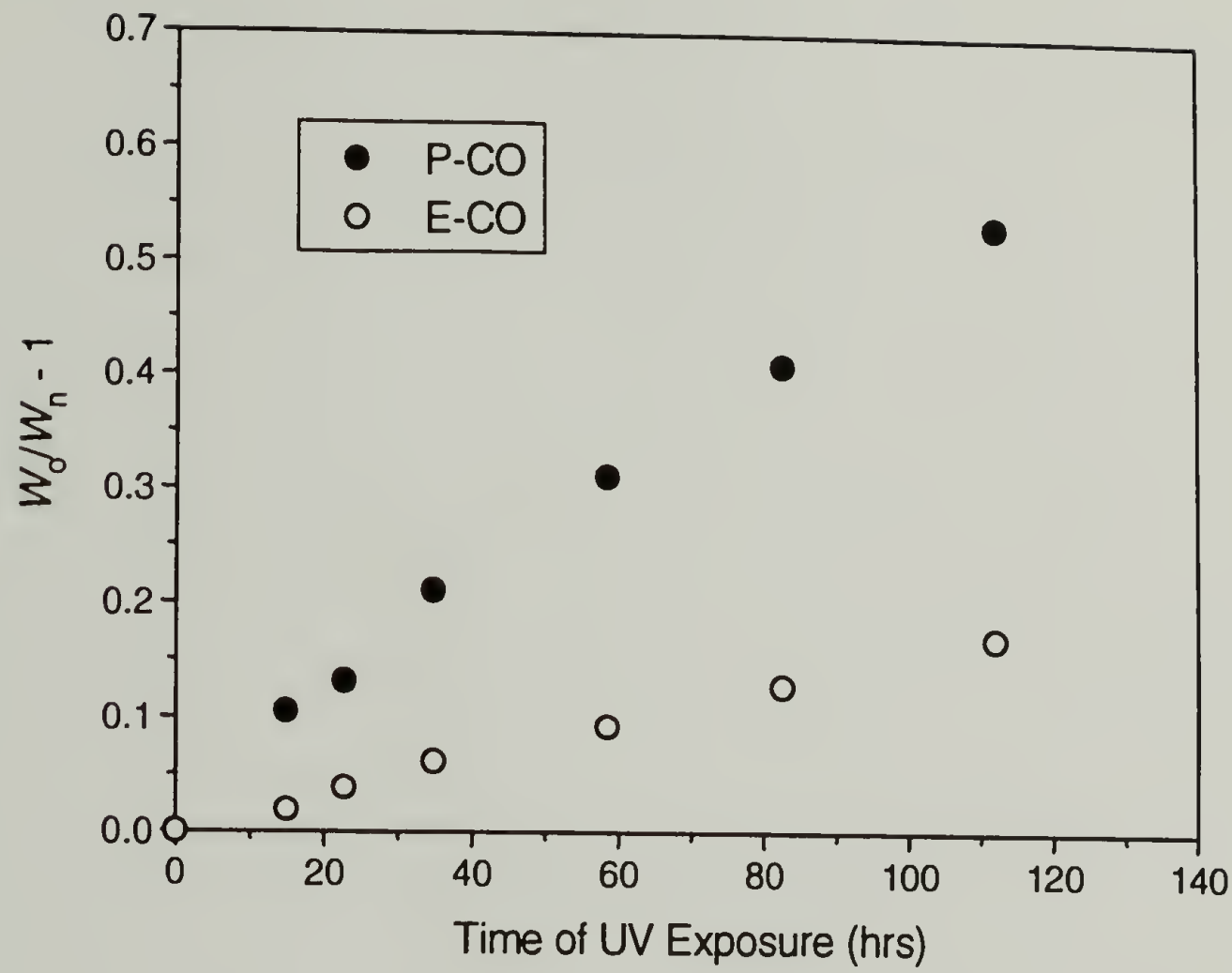

Figure 6.10 Increase of the weight loss of P-CO copolymer (solid circle) and E-CO copolymer (unfilled circle) as a function of the UV exposure time during photolysis in the solid phase : 38 mg of P-CO and E-CO copolymers were compressed-molded under the same pressure. The resulting two films have diameters of 1.9 cm.

ϕ_{II} of the copolymer. However, neither the amount nor the structure of the catalyst residue is known. So we added 0.04 mmol of Pd catalyst to 5.7 g of methanol precipitated P-CO copolymer and solvent casted into films. The ϕ_{II} for this material was found to be 9.7×10^{-3}, which is within experimental error of $\phi_{II} = 0.011 \pm 0.002$ for the copolymer without catalyst added intentionally. Therefore, any Pd residues have no measurable effect on the photodegradation of the P-CO alternating copolymer.

References

(1) Bremer, Y. P. *Polym. Plast. Technol. Eng.* **1982**, *18*, 137.

(2) Guillet, J. E.; Dhanraj, J.; Golemba, F. J.; Hartley, G. H. *Adv. Chem. Ser.* **1986**, *85*, 272.

(3) Heskins, M.; Guillet, J. E. *Macromolecules* **1968**, *1*, 97.

(4) Golemba, F.; Guillet, J. E. *Macromolecules* **1972**, 5, 212.

(5) Amerik, Y.; Guillet, J. E. *Macromolecules* **1971**, *4*, 375.

(6) Guillet, J. E. *Polymer Photophysics and Photochemistry* Cambridge, U.K.: Cambridge University Press, **1985**.

(7) Yang, N. C.; Yang, D. H. *J. Am. Chem. Soc.* **1958**, *80*, 2913.

(8) Leighton, W. G.; Forbes, G. S. *J. Am. Chem. Soc.* **1930**, *52*, 3139.

(9) Hartley, G. H.; Guillet, J. E. *Macromolecules* **1968**, *1*, No. 2, 165.

(10) Franck, J.; Rabinowitch, E. Trans. Faraday Soc. **1934**, *30*, 120.

(11) Noyes, R. M. *Prog. React. Kinet.* **1961**, *2*, 129.

(12) Wagner, P. J.; Hammond, G. S. *J. Am. Chem. Soc.* **1965**, *87*, 4009.

(13) Ausloos, P. J. *Phys. Chem.* **1961**, *65*, 1616.

(14) Nicol, C. H.; Calvert, J. G. *J. Am. Chem. Soc.* **1967**, *89*, 1790.

CHAPTER 7

NEW MISCIBLE POLYMER BLENDS OF PROPYLENE-CARBON MONOXIDE ALTERNATING COPOLYMER WITH POLY(METHYL METHACRYLATE)

7.1 Introduction

Both amorphous and semicrystalline propylene-carbon monoxide (P-CO) alternating copolymers (ACP) have been synthesized by us and other groups.[1-7] It has the general structure of polyketone. P-CO along with ethylene-carbon monoxide copolymer has the potential of being used as photo-degradable material.[8] We have now blended the amorphous P-CO with poly(methyl methacrylate) (PMMA) in order to improve the impact strength of PMMA. The blends were found to be miscible at all composition. Several techniques, such as differential scanning calorimetry (DSC), dynamic mechanical thermal analysis (DMTA), dynamic dielectric thermal analysis (DETA), Fourier transform infrared (FTIR) spectroscopy, and solid state cross-polarization magic angle spinning (CP-MAS) NMR, have been used to provide a broad data base for this new blend system.

7.2 Experimental

7.2.1 Materials

The alternating copolymer was prepared by polymerizing of propylene and CO catalyzed by catalyst **3** as described previously. The copolymerization condition for P-CO is as follows: catalyst (0.02 mmol), methanol (1 mL), 1,2-dichloro-ethane as solvent (150 mL), 80 psig propylene, 720 psig CO, at 0-20 ^{o}C for 24 hours. A 300-mL Paar reactor was dried and purged with argon, and then the catalyst, methanol, and solvent were cannulated into it. Propylene and carbon monoxide were introduced in turn. The mixture was cooled to the polymerization temperature. At the end of a copolymerization the unreacted monomers were vented, and the copolymer was purified by precipitation with methanol and dried in vacuo at ambient temperature for 24 hours. The number average molecular weight of the copolymer is around 20,000. PMMA was purchased from Scientific Polymer Products, Inc. with the number average weight of 35,000 (catalogue No. 037A). The blends were prepared by dissolving the appropriate amounts of each polymer in chloroform and stirred for 3 days, followed by precipitation into a large excess of hexane. The resulted mixture were then repeated washed

and subsequently dried in vacuo at 50 °C for 2 days. No evidence of any solvent residue was seen from TGA measurement. Some film samples for FTIR analysis was prepared by slow solvent casting from chloroform. All blend films were clear and transparent.

7.2.2 Blends Characterization

DSC was performed on a Du Pont 2000 thermoanalysis system with 20 °C/min heating rate. T_gs were taken as the midpoint of heat capacity increment from the second scan. DMTA was done on a Polymer Laboratories DMTA MKI model. GenRad/689M Digibridge controlled by Polymer Laboratories DETA system I was used for the dynamic dielectric thermal analysis (DETA). Cloud-point determinations were performed by using a programmable hot stage in conjunction with a simple He-Ne laser light scattering device.

All solid state NMR measurements were taken on an IBM 200 AF spectrometer equipped with an IBM Solid Accessory and Doty CP-MAS probe. Samples were generally spun at 4.0-4.5 kHz and cross-polarized at 50 kHz fields (6 μs and 5μs 90° pulses for ^{1}H and ^{13}C, respectively). The Hartman-Hahn match was adjusted prior to every run using a di-*tert*-butylbenzene standard. Proton spin-lattice relaxation time in the rotating

frame, $T_{1\rho}^{H}$, was measured through change in cross-polarized carbon signal intensities after variable ^{1}H spin lock time, τ.[9] Proton spin-lattice relaxation time in the laboratory frame, T_1^{H}, was determined via inversion-recovery pulse sequence in a cross-polarization transfer experiment.[10] Quadrature detection and phase alternation was used throughout.

7.3 Results and Discussion

7.3.1 Thermal Analysis

The second scans of DSC trace for pure PMMA, pure P-CO, and a 50:50 blend are shown in Figure 7.1. The glass transition temperatures for pure P-CO and PMMA are 22 °C and 109 °C, respectively. Because T_gs for pure components were separated far enough, T_gs of blends can be used as an indicator for miscibility. Like the 50:50 blend, blends with different compositions all exhibited single T_g behavior. A plot of T_g versus weight fraction of PMMA for a series PMMA/P-CO blends is shown in Figure 7.2. The dash line represents the simple additive behavior of the two components by weight. The experimental results showed a concave derivation from the dash line. The composition variation of T_g can be described satisfactorily by the Gordon-Taylor equation:[11]

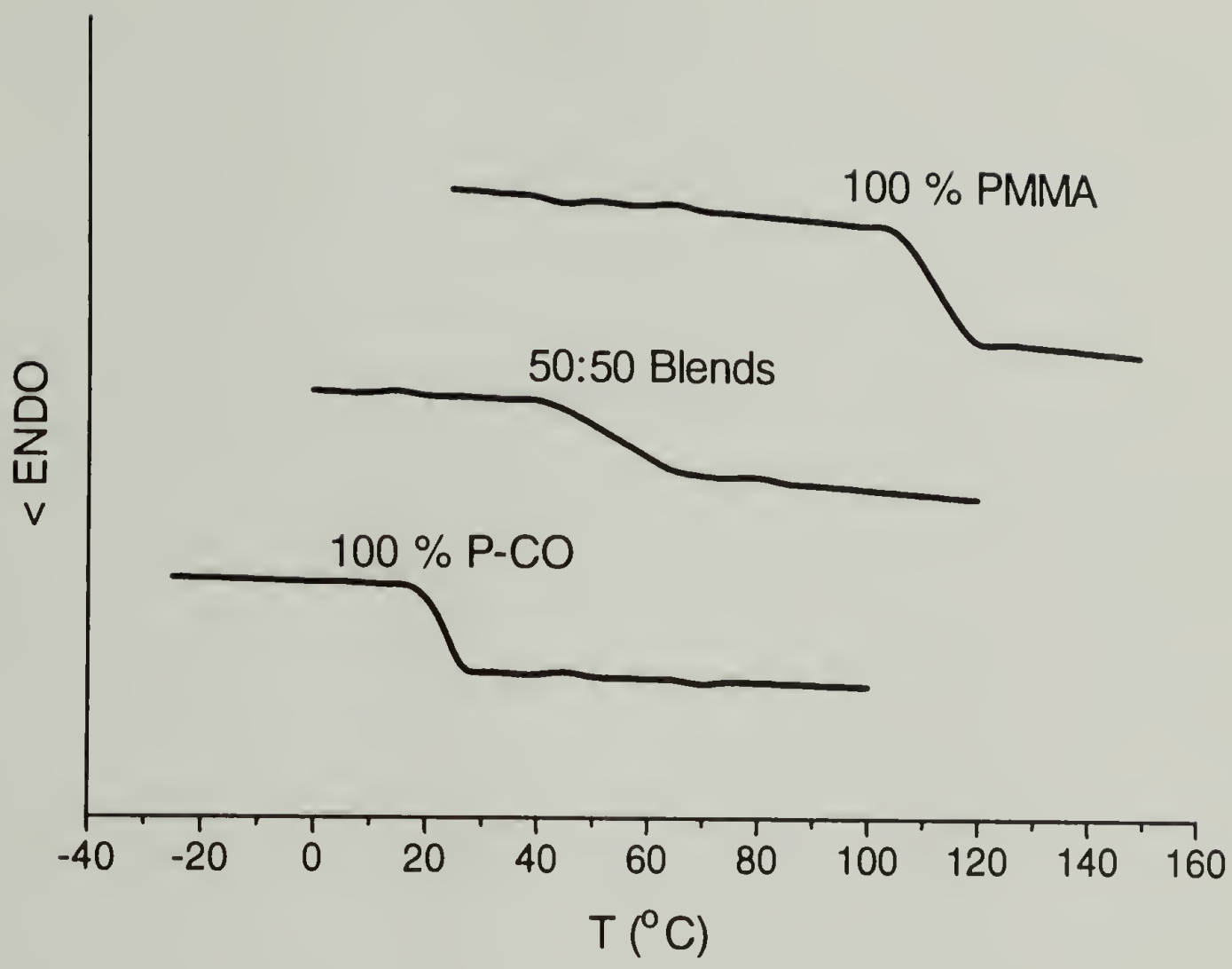

Figure 7.1 Second scans of DSC trace for pure PMMA, pure P-CO, and a 50:50 wt:wt blends.

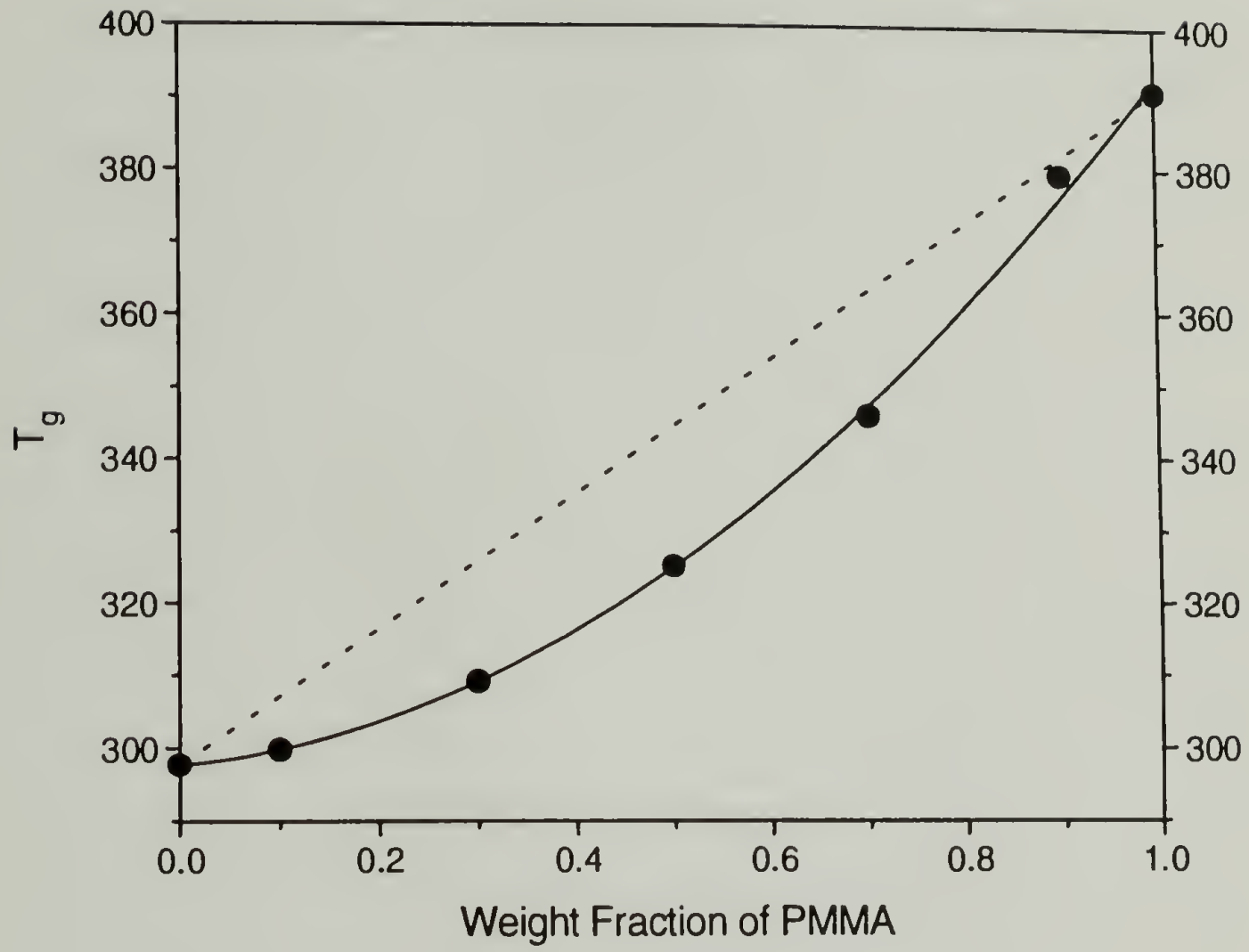

Figure 7.2 T_g as a function of PMMA weight fraction in the blends of PMMA/P-CO. The dash line represents the simple additive behavior of the two components by weight. The experimental results are in filled circles.

$$T_{g,b} = \frac{T_{g,1} + (KT_{g,2} - T_{g,1})W_2}{1 + (K-1)W_2} \qquad (1)$$

where $T_{g,1}$, $T_{g,2}$, and W_2 are the component glass transition temperatures and weight fractions. The fitting parameter K is equal to 0.46. Therefore, the blends are miscible according to the T_g variation.

Cloud-point measurement was performed by using a simple laser scattering device to monitor scattered intensity as a function of temperature. No lower critical solution temperature (LCST) was found for all the blends up to 320 °C, at which P-CO alternating copolymer begins to degrade. The results of cloud-point measurements indicate the blends are miscible.

The mechanical relaxation behavior of the blends was first studied by DMTA. The tanδ is plotted against temperature in Figure 7.3 for pure PMMA and a 30:70 PMMA/P-CO blend. The pure PMMA exhibited both α- and β-relaxation at 125 °C and 30 °C respectively under a frequency of 1 Hz. The β-relaxation of PMMA was generally assigned to the rotation of the -$COOCH_3$ side group;[12] it was suppressed in the blend probably due to the broadened distribution of the relaxation times. The DMTA spectrum of the blend shows a single T_g without observation of β-relaxation of P-CO copolymer. The

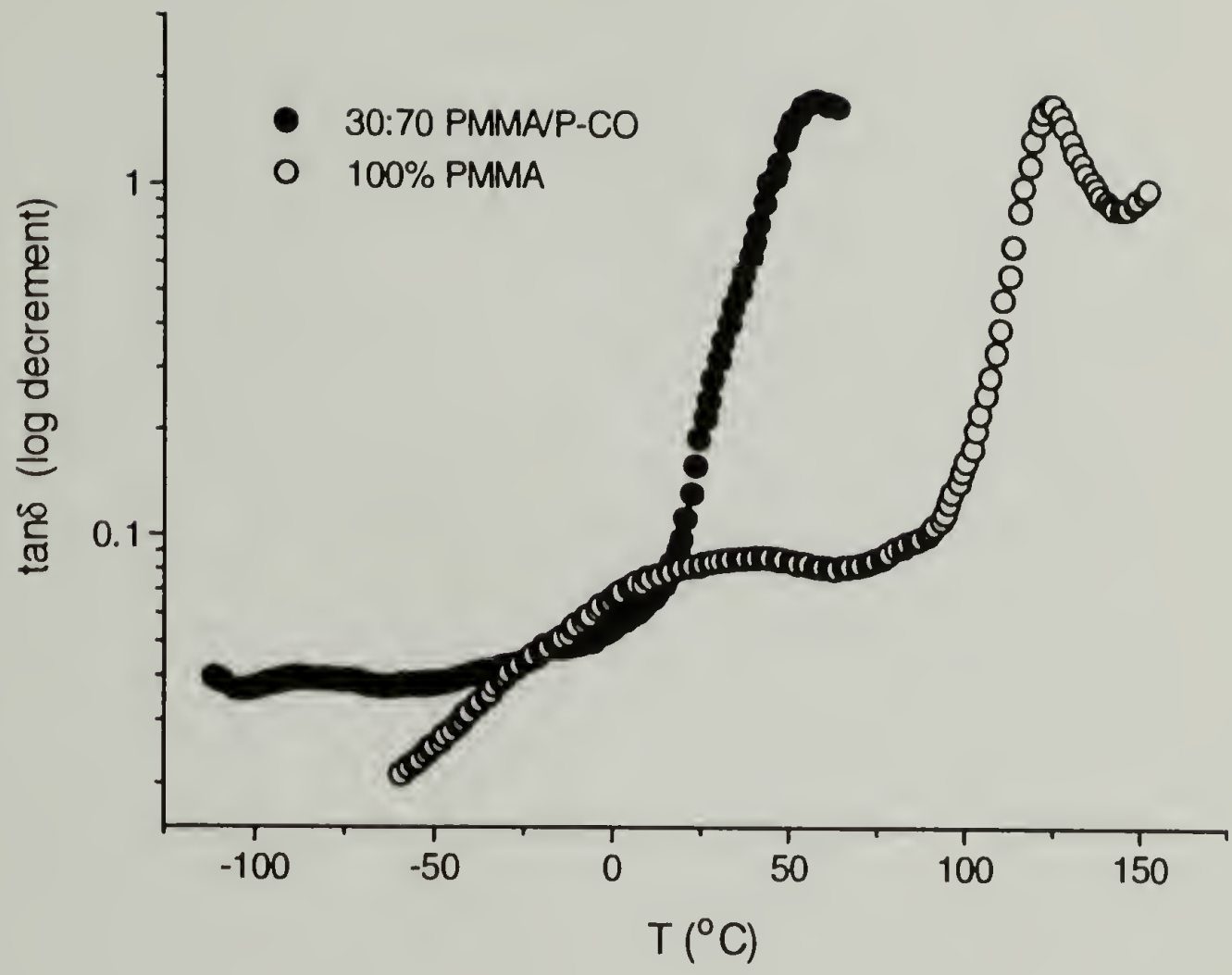

Figure 7.3 DMTA measurement at 1 Hz. Tanδ is plotted versus temperature for pure PMMA and 30:70 PMMA/P-CO blends.

possible β-relaxation of P-CO copolymer can be attributed to the vibration or flipping movement of the carbonyl group; such motion may not affect the mechanical modulus significantly. However, the carbonyl group always exhibits strong dielectric loss peak in dynamic dielectric measurement. The DETA measurements at 1 kHz (Figure 7.4) showed a strong dielectric loss at -60 ^{o}C for the pure P-CO copolymer. Therefore, we can conclude that the β-relaxation is due to the motion of carbonyl group in P-CO ACP.

7.3.2 FTIR Spectroscopy

FTIR studied were performed for the blends of different composition. The IR spectra of carbonyl group stretching region were shown in Figure 7.5. The carbonyl groups of PMMA and P-CO resonate at 1730 and 1707 cm^{-1}, respectively. The most important characteristic band parameters measured in IR spectroscopy are frequency (energy) and intensity (polar character). Both intensity change and frequency shifts provide information on possible specific interactions in polymer blends.[13] As a tool for the discrimination of structural elements, the IR intensities are significantly more sensitive to small changes in structure or bond environment than are the IR frequencies.[14] In the blends of PMMA/P-CO, no significant

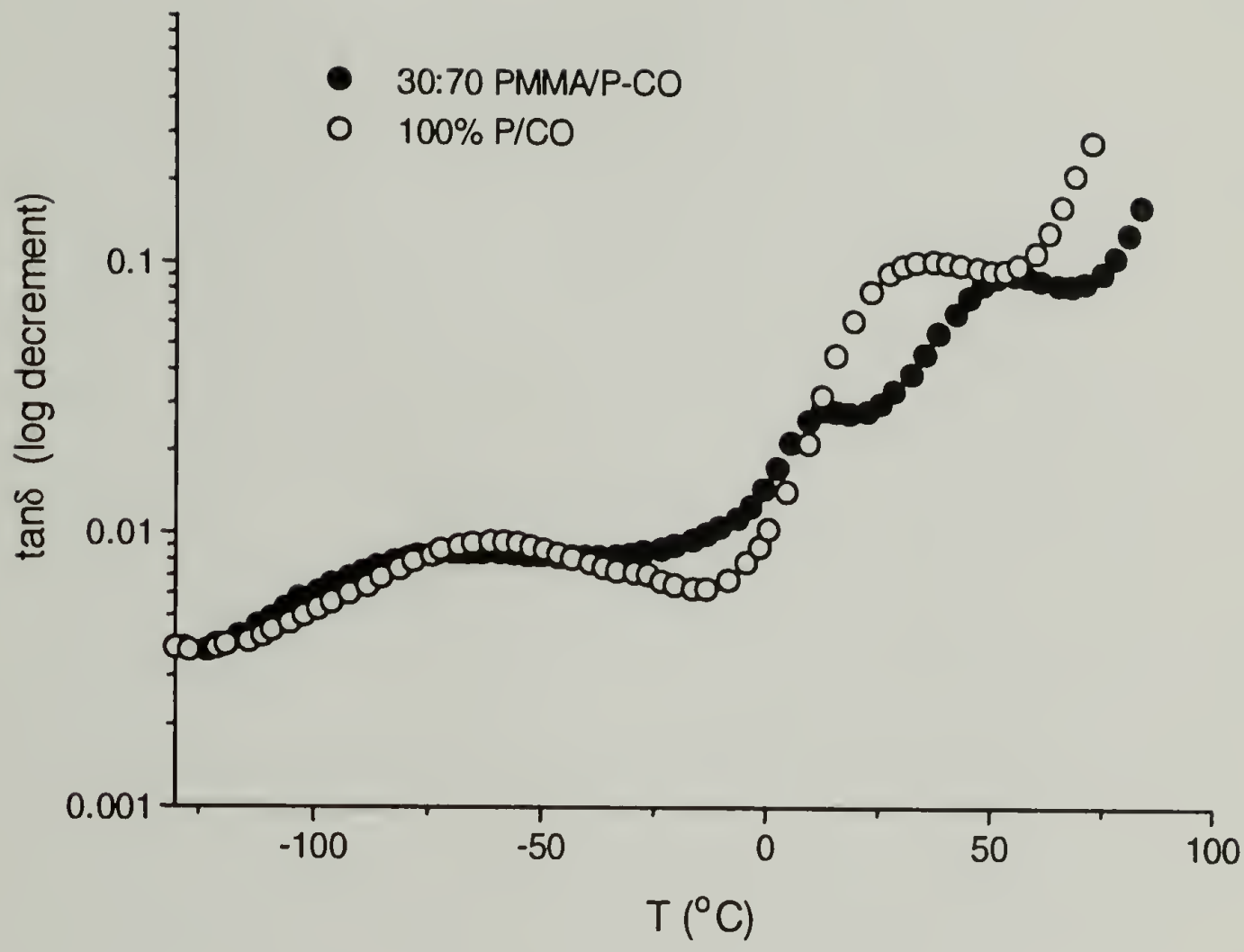

Figure 7.4 DETA measurement at 1 kHz. Tanδ is plotted versus temperature for pure P-CO and 30:70 PMMA/P-CO blends.

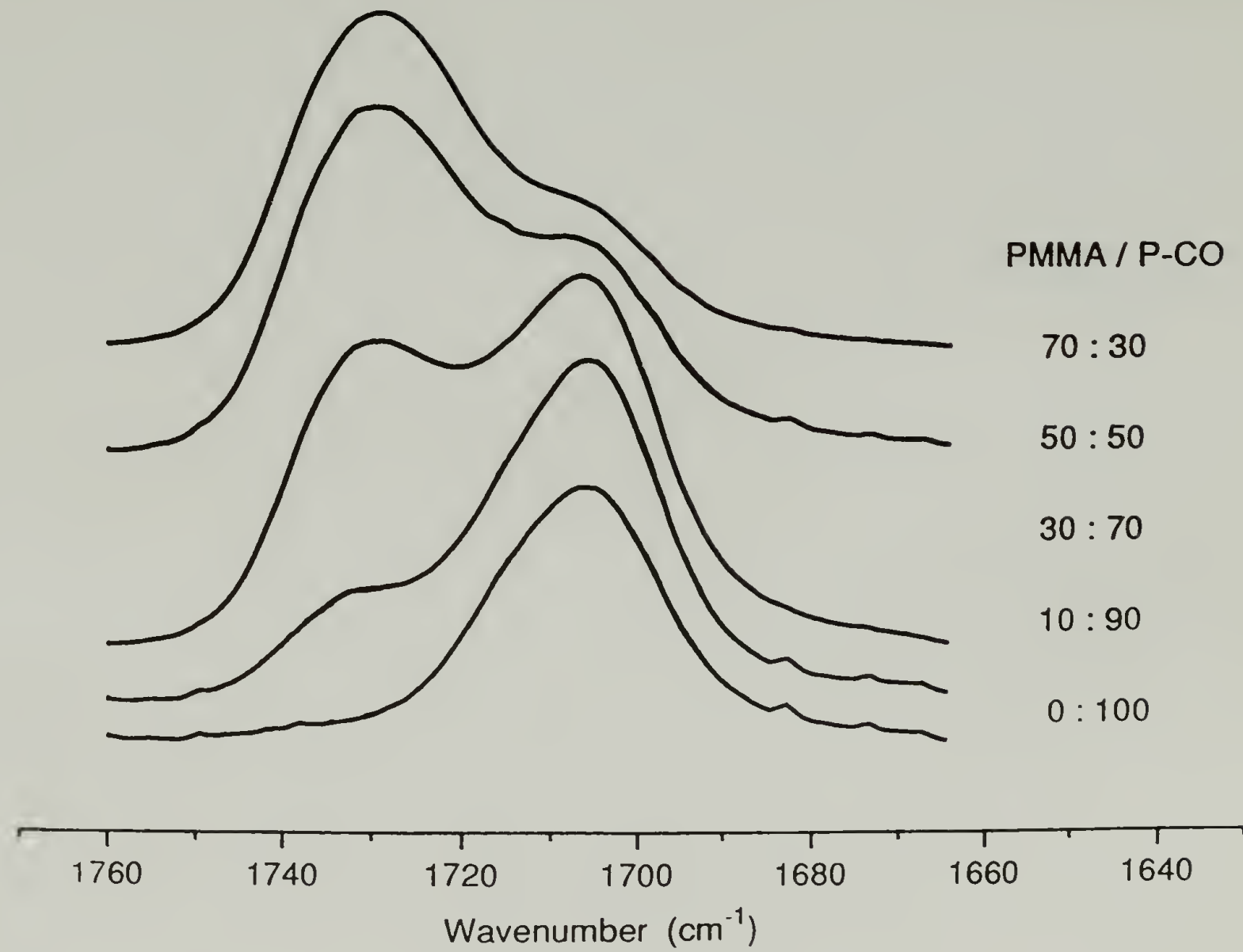

Figure 7.5 IR spectra of carbonyl group stretching region for pure component and blends as indicated. The bands around 1730 and 1707 cm^{-1} are attributed to the carbonyl stretching of PMMA and P-CO, respectively.

frequency shifts were observed for the two carbonyl bands. The intensity changes, however, were very obvious.

The IR intensity, A_S, which is usually referred to an integrated absorbance,[14,15]

$$A_s = \left[\frac{1}{cb}\right] \int_{band} \ln\left(\frac{I_o}{I}\right) d\upsilon \qquad (2)$$

where c is the concentration, b is the path length, I_o is the incident light intensity per unit time, I is the light intensity per unit time emerging from the sample, and υ is the wavenumber. When IR radiation is absorbed by a molecule, the intensity of the absorption depends on the movement of the electronic charges during the molecular vibration. Therefore, the IR intensities should provide information about the electronic charge distributions in molecules and about how the electrons redistribute themselves during molecular vibrations.[14] Each IR intensity can be related to the dipole moment derivative with respect to the normal coordinate.[15] If we set $A_{S,1}$ and $A_{S,2}$ as the IR intensities of carbonyl groups for PMMA and P-CO respectively, the relative IR intensity ratio can be written as

$$\frac{A_{s,1}}{A_{s,2}} = \frac{c_2}{c_1} \times \frac{\text{Band Area 1}}{\text{Band Area 2}} \qquad (3)$$

Since the two carbonyl bands were not severely overlapping, deconvolution of them by curve fitting is easily accomplished. Knowing the areas of two bands and the concentration of the blends, the intensity ratio, $A_{S,1}/A_{S,2}$, was readily calculated. The intensity ratios and band widths at half-height of two carbonyl bands are plotted versus weight fraction of PMMA in Figure 7.6. The intensity ratio changed significantly from 1.44 for the 10:90 PMMA/P-CO blend to 0.32 for the 90:10 PMMA/P-CO blend. In Figure 7.6, it can be seen that the composition variation of intensity ratio is not monotonic. It shows a maximum at ca. 50 wt % PMMA.

The significant effect of blending on the intensity ratio of carbonyl stretching may imply that some groups in the blends interact favorably with one of the carbonyl groups, or two carbonyl groups interact favorably with each other. The variation of width at half-height also supports this argument.

7.3.3 Solid State NMR Relaxation

Many examples of the use of proton spin-lattice relaxation time in laboratory and rotating frame, T_1^H and $T_{1\rho}^H$, and spin diffusion measurements to characterize polymer/ polymer miscibility have been reported.[16-26] A single T_g is taken to indicate the miscibility of blends on the scale of 100 Å; NMR

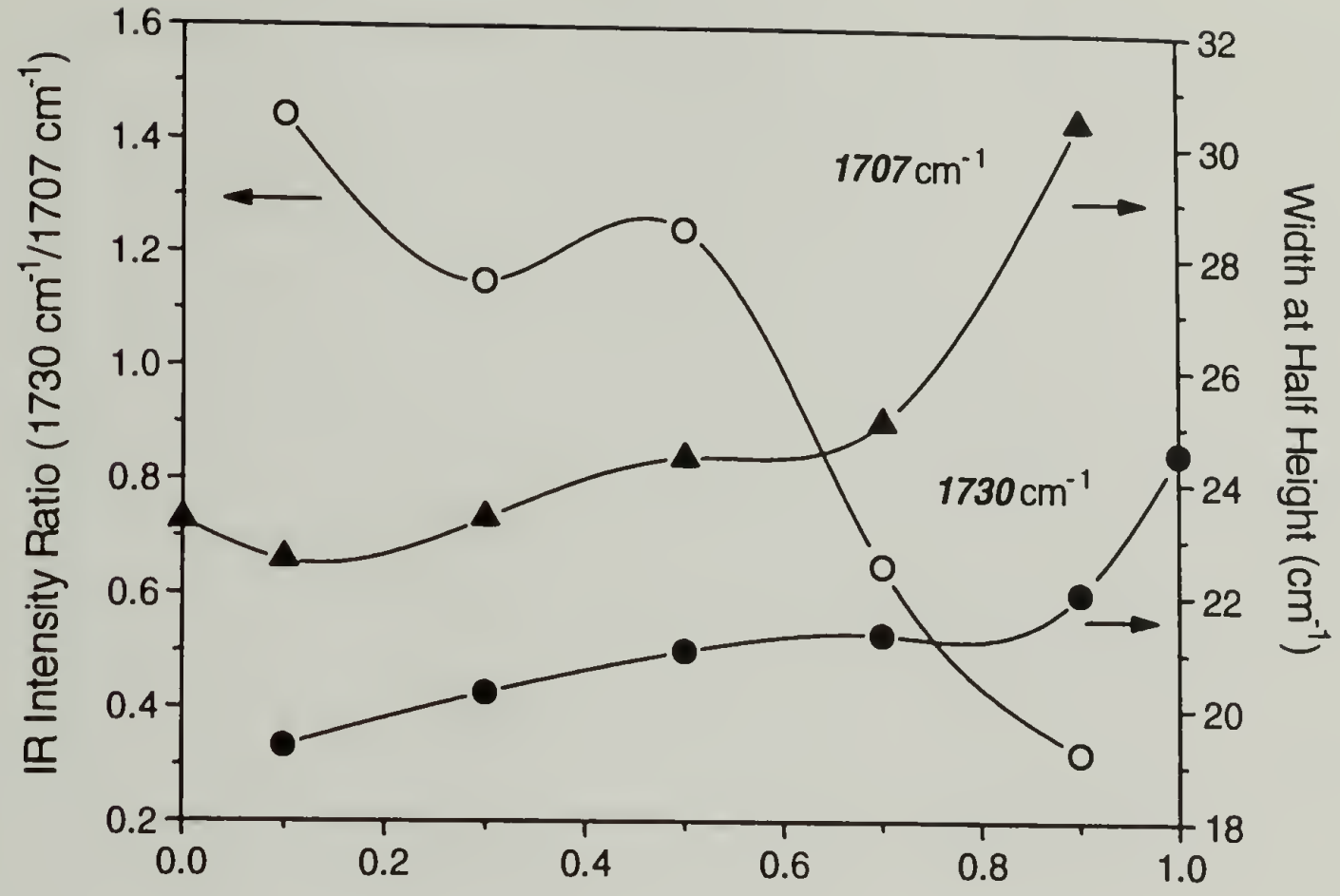

Figure 7.6 The composition dependence of IR intensity ratio and the width at half-height of the two carbonyl bands at 1730 and 1707 cm^{-1}.

relaxation times offer the potential to probe blend miscibility on a different scales. For this reason, solid state NMR was used to further evaluate the PMMA/P-CO blends. Solid state NMR carbon spectra of pure PMMA, pure P-CO, and 30:70 PMMA/P-CO blend are shown in Figure 7.7. Generally speaking, the NMR peaks were well-separated, and relaxation measurement on each individual peak can be performed.

In the solid state experiment, spin energy can propagate between neighboring nuclei by an energy conservation "flip flop" process termed spin diffusion. Spin diffusion is a mechanism for transferring magnetization from one nucleus to another. Spin diffusion is induced by the dipolar interactions of nuclear spins, which produce spin flips between nuclei. This spin flipping leads to an adiabatic transfer of magnetization between neighboring spins. For highly coupled nuclei such as protons, this spin diffusion can be the dominant process for the relaxation.[14] By determining the T_1^H and $T_{1\rho}^H$ values for a blend in comparison to the corresponding values for pure component polymers, it may be possible under certain circumstances to estimate an upper limit to the scale of heterogeneity present in the blend. If the scale of the phase separation in the blend is sufficiently small to permit rapid diffusion of proton spin energy such that a single-component relaxation process is observed, the following equation may be

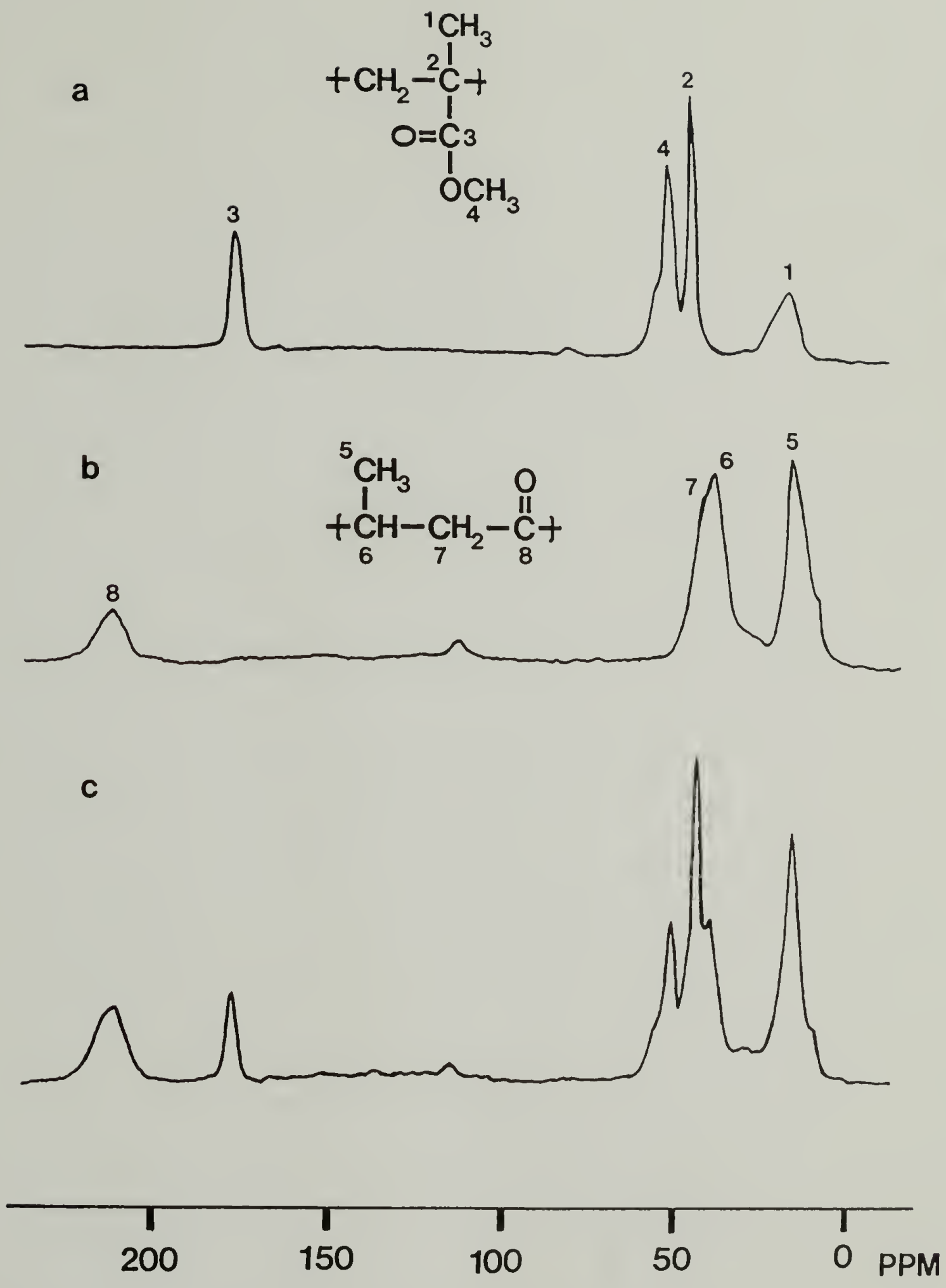

Figure 7.7 Solid state NMR carbon spectra of (a) pure PMMA, (b) pure P-CO, and (c) 30:70 PMMA/P-CO blend.

used to estimate the maximum diffusion path length or upper limit to the domain size,[27,28,23,20,21]

$$\langle L^2 \rangle = \left(\frac{t}{T_2} \right) \langle l_o^2 \rangle \qquad (4)$$

where $<L^2>$ is the mean-square length over which magnetization is transported. $<l_o>$ is the mean jump length which is taken as the distance between neighboring protons, typically 0.1 nm. T_2 is the proton spin-spin relaxation time, and t is the time over which spin diffusion takes place set equal to T_1^H or $T_{1\rho}^H$ in the laboratory or rotating frame. For the PMMA/P-CO blends, substituting in T_2 = 10 μs, the maximum diffusion path lengths for spin-lattice relaxations in the rotating frame (8 ms) and in the laboratory frame (0.5 s) are approximately 30 and 200 Å, respectively. Assuming the spin-lattice relaxation times are different for two pure components, if the blends show single $T_{1\rho}^H$, the blends can be said miscible on the scale of 30 Å, which indicates that the separated phases, if presented, are smaller than ca. 30 Å. Similarly, single T_1^H yields the miscibility on the scale of 200 Å.

Miscibility at 200 Å is required by the single T_g of the blends. Therefore, single T_1^H behavior is expected for the blends. The experimental results confirmed this expectation.

The T_1^Hs were 0.38, 0.46, 0.51, 0.68, and 0.92 s for the pure PMMA, PMMA/P-CO blends of 70:30, 50:50, 30:70, and pure P-CO, respectively.

Measurements of $T_{1\rho}^H$ were made through change in carbon intensity under cross polarization after variable ^1H spin lock time, τ.[9] A typical carbon magnetization intensity versus proton spin lock time plot is shown in Figure 7.8. The carbon signal intensity decay curves were fitted to a standard first-order kinetic expression.[17] If the proton spin system is tightly coupled, the relaxation times should be independent of the carbon peak used to monitor signal decay. This was observed to be the case for this blends system; relaxation times were independent of the peak chosen for the calculation. Figure 7.9 shows the decay curves of ^{13}C signal intensity on a logarithmic scale versus proton spin-lock time for pure PMMA, PMMA/P-CO blends of 70:30, 50:50, 30:70, and pure P-CO. A single exponential decay behavior is observed for all of them. For the pure PMMA, the single-component relaxation process gave a time constant, $T_{1\rho}^H$, of 9.1 ms. Similarly, the $T_{1\rho}^H$ of pure P-CO was calculated to be 5.0 ms. It is readily apparent that the relaxation processes for the blends are intermediate in value as compared to the pure components. These results suggested that the blends are miscible on the scale of 30 Å. In other words the separated phases, if presented, are smaller than

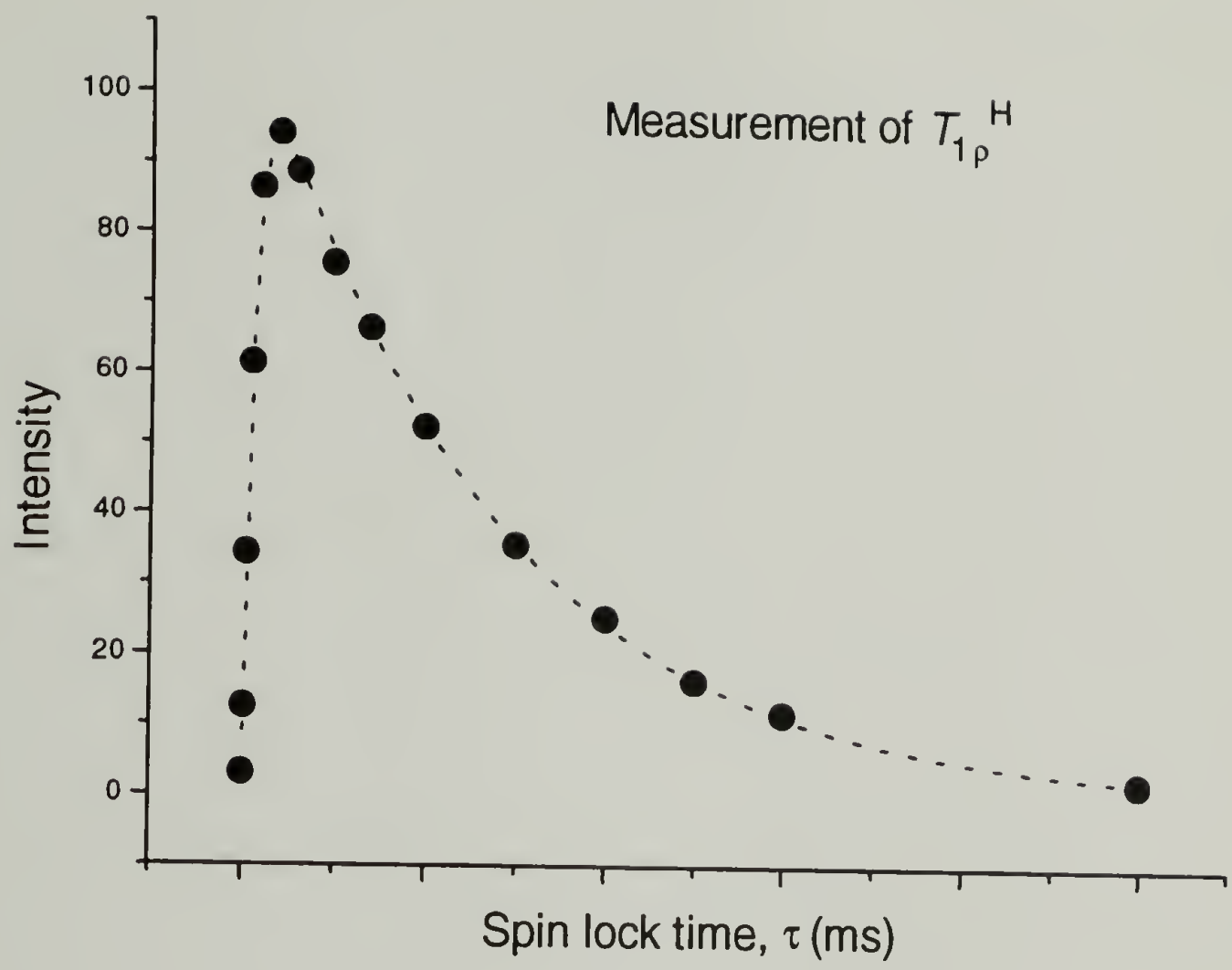

Figure 7.8 A typical carbon magnetization intensity versus proton spin lock time plot.

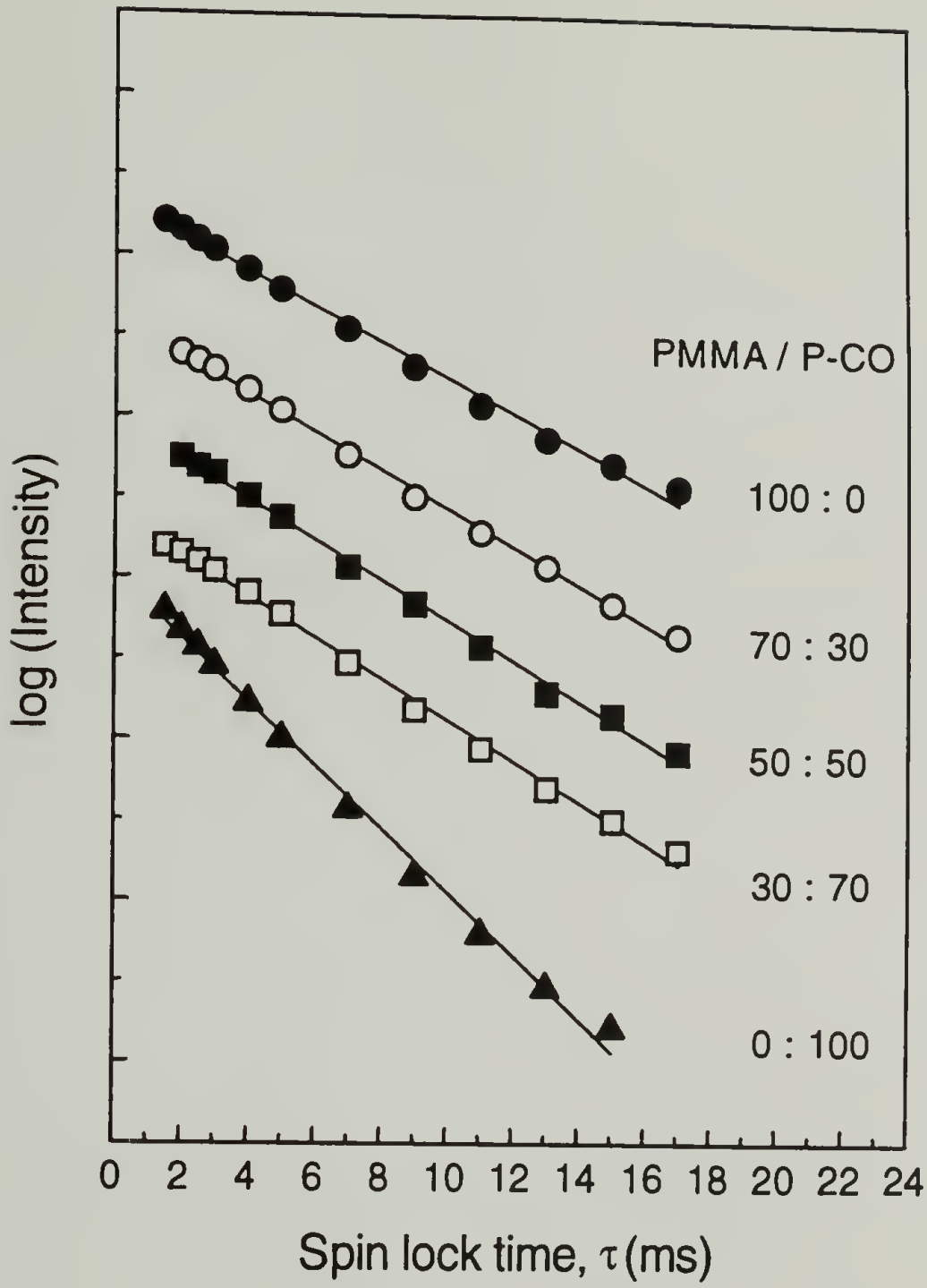

Figure 7.9 Decay curves of ^{13}C signal intensity on a logarithmic scale versus proton spin-lock time, τ, for pure PMMA, PMMA/P-CO blends of 70:30, 50:50, 30:70, and pure P-CO. For clarity each line is begun at a separate origin on the y-axis.

30 Å. However, because of the uncertainty of the exact value of the spin diffusion rate, these upper limit numbers are subjected to error limits of ±50% of the reported value.[20]

7.4 Conclusion

The PMMA/P-CO blends were found to be miscible by both T_g and solid state NMR relaxation studies. The β-relaxation of P-CO was observed by DETA. NMR spin-lattice relaxation in rotating frame measurement showed that the average distance between PMMA and P-CO in the intimately mixed phase is less than 30 Å. The relative IR intensity ratio of two carbonyl bands changed with different blend compositions, which indicated that the specific interaction involving one or both carbonyl groups may be the driving force for mixing.

References

(1) Jiang, Z.; Dahlen, G. M.; Houseknecht, K.; Sen, A. *Macromolecules* **1992**, *25*, 2999.

(2) Batistini, A.; Consiglio, G.; Suter, U. W. *Angew. Chem. Int. Ed. Engl.* **1992**, *31*, 303.

(3) Chien, J. C. W.; Zhao, A. X.; Xu, F. *Polym. Bull.* **1992**, *28*, 315.

(4) Batistini, A.; and Consiglio, G. *Organometallics* **1992**, *11*, 1766.

(5) A. Batistini, G. Consiglio, U. W. Suter, *PMSE Preprint* **1992**, *67*, 104.

(6) Xu, F. Y.; Zhao, A. X.; and Chien, J. C. W. *Markomol. Chem.* **1993**, *194*, 2579.

(7) Wong, P. K.; van Doorn, J. A.; Drent, E.; Sudmeijer, O.; Stil, H. A. *Ind. Eng. Chem. Res.* **1993**, *32(5)*, 986.

(8) Xu, F. Y.; Chien, J. C. W. *Macromolecules* **1993**, *26*, 3485.

(9) Schaefer, J.; Stejskal, E.; Buchdahl, R. *Macromolecules* **1977**, *10*, 384.

(10) McBrierty, V. J.; Douglass, D. C.; Kwei, T. K. *Macromolecules* **1978**, *11*, 1265.

(11) Gordon, M.; Taylor, J. S. *J. Appl. Chem.* **1952**, *2*, 495.

(12) McCrum, N. G.; Read, B. E.; William, G. *Anelastic and Dielectric Effects in Polymeric Solids* New York: Dover Publications, Inc. **1991**.

(13) Coleman, M. M.; Graf, J. F.; Painter, P. C. *Specific Interactions and the Miscibility of Polymer Blends* Lancaster: Technomic Publication, **1991**.

(14) Koenig, J. *Spectroscopy of Polymers* Washington, D. C.: American Chemical Society, **1992**.

(15) Gribov, L. A. *Intensity Theory for Infrared Spectra of Polyatomic Molecules* New York: Consultants Bureau, **1964**.

(16) Albert, B.; Jerom, R.; Teyssie, P.; Smyth, G.; Boyle, N. G.; McBrierty, V. J. *Macromolecules* **1985**, *18*, 388.

(17) Assink, R. A. *Macromolecules* **1978**, *11*, 1233.

(18) Dickinson, L. C.; Yang, H.; Chu, C. W.; Stein, R. S.; Chien, J. C. W. *Macromolecules* **1987**, *20*, 1757.

(19) Stejskal, E. O.; Schaefer, J.; Sefcik, M. D.; McKay, R. A. *Macromolecules* **1981**, *14*, 275.

(20) Parmer, J. F.; Dickinson, L. C.; Chien, J. C. W.; Porter, R. *Macromolecules* **1989**, *22*, 1078.

(21) Gao, Z.; Molnar, A.; Morin, F. G.; Eisenberg, A. *Macromolecules* **1992**, *25*, 6460.

(22) McBrierty, V. J. In *Comprehensive Polymer Science*; Allen, G., Ed.; Oxford: Pergamon Press, **1989**.

(23) McBrierty, V. J.; Douglass, D. C. *Macromol. Rev.* **1981**, *16*, 295.

(24) Voelkel, R. *Angew. Chem., Int. Ed. Engl.* **1988**, *27*, 1468.

(25) Simmons, A.; Natansohn, A. *Macromolecules* **1991**, *24*, 3651.

(26) Chu, C. W.; Dickinson, L. C.; Chien, J. C. W. *J. Appl. Polym. Sci.* **1990**, *41*, 2311.

(27) McBrierty, V. J. *Magn. Reson. Rev.* **1983**, *8*, 166.

(28) Smith, P.; Hara, M.; Eisenberg, A. In *Current Topics in Polymer Science*; Ottenbrite, R. M.; Utracki, L. A. Inoue, S., Eds.; New York: Hanser Publishers, **1987**.

BIBLIOGRAPHY

Albert, B.; Jerom, R.; Teyssie, P.; Smyth, G.; Boyle, N. G.; McBrierty, V. J. *Macromolecules* **1985**, *18*, 388.

Alexander, L. E. *X-ray Diffraction Methods in Polymer Science* New York: John Wiley & Sons, Inc., **1969**.

Allen, N. S.; Edge, M. *Fundamentals of Polymer Degradation and Stabilisation* New York: Elsevier Applied Science, **1992**.

Allinger, N. L. *J. Am. Chem. Soc.* **1977**, *99*, 8127.

Amerik, Y.; Guillet, J. E. *Macromolecules* **1971**, *4*, 375.

Apellmeyer, D. C.; Houk, K. N. *J. Org. Chem.* **1987**, *52*, 959.

Assink, R. A. *Macromolecules* **1978**, *11*, 1233.

Ausloos, P. J. *Phys. Chem.* **1961**, *65*, 1616.

Bamford, C. H.; Norrish, R. G. W. *J. Chem. Soc.* **1938**, 1544.

Bamford, C. H.; Norrish, R. G. W. *J. Chem. Soc.* **1938**, 1521.

Bamford, C. H.; Norrish, R. G. W. *J. Chem. Soc.* **1935**, 1504.

Batistini, A.; Consiglio, G. *Organometallics* **1992**, *11*, 1766.

Batistini, A.; Consiglio, G.; Suter, U. W. *Angew. Chem. Int. Ed. Engl.* **1992**, *31, No. 3*, 303.

Batistini, A.; Consiglio, G.; Suter, U. W. *PMSE Preprint*, **1992**, *67*, 104.

Ben-David, Y.; Portnoy, M.; Gozin, M.; Milstein, D. *Organometallics* **1992**, *11*, 1995.

Ben-David, Y.; Portnoy, M.; Milstein, D. *J. Am. Chem. Soc.* **1989**, *111*, 8742.

Ben-David, Y.; Portnoy, M.; Gozin, M.; Milstein, D. *J. Chem. Soc. Chem. Commun.*, **1989**, 1816.

Bovey, F. A.; Tiers, G. V. D. *J. Polym. Sci.* **1960**, *44*, 173.

Breitmaier, E.; Voelter, W. *Carbon-13 NMR Spectroscopy* New York: VCH **1987**.

Bremer, Y. P. *Polym. Plast. Technol. Eng.* **1982**, *18*, 137.

Broekhoven, J. *Eur. Pat. Appl.* A1, 0,213,671, **1986**.

Brubaker, R. G.; Johnson, W. D. *Coord. Chem. Rev.* **1984**, *53*, 1.

Brubaker, M. M.; Coffman, D. D.; Hoehn, H. H. *J. Am. Chem. Soc.* **1952**, *74*, 1509.

Brumbaugh, J. S.; Whittle, R. R.; Parvez, M.; Sen, A. *Organometallics*, **1990**, *9*, 1735.

Busico, V.; Corradini, P.; De Martino, L.; Proto, A.; Savino, V.; Albizzati, E. *Makromol. Chem.* **1985**, *186*, 1279.

Castonguay, L. A.; Rappe, A. K. *J. Am. Chem. Soc.* **1992**, 114, 5832.

Cavallo, L.; Guerra, G.; Vacatello, M.; Corradini, P. *Macromolecules* **1991**, *24*, 1784.

Chatani, Y.; Takizawa, T. *J. Polym. Sci.* **1961**, *55*, 811.

Chen, J. T.; Sen, A. *J. Am. Chem. Soc.* **1984**, *106*, 1506.

Chen, Y.; Rausch, M. D.; Chien, J. C. W. *J. Am. Chem. Soc.* submitted.

Chen, Y.; Rausch, M.D.; Chien, J. C. W. *Macromolecules* submitted.

Cheng, H. N.; Ewen, J. A.; *Makromol. Chem.* **1989**, *190*, 1931.

Chien, J. C. W.; Zhao, A. X. *Polym. Degrad. Stab.* **1993**, *40*, 257.

Chien, J. C. W.; Zhao, A.; Xu, F. *Polym. Bull.* **1992**, *28*, 315.

Chien, J. C. W.; Tsai, W-M.; Rausch, M. D. *J. Am. Chem. Soc.* **1991**, *113*, 8570.

Chien, J. C. W.; Wang, B. P. *J. Polym. Sci., Part A: Polym. Chem.* **1989**, *27*, 1539.

Chu, C. W.; Dickinson, L. C.; Chien, J. C. W. *J. Appl. Polym. Sci.* **1990**, *41*, 2311.

Coleman, M. M.; Graf, J. F.; Painter, P. C. *Specific Interactions and the Miscibility of Polymer Blends* Lancaster: Technomic Publication, **1991**.

Connor, J. A.; McEwen, G. K.; Rix, C. J. *J. Chem. Soc., Dalton Trans.* **1974**, 589.

Connor, J. A.; Day, J. J.; Jones, E. M.; McEwen, G. K. *J. Chem. Soc., Dalton Trans.* **1973**, 347.

Dickinson, L. C.; Yang, H.; Chu, C. W.; Stein, R. S.; Chien, J. C. W. *Macromolecules* **1987**, *20*, 1757.

Doi, Y.; Asakuru, T. *Makromol. Chem.* **1975**, *176*, 507.

Dorigo, A. E.; Houk, K. N. *J. Org. Chem.* **1988**, *53*, 1650.

Drent, E.; van Brockhoven, J. A. M.; Doyle, M. J.; *J. Organomet. Chem.* **1991**, *417*, 235.

Drent, E. *Eur. Pat. Appl.* A2, 0,272,728, **1987**.

Drent, E. *Eur. Pat. Appl.* A1, 0,264,159, **1987**.

Drent, E. *Eur. Pat. Appl.* 121,965, **1984**.

Dworak, A.; Freeman, W. J.; Harwood, H. J. *Polym. J. (Tokyo)* **1985**, *17*, 351.

Fenton, D. M. *U.S. Pat.* 3,530,109, **1970**.

Flory, P. J. *J. Am. Chem. Soc.* **1967**, *89*, 1798.

Flynn, J. H. in *Aspect of Degradation and Stabilization of Polymers*, Jellinek, H. H. G. Ed., New York: Elsevier Scientific Publishing Co. **1978**.

Franck, J.; Rabinowitch, E. Trans. Faraday Soc. **1934**, *30*, 120.

Gao, Z.; Molnar, A.; Morin, F.; Eisenberg, A. *Macromolecules* **1992**, *25*, 6460.

Garrou, P. E. *Chem. Rev.* **1981**, *81*, 229.

Garrou, P. E. *Inorg. Chem.* **1975**, *14*, 1435.

Gaugh, A. *Great Britain Pat.* 1,081,304, **1967**.

Golemba, F.; Guillet, J. E. *Macromolecules* **1972**, *5*, 212.

Gordon, M.; Taylor, J. S. *J. Appl. Chem.* **1952**, *2*, 495.

Grassi, A.; Zambelli, A.; Resconi, L.; Albizzati, E.; Mazzochi, R. *Macromolecules* **1988**, *21*, 617.

Gribov, L. A. *Intensity Theory for Infrared Spectra of Polyatomic Molecules* New York: Consultants Bureau, **1964**.

Grim, S. O.; Briggs, W. L.; Barth, R. C.; Tolman, C. A.; Jesson, J. P. *Inorg. Chem.* **1974**, *13*, 1095.

Guillet, J. E.; Dhanraj, J.; Golemba, F. J.; Hartley, G. H. *Adv. Chem. Ser.* **1986**, *85*, 272.

Guillet, J. *Polymer Physics and Photochemistry* New York: Cambridge University Press, **1985**.

Hart, J. R.; Rappe, A. K. *J. Am. Chem. Soc.* **1993**, *115*, 6159.

Hart, C. *J. Am. Chem. Soc.* **1957**, *79*, 931.

Hartley, G. H.; Guillet, J. E. *Macromolecules* **1968**, *1*, No. 2, 165.

Heskins, M.; Guillet, J. E. *Macromolecules* **1968**, *1*, 97.

Jiang, Z.; Dahlen, G. M.; Houseknecht, K.; Sen, A. *Macromolecules* **1992**, *25*, 2999.

Jiang, Z.; Sen, A. *Macromolecules* **1992**, *25*, 880.

Kawamura-Kuribayashi, H.; Koga, N.; Morokuma, K. *J. Am. Chem. Soc.* a) **1992**, *114*, 2359. b) **1992**, *114*, 8687.

Kobayashi, T.; Tanaka, M. *J. Organomet. Chem.* **1982**, *233*, C64.

Koenig, J. *Spectroscopy of Polymers* Washington, D. C.: American Chemical Society, **1992**.

Kupin, P. *Zh. Obshch. Khim.* **1959**, *29*, 3738.

Lai, T. W.; Sen, A. *Organometallics* **1984**, *3*, 866.

Langer, A. W.; Burkhardt, T.; Steger, J. J. *Proceedings of the MMI International Symposium on 'Transition Metal Catalyzed Polymerization: Unsolved Problems'*, Midland, MI, **1981**.

Leighton, W. G.; Forbes, G. S. *J. Am. Chem. Soc.* **1930**, *52*, 3139.

Longi, P.; Giannini, U.; Cassata, A. (issued to Montedison) *Belg. Pat.* 774,600, **1971**.

Mann, B. E.; Masters, C.; Shaw, B. L. *J. Chem. Soc., Dalton Trans.* **1972**, 704.

Mann, B. E.; Masters, C.; Shaw, B. L. *J. Chem. Soc. A*, **1971**, 1104.

Manriquez, J. M.; McAlister, D. C.; Sanner, R. D.; Bercaw, J. *J. Am. Chem. Soc.* **1978**, *100*, 2716.

Marsella, J. A.; Folting, K.; Huffman, J. C.; Caulton, K. G. *J. Am. Chem. Soc.* **1981**, *103*, 5596.

McBrierty, V. J. In *Comprehensive Polymer Science*; Allen, G., Ed.; Oxford: Pergamon Press, **1989**.

McBrierty, V. J. *Magn. Reson. Rev.* **1983**, *8*, 166.

McBrierty, V. J.; Douglass, D. C. *Macromol. Rev.* **1981**, *16*, 295.

McBrierty, V. J.; Douglass, D. C.; Kwei, T. K. *Macromolecules* **1978**, *11*, 1265.

McCrum, N. G.; Read, B. E.; William, G. *Anelastic and Dielectric Effects in Polymeric Solids* New York: Dover Publications, Inc. **1991**.

Nakazawa, H.; Ozawa, F.; Yamamoto, A. *Organomet.* **1983**, *2*, 241.

Natta, G.; Corradini, P. *Nuovo Cimento, Supplemento* **1960**, *15*, 1.

Natta, G.; Corradini, P.; Bassi, I.; Porri, L. *Atti. Accad. N. az. Lincei, Cl. Sci. Fis., Mat. Nat., Rend.* **1958**, *24*, 121.

Natta, G.; Pino, P.; Danusso, F.; Mantica, E.; Mazzanti, G.; Moragio, G. *J. Am. Chem. Soc.* **1955**, *77*, 1708.

Nicol, C. H.; Calvert, J. G. *J. Am. Chem. Soc.* **1967**, *89*, 1790.

Noyes, R. M. *Prog. React. Kinet.* **1961**, *2*, 129.

Nozaki, K. *U.S. Pat.* 3,835,123, **1974**.

Nozaki, K. *U.S. Pat.* 3,689,460, **1972**.

Oguni, N.; Shinohara, S.; Lee, K. *Polym. J. (Tokyo)* **1979**, *11*, 755.

Opitz, G.; Adolf, H.; Kleemann, M.; Zimmermann, F. *Angew. Chem.* **1961**, *73*, 654.

Palenik, G. J.; Mathew, M.; Steffen, W. L.; Beran, G. *J. Am. Chem. Soc.* **1975**, *97*, 1059.

Park, H. G. *J. Polym. Sci., Part C* **1968**, *16*, 3455.

Parmer, J. F.; Dickinson, L. C.; Chien, J. C. W.; Porter, R. *Macromolecules* **1989**, *22*, 1078.

Perrin, D. D.; Armarego, W. L. F.; Perrin, D. R. *Purification of Laboratory Chemicals* New York: Pergamon Press, **1980**.

Pino, P.; Muelhaupt, R. *Angew. Chem., Int. Ed. Engl.* **1980**, *19*, 857.

Reppe, W.; Magin, A. *U.S. Pat.* 2,577,208, **1951**.

Rieger, B.; Mu, X.; Mallin, D.; Rausch, M. D.; Chien, J. C. W. *Macromolecules* **1990**, *23*, 3559.

Ruland, W. *Acta Cryst.* **1961**, *14*, 1180.

Schaefer, J.; Stejskal, E.; Buchdahl, R. *Macromolecules* **1977**, *10*, 384.

Sen, A.; Jiang, Z.; Chen, J. T. *Macromolecules* **1989**, *20*, 2012.

Sen, A. *Adv. Polym. Sci.* **1987**, *73/74*, 125.

Sen, A. *Chemtech.* **1986**, 48.

Sen, A.; Lai, T. W. *J. Am. Chem. Soc.* **1980**, *104*, 3520.

Shepherd, L.; Chen, T. K.; Harwood, H. J. *Polym Bull.* **1979**, *1*, 445.

Shorter, J. *Correlation Analysis of Organic Reactivity*, New York: Research Studies Press, **1982**.

Shryne, T. M.; *U.S. Pat.* 3,948,388, **1976**.

Simmons, A.; Natansohn, A. *Macromolecules* **1991**, *24*, 3651.

Smith, P.; Hara, M.; Eisenberg, A. In *Current Topics in Polymer Science*; Ottenbrite, R. M.; Utracki, L. A. Inoue, S., Eds.; New York: Hanser Publishers, **1987**.

Soga, K.; Shiono, T.; Takemura, S.; Kaminsky, W. *Makromol. Chem., Rapid Commun.* **1987**, *8*, 305.

Stejskal, E. O.; Schaefer, J.; Sefcik, M. D.; McKay, R. A. *Macromolecules* **1981**, *14*, 275.

Stutsman, A. *J. Am. Chem. Soc.* **1939**, *61*, 3305.

Suter, U. W.; Neuenschwander, P. *Macromolecules* **1981**, *14*, 528.

Taft, R. W. in *Steric Effects in Organic Chemistry*, Ed., Newman, M. S. New York: Wiley **1956**.

Tani, K.; Tanigawa, E.; Tatsuno, Y.; and Otsuka, S. *J. Organomet. Chem.* **1985**, *279*, 87.

Tsai, W.-M.; Chien, J. C. W. *Makromol. Chem. Macromol. Symp.* **1993**, *66*, 141.

Tsai, W-M.; Rausch, M. D.; Chien, J. C. W. *Appl. Organomet. Chem.* **1993**, *7*, 71.

Voelkel, R. *Angew. Chem., Int. Ed. Engl.* **1988**, *27*, 1468.

Wagner, P. J.; Hammond, G. S. *J. Am. Chem. Soc.* **1965**, *87*, 4009.

Wilson, S. *Chemistry by computer* New York: Plenum Press, **1986**.

Wong, P. K.; van Doorn, J. A.; Drent, E.; Sudmeijer, O.; Stil, H. *Ind. Eng. Chem. Res.* **1993**, *32(5)*, 986.

Xu, F. Y.; Zhao, A. X.; Chien, J. C. W. *Markomol. Chem.* **1993**, *194*, 2579.

Xu, F. Y.; Chien, J. C. W. *Macromolecules* **1993**, *26*, 3485.

Yang, N. C.; Yang, D. H. *J. Am. Chem. Soc.* **1958**, *80*, 2913.

Yomamoto, A. *Organotransition Metal Chemistry* New York: John Wiley & Sons, **1986**.

Yu, Z.; Chien, J. C. W. *J. Am. Chem. Soc.* submitted.

Zhao, A. X.; Chien, J. C. W. *J. Polym. Sci., Part A: Polym. Chem.* **1992**, *30*, 2735.

Ziegler, K. *Belg. Pat.* 53362, **1953**.